Aromatization of Alkenes by Gallium/H-ZSM-5 Zeolite Catalysts

Robin John Nash
BSc. Hons. (Chem.)

Submitted to University of Cape Town
In fulfilment of the requirements for the degree of
Master of Science (Applied Science)

Catalysis Research Unit
Department of Chemical Engineering
University of Cape Town
Rondebosch
Cape Town
South Africa

February 1994

ACKNOWLEDGEMENTS

I would like to gratefully acknowledge the help and guidance given to me by my supervisor, Prof. Mark Dry. I would also like to thank Dr. Jack Fletcher for his role in shaping this project as well as for his advice on how to solve some of the problems that I encountered. Professor Cyril O'Connor deserves an honourable mention for his guidance and the enthusiasm that he inspired in me.

I would furthermore like to thank Peter Richards and Cindy Adamson for their help with some of the experiments and their sense of humour during times when progress was hampered by inevitable setbacks.

To SASOL Ltd., a big thank you for supporting me financially these last two years. Without your help this thesis could never have been written.

Cheers to Barry, for his help with the FTIR analysis, and Leslie for arranging the SEM micrographs.

To the ladies: Debbie, Shehnaaz, Sarah and Mary Jane. Without you I would not have finished this sane.

Thanks to Ashley, Gary, Rein, Dave and Tony. Your helpful comments provided me with insight in times of need. Finally, I must thank my long-suffering lab partner Jannie who had to put up with my antics and who still managed to begin each day with a cheerful greeting and a smile.

SYNOPSIS

Gallium/H-ZSM-5 zeolite catalysts have been extensively researched for the aromatization of liquified petroleum gas (LPG). In 1989 BP and UOP collaborated to commission a pilot plant in Grangemouth, Scotland, for the aromatization of propane and butane. This plant, based on a technology called the Cyclar process, used continuous catalyst regeneration (CCR) and a gallium impregnated ZSM-5 zeolite catalyst to achieve yields of *ca.* 65% aromatics, mainly benzene, toluene and xylenes (BTX) [Guisnet and Gnep, 1992]. As a result of the Fischer-Tropsch process used by SASOL Ltd., South Africa is in an internationally unique position, in that it has a surplus of long chain linear alkenes with carbon numbers in the range C_6-C_8. There could be large economic incentives to convert these alkenes into more valuable products, like alcohols or aromatics. Thus the purpose of this project was to determine if gallium/H-ZSM-5 catalysts, similar to those used in the Cyclar process, would be suitable for the aromatization of long chain alkenes. Three methods were investigated for the introduction of gallium into ZSM-5:

(i) physical mixing with gallium oxide;
(ii) impregnation by incipient wetness with gallium nitrate;
(iii) ion-exchange with gallium nitrate.

The catalysts were tested with regard to their catalytic activity for the aromatization of 1-hexene and 1-octene. It was found that the introduction of gallium into H-ZSM-5 catalysts dramatically enhanced the selectivity towards aromatic products from *ca.* 13% to 70%. However, these catalysts exhibited rapid decrease in BTEX selectivity with time on stream (70% to 20% after 9 hours on stream). No such change was noted for unmodified H-ZSM-5 after similar time on stream. The selectivity to BTEX achieved for 1-hexene and 1-octene aromatization are similar to BTEX selectivities reported in recent literature for light alkane and light alkene aromatization, i.e. *ca.* 70% BTX.

It was found that the best catalysts for aromatization, with regard to initial BTX selectivity, were those where gallium had been added by ion exchange and

impregnation techniques (65% to 73% BTX). The primary cracked products were ethene, propene and the butenes. Selectivity to these cracked alkenes increased with time on stream. The effect of alkene feedstock was negligible with similar BTEX selectivities observed for both 1-hexene and 1-octene feedstocks. The operating conditions, in particular reaction temperature and residence time of the feedstock in the catalyst bed, had a large effect on BTEX selectivities. Maximum selectivity (*ca.* 70%) towards aromatics were observed at high temperatures, 500°C to 550°C, and long residence times of the feedstock over the catalyst bed. The maximum selectivity towards aromatics was 73% for gallium/H-ZSM-5 prepared by impregnation techniques using 1-octene as the alkene feedstock.

While the present results show that gallium/H-ZSM-5 catalysts are active for the aromatization of long chain alkenes, they unfortunately have several unwanted characteristics which may inhibit their use at this stage. These are the rapid decrease in selectivity to BTEX observed with time on stream and the high selectivity to cracked products (*ca.* 25wt%). These problems will have to be overcome before the catalysts find industrial applications.

TABLE OF CONTENTS

LIST OF FIGURES

LIST OF TABLES

NOMENCLATURE

LPG	liquified petroleum gas
BTX	benzene, toluene, xylenes
CCR	continuous catalyst regeneration
B	benzene
T	toluene
p,m-X	p-xylene and m-xylene
o-X	o-xylene
EtB	ethylbenzene
C_1	methane
$C_2=$, $C_3=$	ethene, propene
C_2,C_3	ethane, propane
1-$C_4=$, i-$C_4=$, t-2-$C_4=$, c-2-$C_4=$	1-butene, iso-butene, trans-2-butene, cis-2-butene
i-C_4, n-C_4	iso-butane, n-butane
SBU	structural building unit
Ga(mix)/H-ZSM-5	catalyst prepared by physical mixing of Ga_2O_3 and H-ZSM-5
Ga(impr)/H-ZSM-5	H-ZSM-5 impregnated by incipient wetness with aqueous $Ga(NO_3)_3$
Ga(ionx)/H-ZSM-5	H-ZSM-5 catalyst ion-exchanged with $Ga(NO_3)_3$ solution
H-ZSM-5	protonated form of ZSM-5
NH_4-ZSM-5	ammonium form of ZSM-5
Ga/H-ZSM-5	generic gallium-containing H-ZSM-5 catalyst
DME	dimethyl ether
MFC	mass flow controller
FTIR	Fourier transform infrared spectroscopy
SCCM	standard cm^3/minute
MFI	ZSM-5 class of medium pore-size zeolites

Chapter 1

INTRODUCTION

1. Introduction

The purpose of this project was to research an effective route for the aromatization of linear alkenes. The worldwide relative abundance of liquified petroleum gas (LPG), which has few petrochemical applications, and the strong demand for aromatics make it attractive to produce aromatics via the aromatization of propane and butanes. The Fischer Tropsch process used by SASOL Ltd. in South Africa produces a large amount of linear alkenes. These alkenes are currently converted to make gasoline. There is an incentive to develop a process whereby the C_6 to C_9 alkenes may be converted into higher value products like aromatics.

1.1.The Importance of Aromatic Compounds.

1.1.1 Industrial uses

Aromatic hydrocarbons, in particular benzene, toluene and xylenes (BTX) have two main industrial uses. Due to their high octane number they constitute a significant part of the gasoline pool (ca. 30%), even if due to anti-pollution legislation their use has declined recently. Secondly they are an important source of petrochemicals. BTX hydrocarbons are traditionally obtained by catalytic reforming of naphthas. However light hydrocarbons, in particular LPG, are becoming an attractive feed for the production of aromatics. [Guisnet and Gnep, 1992]. The use of aromatic compounds in industrial processes is widespread. They are used as organic solvents and in the production of polystyrene, to name but two applications.

1.2. Aromatization Processes

1.2.1. The M2-forming process

The M2-forming process, proposed by Mobil, converts a large variety of feedstocks such as pyrolysis gasoline, unsaturated gases from catalytic cracking, paraffinic naphthas and LPGs into aromatics. Depending on the reactivity of the feedstock, the operating temperature varies significantly, varying from below 370°C for alkenes to 538°C for propane. H-ZSM-5 was chosen as the catalyst. This purely acid catalyst is only interesting for the production of high octane compounds from pyrolysis gasoline or paraffinic naphthas [Guisnet and Gnep, 1992].

The following calculated equilibrium product distribution for propene aromatization via the M2-Forming process has been published [Norval et al. 1989] and is shown in Table 1.1. The equilibrium mass percent of the C_3-C_6 alkanes and alkenes were reported to be below 10^{-2} for all conditions. The effect of pressure on the M2-Forming process is to decrease equilibrium selectivity to benzene and increase selectivity to toluene.

Table 1.1 Calculated equilibria for the M2-forming process at 1atm (in wt%)

	527°C	627°C
Hydrogen	0.12	0.35
Methane	37.08	35.91
Ethane	0.06	0.06
Ethene	0.01	0.05
Propene	0.00	0.00
Benzene	56.70	58.88
Toluene	5.82	4.61
Ethylbenzene	0.02	0.02
o-Xylene	0.05	0.03
m-Xylene	0.09	0.06
p-Xylene	0.04	0.03
C_9+ aromatics	0.00	0.00
aromatics sum	62.72	63.63

37,08

99,80

1.2.2. Cyclar process

The Cyclar process was developed jointly by BP and UOP and converts LPG into aromatics in a single step. The process based on continuous catalyst regeneration technology (CCR), uses gallium impregnated H-ZSM-5 as the catalyst. A large scale pilot plant was built in 1989 in Grangemouth, Scotland. The feed used was propane, iso-butane and n-butane. The Cyclar unit consists of reactor regenerator and product-recovery sections (Figure 1.1). The reaction is carried out in a series of adiabatic stacked reactors. Reactor interheaters compensate for the endothermicity of the reaction. The catalyst flows by gravity from one reactor to the next. The catalyst flowing into the final reactor is transferred by lift gas to the regeneration section were it flows by gravity. Lift gas transfers the catalyst to the first reactor [Guisnet and Gnep, 1992]. When propane is used as feed, the aromatic yield is 63.1 wt% and the hydrogen yield is 5.9wt%. The aromatic cut contains 92 wt% BTX, while the coke yield was less that 0.02% of the fresh feed [C.D. Gosling et al. 1991]. The process variables controlling product yields are feed composition, space velocity, reaction temperature and reaction pressure. The demonstration unit closed down at the end of 1991.

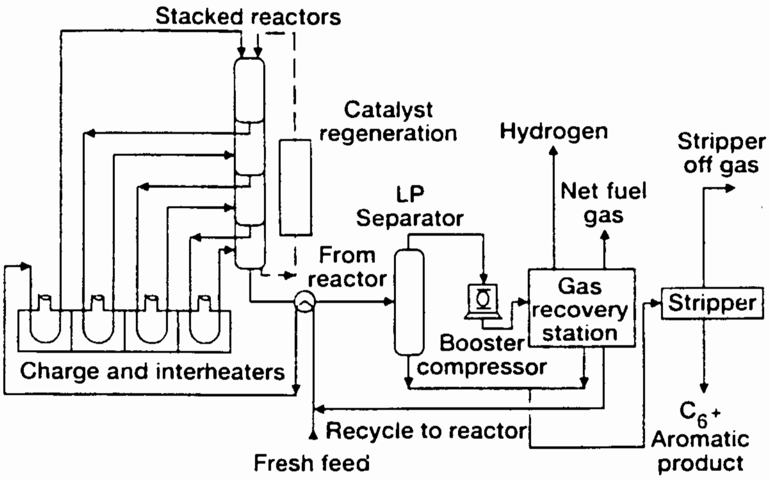

Figure 1.1 Schematic diagram of the Cyclar process for LPG aromatization

The selectivities to products for the aromatization of LPG by the Cyclar process are shown in Table 1.2 [Gosling et al. 1991].

Table 1.2 Cyclar process product distribution

Selectivities [wt%]	Propane feedstock	Butane feedstock
Fuel gas	33	26
Benzene	16	15
Toluene	26	29
Xylenes	13	17
C_9^+ aromatics	5	6
BTX sum	55	61
Hydrogen	7	7

1.2.3. The Aroforming Process

The Cyclar process is not intended to convert light naphtha feedstocks, especially the C_5 and C_6 hydrocarbons, into aromatics, while the Aroforming process, developed by IFP and SALUTEC, has been designed to aromatize a large range of aliphatic hydrocarbons.

Table 1.3 Product yields from the Aroforming process

Selectivities [wt%]	light naphtha feedstock
C_1-C_2	27
C_3	15
benzene	12
toluene	22
C_8 aromatics	12
C_{9+} aromatics	8
BTX sum	56
hydrogen	3

The catalyst is a shape selective zeolite, doped with metal oxides. The process is based on multiple fixed bed isothermal reactors, with some run under regeneration mode whilst the rest are on line. When light naphtha is used as a feedstock, the Aroforming process yields aromatics of *ca.* 54.9%. With LPG the yields are close to that obtained with the Cyclar process [Guisnet and Gnep, 1992].

1.2.4. Platforming

Platforming was the first catalyst reforming process using a noble metal catalyst and became commercial in 1949. It was the prototype for all existing plants. Typical operating conditions are at reaction temperatures between 500°C and 525°C, a pressure of 23.3bar, LHSW of 2 and a hydrocarbon to hydrogen ratio of 6:1. The catalyst is 0.3wt% to 0.5wt% platinum on a high surface area γ-Al_2O_3 support promoted with 1wt% chlorine. The two components of the catalyst perform the major reactions independently. Platinum is the site for dehydrogenation and the promoted alumina the site for isomerization. The loading of the platinum is a compromise, balancing the dehydrogenation activity of the catalyst and the basic cost of metal. Ideally the platinum is atomically dispersed. The loading of chlorine is set to achieve the correct balance of isomerization and cracking activity over the Lewis acid sites. Cracking to carbon can occur at both the platinum and the alumina surface. This limits the life of the catalyst and necessitates the use of higher pressure and higher hydrogen:hydrocarbon ratios than are theoretically required. Improvements in catalyst life and reduction in operating severity have been achieved by the incorporation of a second metal component, such as rhenium or germanium. The catalyst lifetime has also been extended by the introduction of rejuvenation so that a single charge of catalyst can now be used for many years. The deactivating carbon is initially burnt off the catalyst for which the term regeneration was coined. However, this also causes sintering of the platinum. Rejuvenation redistributes the platinum over the alumina and readjusts the chlorine level by treatment with water, chlorine and oxygen. The high yield of aromatics in catalytic reformer product streams makes them key sources of aromatics for chemical feedstocks as well as major components of gasoline [T. Edmonds, 1981].

1.3. Catalysts for Aromatization

1.3.1. Non-acidic catalysts

There are a large number of catalysts which have been reported to be active for aromatization of alkanes and alkenes containing six carbon atoms or more. The reaction proceeds via dehydrogenation and cyclization of the feedstock to aromatic hydrocarbons. The aromatization of alkanes is thermodynamically unfavourable at moderate temperatures. However, due to the stability of the aromatic ring, this unfavourable equilibrium can be displaced almost quantitatively in favour of the aromatic hydrocarbons at temperatures above 300°C, provided a suitable catalyst for ring closure is employed.

Two types of catalysts can be used for the aromatization reaction: reduced metals and metal oxides. The reduced metals are those of Group VIII in the periodic table, preferable nickel or platinum deposited on supports such as alumina, silica or activated carbon. The metal oxides used for the aromatization reaction are mainly chromia, molybdena, or vanadia. The oxides undergo rapid deactivation, however those oxides that are deposited on alumina by impregnation are reported to be more resistant to deactivation[Pines et al, 1981].

Zinc oxide is reported to be active towards alkene isomerization and dehydroaromatization. Dehydroaromatization of propene can be performed at temperatures up to 800°C. No activity from ethene aromatization was observed. A selectivity of 68.6% to benzene was reported using propene as feedstock [Spinicci and Tofanari, 1988, 1981]. The addition of zinc cations to borosilicate increases selectivity towards aromatics to 74%, however rapid deactivation of the catalyst is reported [Ono et al. 1987].

The oxidative dehydrodimerization of propene to 1,5-hexadiene and benzene over a Bi_2O_3-La_2O_3 catalyst has been reported [Cosimo et al. 1986]. The reaction proceeds through a catalyst reduction/oxidation cycle with a rate limiting hydrogen atom abstraction step on the catalyst surface. Dimerization of two allyl radicals results in 1,5-hexadiene from which subsequent dehydrocyclization and aromatization results in benzene.

Pt/KL exhibits higher activity and selectivity towards converting n-hexane to benzene than other platinum containing catalysts. Benzene is formed as a primary product by 1,6-ring closure and methylcyclopentane as a secondary product by 1,5-ring closure of n-hexane. The non-acidic L zeolite is monofunctional having only a platinum metal function. The absence of acid cracking reactions results in high liquid yields. The high selectivity towards benzene can be explained by the geometry of the zeolite support as well as the related influences of cations on the electronic state of platinum. Selectivities to benzene are *ca.* 82% at a conversion of 98% for n-hexane. Activity was reported to decrease after about 60 hours on stream [Lane et al. 1991; Katsumo and Sugimoto 1991; Tauser and Steger 1990]

Te/NaX zeolite catalysts can react with alkanes to form aromatics via dehydrocyclization, isomerization and hydrogenolysis pathways. Dehydrocyclization of n-heptane occurs by sequential dehydrogenation of the alkane to a heptatriene, followed by a gas phase cyclization. Thermal cracking results in the formation of C_1-C_6 products for n-heptane aromatization.

1.3.2. Acidic catalysts

These catalysts have the advantage that they can handle a wide range of feedstocks. In particular they can aromatize hydrocarbon feed with less than six carbon atoms. The most important acidic catalyst for aromatization is H-ZSM-5, which has shape-selective properties which retard coke formation as well as hydrogen transfer properties which facilitate aromatization.

$AlPO_4$-11, an intermediate pore-size molecular sieve, is reported to be active for light alkene aromatization [Norval et al. 1988; Bhatia and Phillips 1988]. Aromatization was performed with reaction temperatures between 400°C and 600°C. The selectivity to aromatics was much lower than that observed over H-ZSM-5 and was attributed to the weak acidity of $AlPO_4$-11. The aromatization mechanism is reported to proceed via an initial partial dehydrogenation to a diene which then participates in a Diels-Alder type dimerization step. $AlPO_4$-11 is a shape selective oligomerization catalyst with low activity towards aromatization reactions due to its weak acidity.

1.3.3. Bifunctional Catalysts

Bifunctional catalysts are necessary to convert LPG into aromatics [Guisnet and Gnep, 1992]. These are essentially acid catalysts with a metal dehydrogenating function.

Platinum on alumina is the historic catalyst for increasing the aromatic yields of light naphthas in the Platforming process as has been previously discussed. The introduction of platinum and rhenium decreases coke formation and increases selectivity to aromatic compounds. The addition of sulphur is reported to increase aromatic yields by selectively poisoning the hydrogenating activity of Pt-Re, hence increasing selectivity to benzene but also increasing the rate of coke formation [Parera et al. 1986]. Chromia/alumina catalysts are reported to exhibit aromatization activity due to co-ordinately unsaturated Cr^{+3} ions [Grunert et al. 1986].

Dimerization and cyclization of 1-butene on tellurium loaded Y-zeolites resulted in a 60% selectivity towards monoaromatic compounds at 475°C at low conversion. Cyclization occurs on acid sites and the reaction proceeds via a Diels-Alder addition [Hungenburg 1981]. Aromatics formation over zinc containing Y zeolites resulted in a high rate of coke formation [Arroyo et al. 1991].

Catalytic reactions of propene on PtFe/SiO2 include hydrogenation, cracking, and dimerization of propene to form benzene. On iron rich catalysts the selectivity towards benzene formation is high, while on platinum rich catalysts methane formation is the main reaction [Guczi et al. 1980].

H-ZSM-5 has been most widely used in research into producing an aromatization catalyst which will have industrial applications. Various metals have been added to ZSM-5 to improve aromatic selectivities. These include zinc, platinum, gallium and copper. Product distributions of several ZSM-5 catalysts are tabulated in Table 1.4.

Table 1.4 Product selectivity for propene and 1-butene aromatization

	Propene		1-Butene	
	H-ZSM-5	Zn-ZSM-5	H-ZSM-5	Zn-ZSM-5
Conversion	94	97	93	99
BTX	43	68	36	77
C_1 & C_2	6	14	5	10
$C_2=$	6	3	8	2
C_3	28	9	27	5
$C_3=$	0	0	9	2
C_4's & $C_4=$'s	12	3	10	2
C_6+	2	0	3	0
B	8	19	7	17
T	20	29	16	27
X & EtB	15	18	13	26
C_9+ aromatics	3	4	3	9

T=500°C, WHSV 5.4g.hour.mol^{-1}, [Ono et al., 1987]

1.4. Characteristics of H-ZSM-5

A summary of the structure and synthesis of ZSM-5 will be discussed below along with some of the reactions catalyzed by this unique zeolite.

1.4.1. Structure of ZSM-5

ZSM-5 is a member of the MFI class of pentasil zeolites.The structure of ZSM-5 is constituted by eight 5-membered rings which form the basic building blocks. The structural building unit (SBU) of ZSM-5 is the 5-1 unit which may combine to form a chain (Figure 1.2). These chains may in turn be linked to give rise to the three dimensional network characteristic of ZSM-5 i.e. a series of sinusoidal and straight channels that intersect each other at right angles.

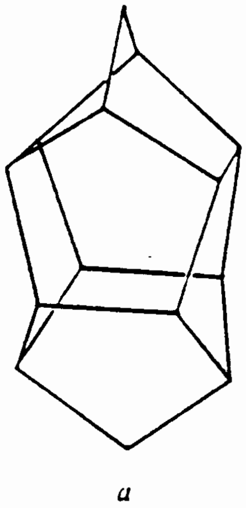

a) Building block of ZSM-5

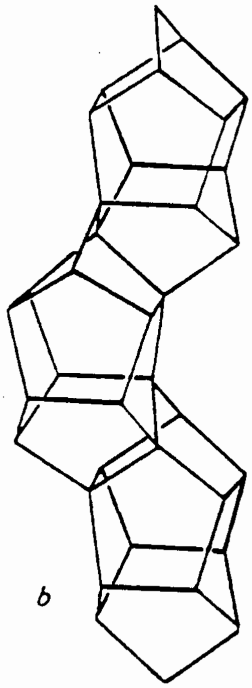

b) Chain of building blocks

Figure 1.2 SBU of ZSM-5

The openings of the straight channels have elliptical cross-sections, while those of the sinusoidal channels have a nearly circular cross-section. The dimensions of the channels are 5.3Å x 5.6Å and 5.1Å x 5.5Å respectively. The channel system thus formed gives rise to the shape selective properties of ZSM-5 (Figure 1.3).

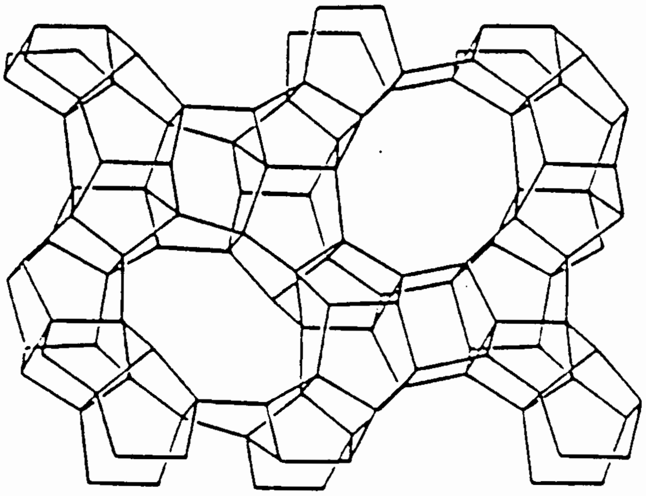
a) Straight channels

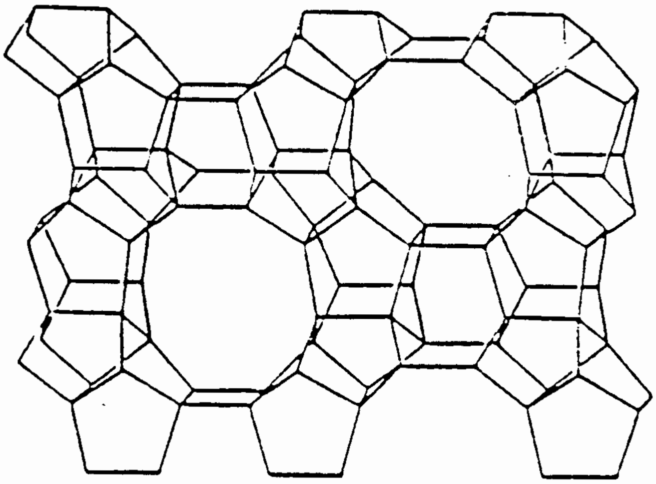
b) Sinusoidal channels

Figure 1.3 Pore system of ZSM-5

A selection of crystallographic data for ZSM-5 is shown in Table 1.5.

Table 1.5 Crystallographic data for ZSM-5

Symmetry of structure	$4_l m2(D_{2d})$
Space group	Pnma
Crystal system	orthorombic or monoclinic
Lattice constants	a = 20.1Å b = 19.9Å c = 13.4Å
Unit cell formula	$Na_nAl_nSi_{96-n}O_{192}\cdot \simeq 16H_2O$ $n < 27$ typically $n \simeq 3$
Framework density of (Si + Al)/1000Å^3	17.9

1.4.2. Synthesis of ZSM-5

The classical synthesis with tetrapropylammonium bromide (TPABr) is discussed briefly below. The synthesis takes place in water and with a relatively high concentration of silica.

There are two types of mechanisms described in the literature. The first is a liquid phase ion transportation, and is ascribed to the synthesis of Argauer and Landolt (1972). The mechanism is a classical nucleation-growth mechanism, in which silica dissolves slowly in the very alkaline synthesis mixture, and silicate monomers are formed by depolymerization-hydration. Aluminium is present as $Al(OH)_4^-$ entities and a hydrous aluminosilicate sol is formed.The gel phase formed from the sol is initially Al rich due to the low concentration of silicate monomers formed by the slow depolymerization of the silica source. The TPA^+ ions, which bring about nucleation order monomeric silicate species into the building blocks of ZSM-5. Crystal growth of the nuclei occurs at the expense of silicate entities in solution and as these are used up, the gels and sols dissolve and Al is incorporated. This gives rise to a Si rich core and an Al rich rim.

The second mechanism is ascribed to a synthesis by Chen et al. (1978). The silica source in this synthesis is waterglass, a sodiumsilicate solution. The silica is present in the form of monomers in equilibrium with silicate polymers. Depolymerization of the silica is therefore not a limiting factor. The synthesis mixture produces a hydrous aluminosilicate gel from predominantly silicate and aluminate monomers, as well as TPA species. It is the mainly monomeric nature of the reacting species that allows the formation of a very homogeneous gel which has a Si/Al similar to that of the reaction mixture. Nucleation is very fast and a large number of nuclei are formed due to the large concentration of silicate and aluminate monomers in close contact with TPA.

1.4.3. Ion exchange

All univalent ions can achieve 100% exchange in ZSM-5. The thermodynamic affinity for exchange for ZSM-5 with a SiO_2/Al_2O_3 ratio of 78 is: $Cs > Rb = NH_4 = H_3O > K > Na > Li$. Multivalent ions are unable to achieve 100% exchange in this structure. Organic ions have exceptionally high selectivities, with full capacity exchange readily attained for all organic ions except those that are larger than the 10-member-ring openings in the structure.

1.4.4. Catalytic properties of ZSM-5

ZSM-5, in its protonated form, designated by H-ZSM-5, is a medium pore-size solid acid catalyst. The types of reactions that can be carried out over ZSM-5 depend on the acidity of the catalyst, which is in turn determined by its Si/Al ratio. It has been studied for alkylation, oligomerization, MTG and disproportionation reactions. ZSM-5 has important industrial applications due to the low rate at which coking occurs. This is a result of the pore system of the zeolite which limits the formation of polynuclear coke precursors. In fact it is the so-called shape selective properties that give ZSM-5 many of its unique catalytic properties. The aromatization of light alkenes becomes significant at temperatures at about 370°C, while the aromatization of alkanes requires temperatures at about 450°C-475°C [Scurrell 1987]. BTX formation is accompanied by the production of light alkanes and alkenes.

1.5. Mechanism for Aromatization on H-ZSM-5

The mechanism for aromatization of liquified petroleum gas (LPG) on H-ZSM-5 has been widely studied [Kitagawa et al. 1985, 1986; Anderson et al. 1985; Gnep et al. 1987; Scurrell 1988; Bandiera 1990]. The mechanism for propane aromatization will now be discussed in some detail.

1.5.1 Propane transformation on H-ZSM-5

The reaction scheme for this reaction is now well established and is shown in Figure 1.4.

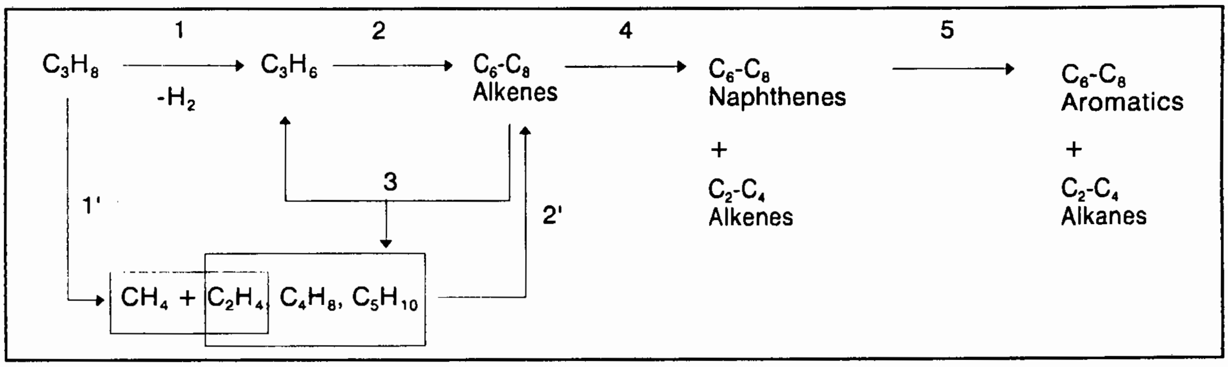

Figure 1.4 Mechanism of propane aromatization on H-ZSM-5

The primary products are propene (and hydrogen) and methane and ethylene in equimolar amounts. These compounds are formed through protolysis of C-H and C-C bonds as shown in (a) and (b) below:

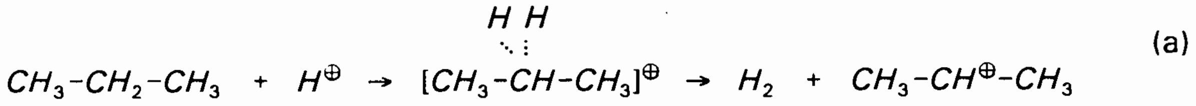

$$CH_3\text{-}CH_2\text{-}CH_3 + H^{\oplus} \rightarrow [CH_3\text{-}\overset{H\,H}{CH}\text{-}CH_3]^{\oplus} \rightarrow H_2 + CH_3\text{-}CH^{\oplus}\text{-}CH_3 \qquad \text{(a)}$$

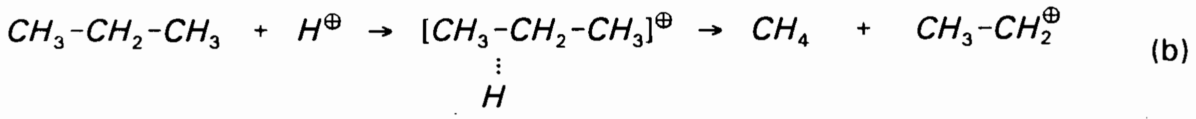

$$CH_3\text{-}CH_2\text{-}CH_3 + H^{\oplus} \rightarrow [CH_3\text{-}\underset{H}{CH_2}\text{-}CH_3]^{\oplus} \rightarrow CH_4 + CH_3\text{-}CH_2^{\oplus} \qquad \text{(b)}$$

These carbenium ion intermediates, proposed in order to explain the reactions of alkanes in superacid medium, would be responsible for the initiation step of alkane transformation with acid catalysts at high temperature [Haag et al. 1984; Planelles et al. 1985; Hall et al. 1988, 1990]. On H-ZSM-5 cracking is faster that dehydrogenation and the ratio of cracking to dehydrogenation is close to 2.5 no matter what the Si/Al ratio [Guisnet and Gnep, 1992].

Propene and ethene resulting from reaction 1 and 1′ oligomerize, these oligomers crack to C_2-C_5 alkenes or undergo cyclization followed by aromatization. The C_2-C_5 alkenes react with propene or ethylene to form C_6-C_8 alkene oligomers, which can be cracked or transformed into aromatics. Under the same conditions, propene leads to the same products as propane but more rapidly (about 500 times at 350°C). It can thus be concluded that the formation of olefinic compounds from dehydrogenation and cracking of propane is the limiting step of propane aromatization. Ethene, butenes and C_{5+} are the primary products of propene transformation. These alkenes undergo secondary transformations leading to C_6-C_8 aromatics and to C_2-C_4 alkanes. Whatever the conversion there are, as a result of hydrogen transfer, about 3 mole of alkanes formed per mole of aromatics.

Reactions 2-5 occur through carbenium ion intermediates. The mechanisms of reactions 2,2′ and 3 are well-known. Thus the reaction of propene with butene (reaction 2′) involves three steps.

$$\text{C-C=C-C} + \text{H}^{\oplus} \rightarrow \text{C-C}^{\oplus}\text{-C-C} \qquad \text{...(c)}$$

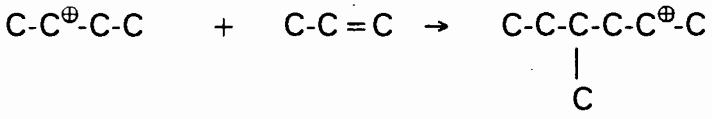

$$\text{C-C}^{\oplus}\text{-C-C} + \text{C-C=C} \rightarrow \text{C-C-}\underset{\underset{\text{C}}{|}}{\text{C}}\text{-C-C}^{\oplus}\text{-C} \qquad \text{...(d)}$$

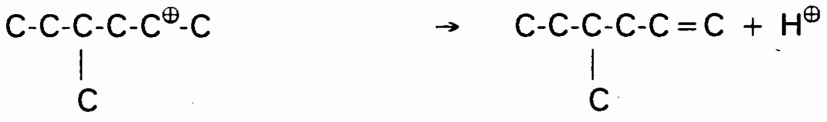

$$\text{C-C-}\underset{\underset{\text{C}}{|}}{\text{C}}\text{-C-C}^{\oplus}\text{-C} \rightarrow \text{C-C-}\underset{\underset{\text{C}}{|}}{\text{C}}\text{-C-C=C} + \text{H}^{\oplus} \qquad \text{...(e)}$$

Cracking of methylhexenes is obviously the opposite reaction. The cyclization reaction is more complex, as it involves first the formation of an alkenyl carbenium ion through a hydride transfer reaction:

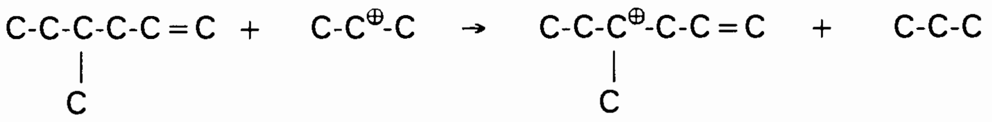

$$\text{C-C-}\underset{\underset{\text{C}}{|}}{\text{C}}\text{-C-C=C} + \text{C-C}^{\oplus}\text{-C} \rightarrow \text{C-C-}\underset{\underset{\text{C}}{|}}{\text{C}^{\oplus}}\text{-C-C=C} + \text{C-C-C} \qquad \text{..(f)}$$

The isomerization of carbenium ions through hydride shift is very fast, thus all the carbenium ions with a methylhexenyl skeleton are rapidly converted in the thermodynamic equilibrium mixture. Depending on the alkenyl carbenium ion the cyclization can lead to a five membered or six membered ring.

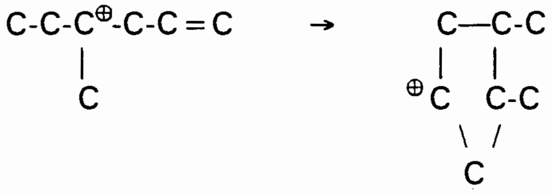

...(g)

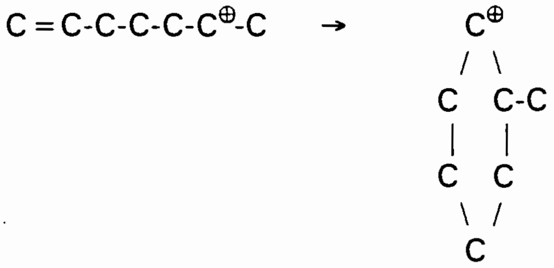

...(h)

In the first case an isomerization step, through a protonated cyclopropane intermediate allows the formation of a six membered ring [Gnep et al. 1987]. The direct cyclization into a six-membered ring is excluded in the case of olefinic C_6 carbenium ions as it would require the formation of an unstable primary carbenium ion. Reaction 5 is the transformation of cyclohexyl-carbenium ions into a benzenic compound through hydrogen transfer reactions. While these hydrogen transfer reactions allow the formation of aromatic compounds from propane, they lead unfortunately to the reactant (propane) and other alkanes. These alkanes must be cracked dehydrogenated and/or cracked into alkenes through reaction 1. As the alkanes, especially ethane and methane, are relatively unreactive, this limits the aromatization process.

1.6. The Effect of a Dehydrogenating component on ZSM-5

Of a wide variety of hydrogenating components tested, gallium and zinc seem to give the best results. Gallium containing ZSM-5 catalysts were preferred industrially as zinc was lost as a result of its volatility. However various bimetallic hydrogenating components could also be used e.g. Zr_2Fe [Chetina et al. 1992].

1.6.1. Platinum

Platinum and palladium are often chosen as the hydrodehydrogenation components of bifunctional zeolite catalysts used in industrial processes. Pt/H-ZSM-5 catalysts have been tried in propane aromatization but their stability and selectivity are not satisfactory. Platinum increases the rate of propane transformation. The activity increases at first with increase in platinum content, but then remains practically constant for platinum content >0.5wt%. Deactivation is faster on Pt/H-ZSM-5 than with H-ZSM-5. The product distribution is different from that found on H-ZSM-5 for propane conversion, the main differences being:

i. Propene becomes the main primary product.
ii. Other alkenyl compounds are formed only in very small amounts
iii. The selectivity for methane is lower on Pt/H-ZSM-5 for conversions below 80%, but greater for higher conversions.
iv. The product distribution of aromatics are 10% benzene, 45% toluene and 45% C_8 aromatics on Pt/H-ZSM-5, against 25% benzene, 50% toluene and 25% C_8 aromatics on H-ZSM-5. The yields of aromatics at the same conversion of propane on H-ZSM-5 and Pt/H-ZSM-5 are similar.

The aromatization of propane proceeds by a bifunctional pathway. Platinum sites dehydrogenate propane to propene and the naphthene intermediates to aromatics while the acid sites catalyze the oligomerization of propene and the cyclization of the oligomers. The deactivation of these catalysts is mainly due to the formation of coke. It is reported that it is probably the greater rate of coke formation on Pt/H-ZSM-5 which causes these catalysts to deactivate more rapidly than H-ZSM-5

[Gnep et al. 1987]. Pt/H-ZSM-5 catalysts are no more suitable than H-ZSM-5 for propane aromatization. While their initial activity is greater, their stability is lower. Moreover, at high conversions the production of methane and ethane, which cannot be recycled, is very significant. The addition of copper, tin, gallium or iridium to platinum limits the hydrogenolysis activity of platinum and thus improves selectivity to aromatics [Inui et al. 1989, Romera et al. 1990, Scire et al. 1989, Maggiore et al. 1991].

1.6.2. Zinc

Zinc is an effective promoter and can be added by ion exchange or by impregnation. The preferred method is by ion exchange on NH_4-ZSM-5 using zinc nitrate solution followed by calcination. Effective promotion has been claimed for zinc levels of 0.4wt% to 2wt% with typical values being around 1wt% [Sneddon 1990]. For zeolites with a Si/Al ratio of 40, this is well below the ion exchange capacity of the zeolite, assuming exchange is via doubly charged zinc cations. However, under the reducing conditions of alkane conversion, zinc is slowly eluted from the catalyst. The conversion of alkanes to aromatics results in strongly reducing reaction conditions because hydrogen is produced in the first step of the reaction as well as the formation of coke which also produces hydrogen. The following sources can be referenced for additional information on the use of zinc as a promoter for hydrocarbon aromatization [Le Van Mao et al. 1986, Roessner et al. 1992, Osaka et al. 1992, Kanai and Kawata 1988, Mole and Anderson 1985].

1.7. Chemistry of Gallium

1.7.1. Discovery and Distribution

Gallium is one of the rarest of the elements, occurring widely distributed, but only in very minute quantities. Gallium was discovered in 1875 by the French Chemist Lecoq de Boisbaudran who named it gallium in honour of his native France. The metal was detected by spectroscopic means. He later isolated over a gram a gallium from several hundred kilograms of zincblende.

1.7.2. Industrial Uses

The uses of gallium are restricted by price. The most important use is in intermetallic compounds (particularly with As, Sb, or P) for use in semiconductors. Intermetallic compounds with gallium have application as high-temperature rectifiers and transistors, solar batteries and other devices where the photovoltaic effect can be used. On account of its low vapour pressure, the metal is used in liquid seals for vacuum apparatus. Gallium is also used as an activator in glowing paints. The absorbtion of ^{72}Ga by bone leads to its use in the diagnosis of bone cancer.

1.7.3. Toxicity

The toxicity of compounds due to their gallium content is low, it depends on the type of compound and the means of administration. Individuals exposed to gallium compounds during the production of the metal suffered from tooth decay, pains in joints and bones, nervous and gastrointestinal disorders, heart pains and general debility.

1.7.4. Physical properties of gallium metal

Gallium is a greyish metal with a colour resembling that of steel. Gallium is hard with a low malleability. It has a low melting point, although its vapour pressure is extremely low. Some of the physical properties of gallium metal are summarized in Table 1.6.

Table 1.6 Physical properties of gallium [Bailar 1973]

Melting point	30.15°C	
Boiling point	2403°C	
Natural isotopes	^{69}Ga (60.5%)	^{71}Ga (39.5%)
Standard reduction potential	-0.52V	
Atomic radius	1.53Å	
Ionic radius	0.62Å	
Density	5.904 g/cm^3	
Molar enthalpy of vapourization	5.29 kJ/mol	
Molar heat capacity	25.86 kJ/mol	
Pauling electronegativity	1.8	
Electrical resistivity	17.4 10^{-8} Ω.m	
Thermal conductivity	40.6 W/m.K	
Abundance	18 ppm	
Spectroscopic identification	2944Å	2874Å

1.7.5. Physical properties of gallium oxides

Gallium(III) oxide is formed on heating gallium in dry air or by thermally decomposing gallium nitrate or hydroxide at 200°C to 250°C. Of the five modifications $\alpha,\beta,\gamma,\delta$ and ϵ, the β form is the most stable. The others are converted into it at temperatures above 1000°C. It can be reduced at 600°C to the metal with hydrogen or carbon monoxide. With moderate heating it dissolves in dilute mineral acids. After heating to redness, Ga_2O_3 is insoluble in these acids, concentrated nitric acid and aqueous alkalis. At high temperatures the oxide GaO has been detected spectroscopically. At 500°C *in vacuo* gallium metal reduces Ga_2O_3 to Ga_2O, which sublimes on the cooler parts of the container as a dark brown powder. Above 700°C *in vacuo,* it disproportionates to Ga_2O_3 and Ga. It is stable in dry air. Ga_2O is a strong reducing agent and is oxidized to Ga_2O_3 by permanganate or on heating in air.

Some of the physical properties of β-Ga_2O_3 are summarized in the Table 1.7.

Table 1.7 Physical properties of β-Ga_2O_3 [Bailar 1973]

Melting point	1740 ± 20°C	
$\Delta H_{sublimation}$	527kJ/mole	
$\Delta S_{sublimation,298K}$	205kJ/mole.deg	
Vapour pressure at 550°C	$3.4x10^{-23}$kPa	
Heat capacity equation	$111.1 + 32x10^{-3}T - 24.4x10^{5}T^{-2}$ J/mole.deg	
ΔH_f^o	-1089kJ/mole	
ΔG_f^o	-998kcJ/mole	
Density	$5.88g/cm^3$	
Crystal structure	monoclinic	
Infrared absorbtion	$696.8cm^{-1}$ (strong)	$740.7cm^{-1}$ (medium)

1.8. The Effect of Gallium

1.8.1. Catalytic effect of gallium

As has been previously stated, there are four methods by which gallium can be incorporated into ZSM-5, viz. ion-exchange and impregnation with gallium salts, physical mixing with gallium oxide and by the synthesis of gallosilicates. The first three methods are post synthesis modifications of ZSM-5 with gallium, while the synthesis of gallosilicates and galloaluminosilicates with a MFI structure are produced by the last method.

It was shown [Kitagawa et al. 1986] that the total conversion (of the feed) and the selectivity to aromatics of gallium exchanged H-ZSM-5 catalysts increase sharply until the gallium content reaches the value corresponding to a degree of ion exchange of 100%. Further increase in gallium content causes only a slight increase in conversion and selectivity to aromatics. Ga^{+3} cations are reported to be the most effective gallium species for aromatization, and the role of gallium would be to increase the rate of aromatization of the lower alkenes. These species would not play any role in the activation of propane to propene.

However these results have recently been questioned [Gnep et al. 1987] as the conversion and selectivity to aromatics are generally found to increase well above the value corresponding to maximum theoretical exchange. Similarly there is probably no exchange of the protonic sites since the acidities of H-ZSM-5 and Ga/H-ZSM-5 are identical. Gallium was reported, however, to increase the rate limiting step of propane conversion, i.e. dehydrogenation of propane to propene. The initial rate of propene formation is four times higher on H-ZSM-5 impregnated with 6wt% gallium. Gallium also has an effect on the rate and selectivity of aromatics formation from the lower alkenes. It was thus suggested [Gnep 1987] that propane aromatization on Ga/H-ZSM-5 catalysts occurs via a bifunctional process whereby gallium species dehydrogenate propane into propene and the naphthene intermediates into aromatics. The acid sites catalyze oligomerization of propene and cyclization of oligomers. Aromatics formation occurs more rapidly on gallium species (dehydrogenation of naphthenes) than on acid sites (hydrogen transfer from naphthenes to light alkenes). Indeed for propene conversion on Ga/H-ZSM-5 the production of 1 mole of aromatic products is accompanied by the liberation of 1.8 moles of hydrogen. No hydrogen is formed on H-ZSM-5 [Guisnet and Gnep 1992].

Under the conditions of propane aromatization, Ga_2O_3 (without ZSM-5) catalyzes the dehydrogenation of propane into propene and of methylcyclohexene into toluene, but is practically inactive in 1-hexene, 1-heptene and methylcyclohexane aromatization [Gnep et al. 1989]. 1-Hexene and 1-heptene are rapidly isomerized and cracked. It was thus concluded that gallium species do no play a significant role in the cyclization step and that on Ga/H-ZSM-5 catalysts the cyclization occurs primarily through an acid mechanism as on H-ZSM-5.

However these results were partially contradicted in a different study whereby Ga_2O_3 (also without ZSM-5) was observed to rapidly and selectively transform 1-hexene and hexadiene into aromatics with virtually no cracking products

[Meriaudeau et al. 1989]. Cyclohexene and cyclohexadiene, but no cyclohexane were observed in the product spectrum of 1-hexene transformation, which shows cyclization proceeds via hexadiene and hexatriene intermediates and not directly from 1-hexene. The authors concluded that Ga_2O_3 dehydrogenates C_6-C_8 alkenes into dienes and trienes. The trienes are cyclized through a non-catalytic gas phase reaction [Le van Mao et al. 1989].

However, on Ga/H-ZSM-5, the formation of naphthenes proceeds mainly through cyclization on acid sites of dienes resulting from alkene dehydrogenation on gallium species [Meriaudeau and Naccache 1991]. Thus to summarize, the mechanism whereby C_6-C_8 alkenes are cyclized to naphthenes differ only in the mode of formation of the alkenyl carbenium ion on which cyclization occurs. Gnep et al. [1989] proposes direct formation through hydrogen transfer on the acid sites (a), while Meriaudeau and Naccache [1991]. propose dehydrogenation on the gallium species then protonation of the diene on the acid sites (b).

$$C_nH_{2n} \xrightarrow{R^\oplus, -R} (C_nH_{2n-1})^\oplus \qquad (a)$$

$$C_nH_{2n} \xrightarrow[-H_2]{Ga} C_nH_{2n-2} \xrightarrow{H^\oplus} (C_nH_{2n-1})^\oplus \qquad (b)$$

The differences between the selectivities of hexene transformation on Ga_2O_3, isomerization and cracking according to Gnep et al. [1989] and isomerization and aromatization according to Meriaudeau and Naccache [1991], could be due to differences in the operating conditions and in the Ga_2O_3 samples [Guisnet and Gnep 1992].

The two modes of cyclization coexist on Ga/H-ZSM-5 catalysts, with their relative activity depending on the number and strength of the acid sites as well as the amount and activity of the gallium species. It can thus be concluded that aromatization of propane on Ga/H-ZSM-5 catalysts occurs via bifunctional catalysis. The gallium species catalyze dehydrogenation of propane into propene and of naphthenes into aromatics. They probably are also active in a small way for cyclization reactions by dehydrogenating the C_6-C_9 alkenes into dienes. The acid sites catalyze the oligomerization of light alkenes and the cyclization of C_6-C_9 alkenes. The main unwanted reactions, cracking of alkanes via carbenium ion intermediates and hydrogen transfer reactions, occur on acid sites [Guisnet and Gnep 1992].

It must be emphasized that the bifunctional process requires not only the reactions on the acid sites and on the gallium species but also the diffusion of the intermediate species between acid sites and gallium species.

1.8.2. Hydrogen back spillover

Another reaction pathway was proposed whereby the gallium species would have no dehydrogenation or hydrogenation activity and their main role would be to favour the removal of the hydrogen species released by the zeolitic acid sites [Le Van Mao et al. 1991, 1990, 1986; Inui et al. 1989]. This concept is known as hydrogen back spillover. However experiments with Ga_2O_3 show that gallium species have a dehydrogenating activity as has been discussed above. Hydrogen back spillover was proposed to explain the great aromatization activity of hybrid catalysts in which the gallium species were far from the zeolite acid sites (order of μm). Hybrid catalysts constituted by a mechanical mixture of H-ZSM-5 and co-precipitate of gallium and silica oxides embedded within a clay matrix were more active for butane aromatization than gallium impregnated H-ZSM-5 [Le Van Mao and Yao 1991].

The large distance between the gallium species and the zeolite acid sites does not, however, allow the exclusion of the possibility of a bifunctional mechanism even if the diffusion of the intermediate species does become the limiting step. It was concluded that aromatization occurs mainly through bifunctional catalysis on Ga/H-ZSM-5 catalysts in which gallium species and zeolite acid sites are adjacent to each other, while hydrogen back spillover would be mainly responsible for the great aromatization activity of hybrid catalysts [Guisnet et al. 1992].

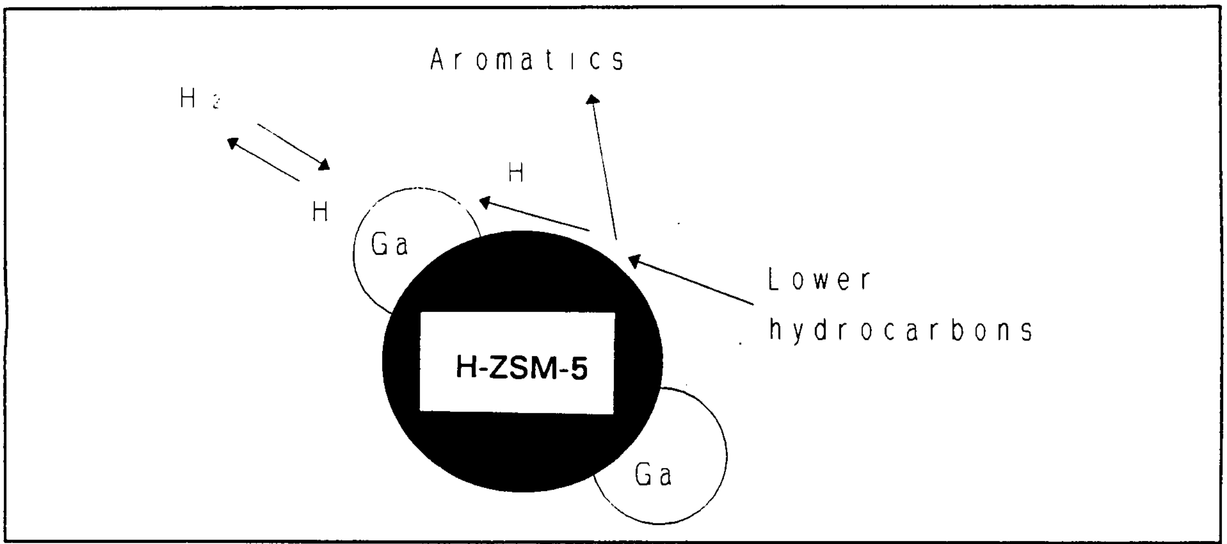

Figure 1.5 Schematic diagram of hydrogen back spillover

1.8.3. Mechanism of propane dehydrogenation on gallium species

The mechanism for propane transformation is shown in Figure 1.6.

Aromatization Process

$$\begin{tikzcd}
C_3H_8 \arrow[r, "Ga"] & C_3H_6 \arrow[r, "H^+"] & \begin{array}{c}C_6\text{-}C_8\\ \text{Alkenes}\end{array} \arrow[r, "{H^+,Ga}"] \arrow[d, shift left, "H^+"] & \begin{array}{c}C_6\text{-}C_8\\ \text{Dienes}\end{array} \arrow[r, "H^+"] & \begin{array}{c}C_6\text{-}C_8\\ \text{Naphthenes}\end{array} \arrow[r, "Ga"] & \begin{array}{c}C_6\text{-}C_8\\ \text{Aromatics}\end{array} \\
 & & \begin{array}{c}C_2\text{-}C_5\\ \text{Alkenes}\end{array} \arrow[u, shift left] & & &
\end{tikzcd}$$

Secondary Reactions

On acid sites:

$$C_3H_8 \xrightarrow{H^+} C_2H_4 + CH_4 \ (C_3H_6 + H_2)$$

Hydrogen transfer

$$\begin{array}{c}C_6\text{-}C_8\\ \text{Naphthenes}\end{array} + \begin{array}{c}C_2\text{-}C_5\\ \text{Alkenes}\end{array} \longrightarrow \begin{array}{c}C_6\text{-}C_8\\ \text{Aromatics}\end{array} + \begin{array}{c}C_2\text{-}C_5\\ \text{Alkanes}\end{array}$$

Figure 1.6 Mechanism of propane aromatization on Ga/H-ZSM-5

The dehydrogenating activity of gallium is greatly improved by the protonic acid sites of H-ZSM-5. The rate of propane dehydrogenation is 200 times higher on gallium impregnated H-ZSM-5 than on gallium impregnated Na-ZSM-5 [Meriaudeau and Naccache 1990]. Moreover the dehydrogenating activity of the sodium exchanged Ga/H-ZSM-5 decreased by a factor of 80, while proton exchange of Ga/Na-ZSM-5 increased by 150 its dehydrogenating activity. A bifunctional mechanism was proposed. The steps involve:

(i) dissociative adsorption of propane with formation of gallium hydride and gallium alkoxide species;
(ii) rapid exchange of the propyl carbenium ions with zeolite protons through an alkyl surface migration reaction;
(iii) desorption of propene from the zeolite;
(iv)- The role of the protonic sites would be to bypass the slow direct transformation of gallium alkoxide species into a gallium hydroxide species;

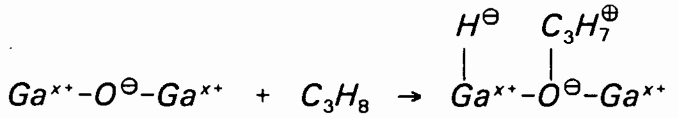

$$Ga^{x+}\text{-}O^{\ominus}\text{-}Ga^{x+} + C_3H_8 \rightarrow \overset{H^{\ominus}}{\overset{|}{Ga^{x+}}}\text{-}\overset{C_3H_7^{\oplus}}{\overset{|}{O^{\ominus}}}\text{-}Ga^{x+} \qquad \ldots(i)$$

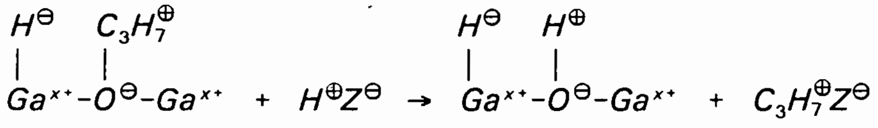

$$\overset{H^{\ominus}}{\overset{|}{Ga^{x+}}}\text{-}\overset{C_3H_7^{\oplus}}{\overset{|}{O^{\ominus}}}\text{-}Ga^{x+} + H^{\oplus}Z^{\ominus} \rightarrow \overset{H^{\ominus}}{\overset{|}{Ga^{x+}}}\text{-}\overset{H^{\oplus}}{\overset{|}{O^{\ominus}}}\text{-}Ga^{x+} + C_3H_7^{\oplus}Z^{\ominus} \qquad \ldots(ii)$$

$$C_3H_7^{\oplus}Z^{\ominus} \rightarrow C_3H_6 + H^{\oplus}Z^{\ominus} \qquad \ldots(iii)$$

$$GaOC_3H_7 \rightarrow GaOH + C_3H_6 \qquad \ldots(iv)$$

Two other bifunctional mechanisms were proposed to explain the positive effect the protonic sites have on the dehydrogenating activity of the gallium species. The zeolite protons combine with the hydride ions, abstracted from propane by a gallium Lewis species L, to form molecular hydrogen. The carbenium ions take the place of the protons [Bayense et al. 1991].

$$C_3H_7^{\oplus} \quad + \quad H^{\oplus}Z^{\ominus} \quad + \quad L\text{-}H \rightarrow C_3H_7^{\oplus}Z^{\ominus} \quad + \quad H_2 \quad + \quad L^{\oplus}$$

However, it was proposed [Buckles et al. 1991] that the concerted action of gallium species and of protonic sites in the initial C-H bond scission would be the rate limiting step of dehydrogenation.

$$C_3H_8 \xrightarrow{Ga} \overset{\delta^- \ \delta^+}{H\text{-}CH(CH_3)_2} \xrightarrow{H^{\oplus}Z^{\ominus}} H_2 \quad + \quad C_3H_7^{\oplus}Z^{\ominus}$$

1.8.4. Gallium active species

Gallium catalysts prepared by ion exchange or impregnation of H-ZSM-5, physical mixtures of Ga_2O_3 and H-ZSM-5 and gallosilicates or galloaluminosilicates will briefly be discussed with regard to their catalytic properties. As was previously discussed, there is probably no exchange of gallium in the zeolite and after a calcination treatment the gallium species in the catalyst prepared by ion exchange or by impregnation are most likely Ga_2O_3 deposited in the pores or on the outer surface of the zeolite crystallites. Ga_2O_3 is primarily located on the outer surface [Meriaudeau and Naccache 1991]. Ion-exchanged and impregnated catalysts and physical mixtures of Ga_2O_3 and H-ZSM-5 therefore differ only in the dispersion of Ga_2O_3 and the distance between the gallium species and the acid sites [Guisnet and Gnep 1991].

However with gallosilicates and galloaluminosilicates it is possible to compare the dehydrogenating activities of framework and extraframework species. Steaming of these MFI catalysts causes extraction of gallium from the framework and the formation of extraframework gallium species. The catalytic properties of GaMFI catalysts depend on the mode of introduction of gallium, gallium content, size of the crystallites and activation treatment. The following conclusions have been drawn:[Guisnet and Gnep 1992]

i. The exchange or the impregnation of H-ZSM-5 zeolites by gallium salts give more active catalysts than Ga_2O_3/H-ZSM-5 physical mixtures. However, the more intimate the mixture, the more active the catalyst.

ii. Deactivation by coke of GaMFI catalysts is more rapid than that of H-ZSM-5 and the Ga_2O_3/H-ZSM-5 mixtures deactivate more rapidly than the gallosilicates and galloaluminosilicates i.e. Ga_2O_3/H-ZSM-5 > GaMFI > H-ZSM-5

iii. Selectivity to aromatics is greater with MFI gallosilicates than with other gallium catalysts.

Most of these observations can be related to the fact that activities for alkane aromatization of the GaMFI catalysts are mainly determined by the protonic sites and by the gallium species, in particular by their proximity and the balance of their activities. Thus gallium impregnated H-ZSM-5 catalysts are more active than the Ga_2O_3/H-ZSM-5 mixtures, because of the closer proximity of the gallium species and the acid sites. This activity is also probably due to the better dispersion of the gallium species hence their greater dehydrogenation activity. An important fact, that has been underlined by various authors [Bayense et al. 1991; Kanai and Kawata 1989], is that the dehydrogenating activity of framework gallium atoms is much lower than the extra framework species. Extraframework gallium species are necessary to obtain an active and selective catalyst for aromatization. The positive effect of mild steaming of gallosilicates and galloaluminosilicates on aromatics selectivity can be explained by the formation of extraframework gallium species, highly active for dehydrogenation. A high dispersion of these species in the zeolite crystallites could be the main parameter governing their activity, stability and selectivity, as this determines their dehydrogenation activity and their proximity to acid sites [Guisnet and Gnep 1991].

Gallosilicates and galloaluminosilicates, when treated under the appropriate conditions to create extra framework gallium species, are the most active and selective catalysts for propane aromatization. However oxidative treatment during regeneration for coke removal can, if conditions are too severe, cause destruction of their catalytic properties. This is the reason why gallium impregnated catalysts are preferred in industrial process.

In recent literature [Dooley et al. 1992, 1993] it is reported that the Ga^{+1} species is not active for aromatization, but that the active species probably consists of a Ga^{+3} species which is stable under reaction conditions. The gallium in ion exchanged ZSM-5 can be reduced to Ga^{+1} up to a limit determined by the number of anionic framework sites. These catalysts are not as active as catalysts that have been substantially reoxidized in air or by traces of oxygen in inert gases. Reoxidation does not generate β-Ga_2O_3, but a higher energy dispersed Ga^{+3} which appears to be highly active for production of aromatics from alkanes. The following conclusions were drawn with regard to the active gallium species in H-ZSM-5 [Dooley et al. 1992, 1993]:

i. Ga/H-ZSM-5 catalysts contain Ga^{+3}/Ga^{+1} in the form of a redox pair. The extent of reduction to Ga^{+1} is limited by the availability of anionic lattice sites.
ii. Optimal catalysts for alkane aromatization are prepared by reduction with hydrogen to disperse the gallium, followed by reoxidation to a dispersed Ga^{+3} phase. In practice most of the Ga^{+3} would be in the form of $[GaO]^+$ ions, as the ultimate product of reoxidation, dispersed Ga_2O_3, is formed very slowly at 550°C
iii. A substantially reduced catalyst is both less active and selective for aromatics formation. Such catalysts show lower hydrocracking activities than either unreduced or reoxidized materials, because of the reduction in Bronsted acidity associated with the transformation to Ga^+Z^- sites.
iv. TGA studies show that $Ga(OH)_2^+$ is the exchanging ion in ion-exchanged Ga/H-ZSM-5 catalysts and that these can be reduced to Ga^+ with hydrogen.

1.8.5. Influence of activation treatments

The effect of hydrogen pretreatment on catalysts prepared by impregnation or by physical mixing of Ga_2O_3 and H-ZSM-5 will now be discussed.

After calcination gallium would be in the form Ga_2O_3 and would be located mainly on the outer surface of the catalyst crystallites. A positive effect of hydrogen pretreatment on the aromatization activity of these catalysts was observed [Changyu et al. 1988; Price and Kanazirev 1990; Kanazirev et al. 1990; Kanazirev et al. 1991]. This increased activity could be attributed to increased dehydrogenating activity of the gallium species caused by increased dispersion and or by reduction of the gallium species. TPR results and techniques for characterizing hydrogen treated samples show that following phenomena occur during hydrogen treatment of Ga/H-ZSM-5 samples:

(i) Reduction of Ga_2O_3 species
(ii) Increase in the dispersion of gallium species
(iii) Migration of gallium species within the zeolite crystallites
(iv) Exchange of protonic sites by gallium

TPR profiles of Ga/H-ZSM-5 catalysts show a small peak of hydrogen consumption at 25°C-125°C attributed to hydrogen adsorption on Ga_2O_3 and two significant peaks at 475°C-625°C and 825°C-1027°C attributed to Ga_2O_3 reduction [Petit et al. 1989, Joly et al. 1991]. The reduction of Ga_2O_3 requires the presence of acid sites. No reduction of pure Ga_2O_3 or Ga_2O_3/ NaX mixture takes place and only a very limited reduction of Ga_2O_3/silicate was observed [Price et al. 1990]. Other characteristics, gallium content, dispersion of Ga_2O_3 species, distance between Ga_2O_3 and acid sites, nature of Ga_2O_3 phase (α,β) also influence the reduction process.

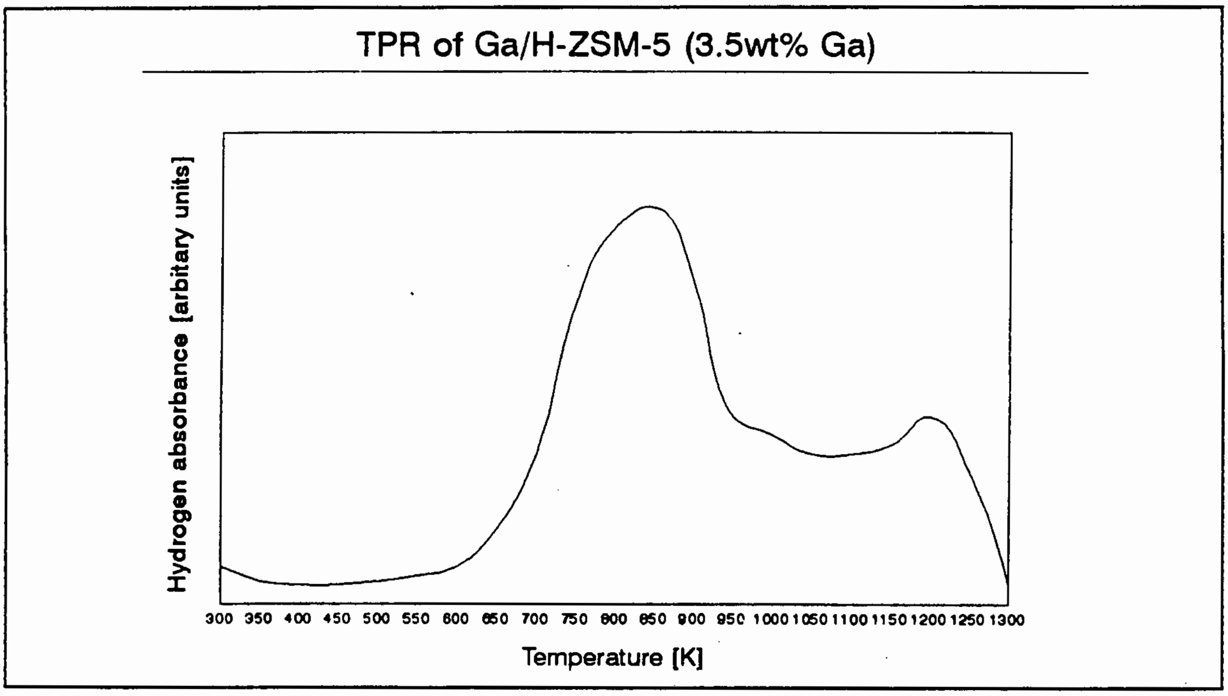

Figure 1.7 TPR of Ga/H-ZSM-5

The degree of Ga_2O_3 reduction depends on the operating conditions, particularly the temperature, gallium content and gallium/acid site ratio.

The following pathway has been proposed [Price and Kanazirev 1990] for the reduction of β-Ga_2O_3/H-ZSM-5 intimately mixed catalysts. The reduction of gallium was limited to one atom of gallium per acid site.

(i) Reduction of Ga_2O_3

$$Ga_2O_3 + 2H_2 \rightarrow Ga_2O + 2H_2O$$

(ii) Migration of Ga_2O to the acid sites

(ii) Reaction of Ga_2O with the protonic sites

$$Ga_2O + 2H^+Z^- \rightarrow 2Ga^+Z^- + H_2O$$

The migration of gallium species (Ga_2O) to the acid sites would be the limiting step and would occur through a solid state process rather than through transport of volatile gallium species [Price and Kanazirev 1990]. It must be noted that step (iii) leads to a neutralization of the zeolite protonic sites. A decrease in the number of acid OH groups was found by IR spectroscopy [Meriaudeau and Naccache

1991]. However as the protonic sites are involved in the oligomerization and cyclization steps of the bifunctional aromatization pathway, the catalytic activity should be decreased. This was not observed. Thus either the neutralization of the protonic sites or the bifunctional mechanism must be questioned.

STEM analysis of Ga/H-ZSM-5 samples before and after hydrogen reduction shows a decrease in the size of the gallium particles [Joly et al. 1991]. XPS and TEM coupled with EDX microanalysis show migration of gallium species within the zeolite crystallites. Hydrogen treatment of Ga/H-ZSM-5 improves the dispersion and nature (hence the dehydrogenating activity) of the gallium species in the catalyst. These phenomena take place even at low hydrogen partial pressures and in the range of temperatures chosen for the aromatization process. Thus the above mentioned reduction must take place during aromatization. The higher dehydrogenation activity of Ga_2O_3 in the presence of H-ZSM-5 could be simply due to the reduction of the gallium species (and to an increase in their dispersion) during propane aromatization.

It was reported [Dooley et al. 1992] that there was negligible loss of Ga_2O in pretreatments, which can be understood if the Ga_2O reacts immediately with the zeolite as proposed in the reaction scheme above. In practice even reoxidized Ga/H-ZSM-5 catalysts contain some gallium as cations ($[GaO]^+$) as the final stage of reoxidation to Ga_2O_3 is slow.

1.9. Deactivation

The main cause of deactivation of zeolites is the formation and the retention of high molecular mass secondary products inside the pores and on the outer surfaces of the crystallites. Coking and deactivation depend on the nature of the active sites on the zeolite as well as on reaction conditions such as temperature and the reactant molecules. The formation of coke at low (120°C) and high (450°C) temperatures with respect to rate of formation, the location, composition and mode of formation of the coke for the transformation of propene and toluene will be discussed below.

1.9.1. Deactivation at low temperature

At 120°C there were practically no products, besides coke which was not present in the product stream, observed during the transformation of propene and toluene over H-ZSM-5. Traces of isopropyltoluene were found for propene/toluene mixtures. A small amount of C_{12}-C_{22} oligomers were observed for propene transformation. The rate of coke formation was much faster from propene than from toluene. The maximum coke extracted after a 24hr run was 5% of the zeolite mass, however this discounts coke located inside the pores. The composition of the coke depended to a large extent on the reactant. From toluene three main families of coke were found, the components resulting from the association of 2 or 3 toluene molecules. The coke formed from propene contains C_{12} to C_{35} aliphatic compounds (b.p. 175°C-488°C, coke 9wt% of the zeolite mass), while the coke formed from propene/toluene mixtures was mono-,bi- or triisopropyltoluenes (b.p. 265°C-380°C, coke 0.5wt% of the zeolite mass) resulting from the alkylation of toluene by propene [Magnoux et al. 1992].

At this temperature there are practically no desorbed products. For propene, coke is constituted of alkanes, alkenes and cyclanes having 12 to 35 carbon atoms. These compounds result from a variety of reactions involving rearrangement and cracking of oligomers, condensation of alkenyl cracking products with propene, cyclization and hydrogen transfer between oligomers. The low density of acid sites on H-ZSM-5 and the steric constraints at their vicinity limits hydrogen transfer reactions and oligomerization of branched alkenes [Magnoux et al. 1992]. With toluene the coke component results from the condensation of 2 or 3 toluene molecules, with methyldiphenyl and triphenylmethane being formed. The formation of these compounds is slow as their formation requires strong acid sites and the steric constraints of the zeolite channels limit these bimolecular reactions.

1.9.2. Deactivation at high temperatures

At 450°C the composition of the coke is relatively independent on the reactant. The main coke components were methylpyrenes and methylfluorenes. It the case of toluene, methylphenanthrene and anthracene were also observed. Whatever the reactant the rate of coke formation is very slow. For propene and propene/toluene mixtures it is much slower than the conversion into desorbed products. The main coke components are always alkylpyrenes with the trimethylpyrenes being predominant. The other coke components are flourenic compounds. Two hypotheses can be advanced to explain the similarity between the coke formed by propene and toluene [Magnoux et al. 1992]:

(i) Alkylpyrenes and fluorenes result from the same reactions, probably between aromatic and alkenyl compounds. This is possible for propene/toluene mixtures as well as for propene, as propene is rapidly transformed into C_2-C_7 alkenes and benzenic compounds. However, this is improbable for toluene as only traces of alkenes are observed in the reaction products.

(ii) Coke components result from different reaction paths and the their formation involves different intermediates. The kinetic diameter of these intermediates is smaller than the pore apertures, hence they can desorb from the zeolite. However the desorption of certain of these intermediates is slower than their rate of transformation to bulky compounds larger than the pore apertures. Thus these bulky compounds remain sterically blocked at the channel intersections and constitute the coke components.

1.9.3 Location of the coke molecules

Whatever the reaction temperature and the reactant all the coke components are soluble in methylene chloride after dissolution of the zeolite in hydroflouric solution. However more than 95% of the coke cannot be recovered by a 24 hour soxhlet treatment of the coked zeolite by methylene chloride [Magnoux et al. 1992]. This shows that the coke molecules are blocked inside the pores.

The coke molecules formed at low temperatures from propene are aliphatic hydrocarbons (C_{12}-C_{35}) with a limited degree of branching. The kinetic diameter of the compounds is less than 5Å with a length of 10Å-35Å. They are thus located in the channels (the distance between two channel intersections is 10Å). The volume occupied by these molecules is estimated at 70% of the pore volume of the zeolite. The coke formed from toluene at low temperature have kinetic diameters close to that of the channels, hence their migration in the zeolite channels is slow.

At high temperatures, the coke formed has a low vapour pressure at the reaction temperature. Hence coke retention in the zeolite pores is the result of steric blockage at channel intersections. The molecular cross section of the coke molecules is greater than that of the pore apertures and close to that of the channel intersections [Magnoux et al. 1992].

Deactivation is hence rather more likely to be due to site blocking rather than to site poisoning or consumption of active OH groups [Karge and Boldingh, 1988], with the initial rate of coke formation affected by the number of active sites. The final level of coke deposition reflects the available pore volume of the zeolite.

1.9.4. Coke formation from 1-hexene and 1-octene

At 120°C, with 1-hexene as feedstock, the retained product was dominated by the C_{12} dimer. However cracking and oligomerization also took place [Anderson et al. 1989]. The retained material was largely alkanes (C_8-C_{15}) with a distribution maximum at C_{12}. There was some chain branching present. The alkylbenzenes (C_7-C_{12}) from the gas phase product (25wt%) is probably closely linked to the alkane formation, with alkylbenzene being the end products in the hydrogen abstraction reactions required for the conversion of alkenes to alkanes. The thermodynamic feasibility of this may be demonstrated by considering the following reaction for which the equilibrium constant at 120°C is 3.3×10^6:

$$4C_6H_{12} \rightleftarrows C_6H_6 + 3C_6H_{14}$$

As the reaction temperature was increased above 120°C, higher molecular weight, unsaturated, cyclic products became of increasing importance. In particular alkylcyclopentadienes were the major residue product at temperatures between 180°C and 240°C. At temperatures above 320°C alkylnaphthalenes, alkylindanes and alkylindenes, as well as lesser amounts of alkylphenanthrenes were the major residue products, while in the gaseous phase alkylnaphthanes and alkylbenzenes were the most significant components, apart from cracked products [Anderson et al. 1989]. With 1-hexene, oligomerization, cracking, skeletal isomerization and double bond shift are all facile acid-catalyzed reactions and the formation of alkylcyclopentadienes may be formulated from an alkylpentadienyl carbocation. The formation of alkylbenzenes occurs at all temperatures in relatively modest amounts. Akylbenzenes may be formed by either alkylcyclopentadienyl carbocations which may undergo ring expansion to alkylcyclohexenyl carbocations followed by hydrogen abstraction to form the alkylbenzene. Alternatively, alkylbenzenes may be formed by ring opening from alkylindanes and alkylindenes. The use of n-hexane as reactant gives broadly similar results to those obtained from 1-hexene.

The residue formed from 1-hexene at 120°C to 240°C renders the pores inaccessible to nitrogen sorption [Anderson et al. 1989]. The residue occupied 55% of the specific pore volume. It was thus concluded that the residue in this temperature range was non-uniformly distributed, being concentrated toward and on the outer surface of the zeolite so as to block the entire pore volume. At 320°C to 445°C the accessible pore volume was 85%-100% of the total pore volume, while the residue content was 3wt%. Clearly this residue must exist largely on the external surface of the zeolite and in a manner which left most of the internal pore system open.

The residue formed at low temperatures had a boiling point distribution (at 1atm) below 280°C and many had boiling point distributions below 530°C. Therefore significant amounts of these components could not have accumulated on the external zeolite surface, which implies their accumulation in the pore system. Thus the unblocking of the pores of H-ZSM-5 treated with 1-hexene at temperatures above 320°C was due to migration of residue out of the pores to the external surface, where part was lost by migration and part was converted into higher molecular weight products, which were retained on the zeolite surface. These higher molecular weight products were mainly higher alkylaromatics (C_{11}-C_{17} alkylnaphthalenes and C_{15}-C_{17} alkylphenanthracenes) which were formed at the external surface rather than in the pores because of steric constraints within the zeolite pore system [Anderson et al. 1989].

The composition of the retained residue from 1-octene conversion is broadly similar to that of 1-hexene with respect to alkanes (exclusive component at 120°C, decreasing rapidly at higher temperatures), alkylcyclopentadienes (important at intermediate and higher temperatures) and alkylnaphthalenes (formed only at 320°C). However, alkylbenzenes with 1-octene, increased rapidly at temperatures above 180°C and were the dominant residue component (46wt%) at 320°C [Anderson 1991]. This behaviour is different to that reported for 1-hexene, when alkylbenzenes were always comparatively small (2wt%). The large amount of alkylbenzene product from 1-octene is attributed to direct hydrogenative reactant cyclization, proceeding via a C_8 diene. This should give C_8 alkylbenzenes as a primary product, however the co-occurrence of extensive alkylation and side-chain cracking reactions will tend to mask this as an indicator. Apart from this facile direct formation of alkylbenzenes from 1-octene, the similarity between 1-octene and 1-hexene in regard to residue products versus temperature suggests the operation of a route to naphthalenes via cyclopentadienes for 1-octene, similar to that established for 1-hexene.

The main conclusions that can be drawn are common to both systems, in that at lower temperatures the retained residue exists mainly within the zeolite pores in a manner that blocks the entire pore volume. At increasing treatment temperatures the amount of retained residue decreased and as a result the amount of accessible pore volume increased [Anderson et al. 1991].

1.10. Effect of Feedstocks on Aromatization Selectivity

Thermodynamic data reveal that alkanes can only be directly converted into aromatics at high temperatures. Butane, for example, can be catalytically converted into xylenes at temperatures over 400°C but alkene formation from the alkane is only favoured at much higher temperatures. Alkenes are much more reactive and butene can be converted to xylenes over the temperature range considered [Seddon 1990]. Thermodynamic data also reveals that alkane to aromatic conversion becomes more favourable as the size of the alkane increases and that aromatics formation is favoured over corresponding alkene formation [Scurrell 1987]. Methane and ethane are considered non-aromatizable compounds due to the high thermodynamic barriers to their conversion to aromatics. Iso-alkanes are more reactive than n-alkanes, giving more hydrogen (H_2) but less aromatics.

1.10.1. Reactivity of C_2-C_4 alkanes

Butanes are more reactive than propane and much more reactive than ethane. This trend is independent of the catalyst used for aromatization. With H-ZSM-5, butane and iso-butane react at similar rates, 4 times faster than propane and 100 times faster than ethane. Aromatics are always secondary products. The distribution of C_6-C_8 aromatic products are similar from C_3-C_4 alkanes; about 20% benzene, 50% toluene and 30% C_8 aromatics. From ethane only toluene (60%) and benzene (40%) are initially formed, with C_8 aromatics only appearing at high conversions.

Gallium affects the distribution of the primary products of ethane, propane and n-butane transformation, increasing the selectivities to dehydrogenation products and decreasing that to cracking products. With iso-butane, gallium does not modify the selectivities to butenes, propene and methane. Gallium increases significantly the selectivity to aromatic products with ethane, propane and n-butane transformation, but has a limited effect with iso-butane. It was concluded from this and other data that on Ga/H-ZSM-5 the aromatization of ethane, propane and n-butane occurred mainly through a bifunctional pathway, while that of iso-butane through a acid pathway [Guisnet et al. 1992].

1.10.2. Naphthenes

In the study of n-hexane, cyclohexane, n-heptane and methylcyclohexane transformation over H-ZSM-5 and Ga/H-ZSM-5 it was shown that the aromatic molar product distribution is affected by the type of catalyst. On H-ZSM-5 n-hexane and cyclohexane showed similar results while n-heptane and methylcyclohexane showed similar results. On Ga/H-ZSM-5 the fraction of the aromatic isomer of the transformed molecule is higher than with acidic catalysts. [Giannetto et al. 1991]. This change is more pronounced for cycloparaffins and is related to the dehydrogenating activity of the gallium species. Over H-ZSM-5, toluene is the major aromatic product. Some results are shown in Table 1.8 [Giannetto et al. 1991].

There is evidence for direct aromatization of cycloalkanes due to the high selectivity to benzene and toluene for the cyclohexane and methylcyclohexane feed stocks respectively. With aliphatic compounds aromatization takes place over the gallium species by the bifunctional mechanism previously reported. Thus the gallium species participate in a monofunctional reaction, favouring the direct formation of aromatic products, as well as by the commonly accepted bifunctional reaction mechanism.

Table 1.8 Aromatic yields for C_6-C_7 alkanes

	H-ZSM-5			Ga/H-ZSM-5		
Feed	B	T	C_8 aromatics	B	T	C_8 aromatics
n-C_6	28	45	27	40	38	22
Δ-C_6^{a}	25	45	30	73	20	7
n-C_7	16	44	40	16	50	34
m-Δ-C_6^{b}	16	44	40	26	62	12

(a) cyclohexane; (b) methylcyclohexane

1.11. Research Objectives

The objective of this research was to investigate the feasibility of aromatizing long chain alkenes (1-hexene and 1-octene) into aromatics, mainly BTX over gallium-modified H-ZSM-5 catalysts. The effect of temperature, WHSV, method of loading gallium onto the zeolite, hydrogen pretreatment and reactant was investigated. Gallium/ZSM-5 has been extensively studied for the aromatization of LPG, but has not been investigated for the aromatization of long chain alkenes. Thus this work is novel in the sense that the reactants which were used have not been systematically tested with a view to optimizing BTX selectivity.

Three methods of adding gallium to H-ZSM-5 were investigated, viz.

(i) Physical mixing with Ga_2O_3;
(ii) Ion exchange with a $Ga(NO_3)_3.9H_2O$ solution;
(iii) Impregnation by incipient wetness with a $Ga(NO_3)_3.9H_2O$ solution.

The effect of adding gallium to H-ZSM-5 was quanitified by comparing the yields of the gallium/H-ZSM-5 to unmodified H-ZSM-5 for both 1-hexene and 1-octene. The effect of the different reactants on deactivation and product selectivity over a range of temperatures was also investigated.

Chapter 2

EXPERIMENTAL

2. Experimental

2.1. Catalyst Synthesis and Modification

2.1.1. ZSM-5

ZSM-5 with a Si/Al ratio of 35 was synthesized according to the method of Arguer and Landolt [1972]. The catalyst was detemplated by calcination in N_2 (30ml/min) at 500°C for 6 hours, followed by calcination in air (30ml/min) at 500°C for a further 6 hours. The Na-ZSM-5 form was ion-exchanged twice with two equivalents of NH_4Cl to give the ammonium form, NH_4-ZSM-5. The catalysts used in this project consisted of two 15g batches, synthesized separately, but under identical conditions. These two batches were sieved together and mixed to give 30g of NH_4-ZSM-5 which was used throughout the project.

2.1.2. Gallium(impr)/H-ZSM-5

The gallium impregnated catalyst was synthesized by standard incipient wetness techniques. $Ga(NO_3)_3.9H_2O$ was used as the gallium salt. The gallium loading was 5wt% of the total catalyst mass. The catalyst was dried at room temperature for 12 hours, then calcined in N_2 under the standard calcination program used during the project (see 2.3.8.1.). The gallium loading was 5% by mass.

2.1.3. Gallium(ionx)/H-ZSM-5

The ion-exchanged catalyst was prepared by two successive ion-exchanges of NH_4-ZSM-5 with 2M $Ga(NO_3)_3.9H_2O$ solution. The catalyst was washed with 400ml of de-ionized water after each ion-exchange. The catalyst was dried overnight and calcined in N_2 under the standard calcination program used during the project (see 2.3.8.1.). The catalyst name, "Ga(ionx)/H-ZSM-5" refers to the synthesis method only as ion exchange with multivalent ions does not easily occur with H-ZSM-5 (section 1.4.3). The gallium loading was found to be 18% by mass.

2.1.4. Gallium(mix)/H-ZSM-5

The physically mixed catalysts were prepared by ballmilling H-ZSM-5 with β-Ga_2O_3 for 3hrs. The catalysts were calcined in N_2 (see 2.3.8.1). The gallium loading was 5% by mass.

2.1.5. β-Ga_2O_3

β-Ga_2O_3 was synthesized by heating mixed phase Ga_2O_3 in air in a muffle furnace at 1200°C for 24hrs. XRD patterns indicated the formation of the β-Ga_2O_3 phase had occured to completion.

2.2. Catalyst Characterization

2.2.1. Catalyst structure

Standard XRD patterns were compared with those for our catalyst to give an indication of the catalyst structure and degree of crystallinity. XRD was performed on a Phillips XRD spectrometer using Cu-Kα (1.541Å) radiation, 30mA, 40kV.

2.2.2. TPR

TPR was carried out using the following general conditions:

Table 2.1 TPR procedure

Temperature range	100°C to 1000°C
Sample mass	200mg
Ramp to calcination temp.	10°C/minute to 550°C in air at 60ml/minute
Plateau	4 hours
Cool to 100°C	5°C/minute
Ramp to reduction temp.	10°C/min to 1000°C in 5.4% H_2 in N_2 at 60ml/minute
Plateau	30 minutes

2.2.3. AA analysis

The amount of gallium present on the catalyst was determined by AA analysis on a Varian SpectrAA-30 spectrometer using a gallium hollow cathode lamp supplied by SPEC.

2.2.4. FTIR

FTIR analysis of catalyst samples were performed using a Nicolet 5ZDX FTIR spectrometer with a resolution of 4cm^{-1}. All samples were made from KBr wafers.

2.2.5. SEM

SEM analysis was performed with a Cambridge Instruments S200 scanning electron microscope.

2.3 Reactor Configuration and Experimental Procedures

2.3.1. Reactor system

A schematic diagram of the reactor system is shown in Figure 2.1. The reactor is a simple plug flow reactor, consisting of a borosilicate glass tube (16mm ⊘ I.D.). A mass flow controller (MFC) allowed the feeding of air, hydrogen or nitrogen at controlled flowrates. Analysis is by online gas chromatography. Dimethyl ether (DME) is added downstream of the reactor and used as an internal standard. A double stage saturator containing the alkene reactant and using nitrogen as a carrier gas enabled the feedstock to be supplied at a constant rate. A catchpot at 0°C allowed the heavier compounds, C_5+, to be trapped for off-line analysis. The lines upstream of the reactor were heated to 60°C while those downstream of the reactor were heated to 210°C.

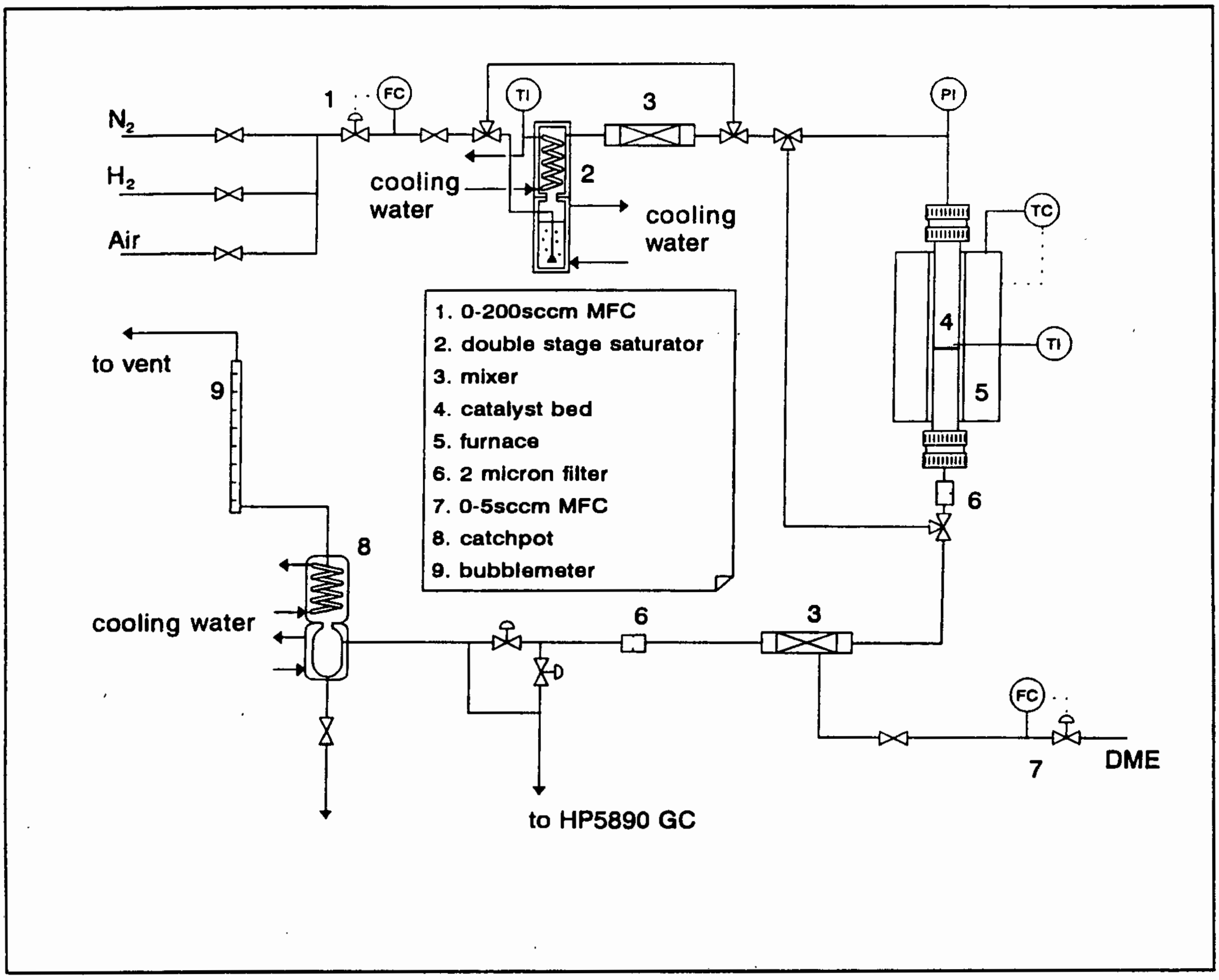

Figure 2.1 Schematic diagram of reactor system

2.3.2. The catalyst bed

The catalyst bed was supported by a quartz wool plug, through which a thermocouple, linked to a temperature indicator, protruded. The ZSM-5 catalyst used during experimentation was in powder form (ca. 3μm average crystallite size) which limited the depth to which the catalyst bed could be packed. Packing the bed too deeply resulted in an unacceptably high pressure drop across the bed. Initial experimentation was with a shallow bed, about 5mm in length. However, temperature ramps of up to 70°C occurred during air calcination of coked catalysts. In order to maintain a more constant reactor temperature during calcination, the catalyst was mixed with quartz sand with a particle size between 75μm and 210μm, in a ratio of ca. 1:25 catalyst to quartz sand. This allowed the use of a longer catalyst bed as the quartz sand dissipated the reaction heat during calcination and catalytic testing. Thus unwelcome temperature runaways in the catalyst bed were eliminated. All catalytic testing reported in the project was made using a catalyst bed packed as shown in Figure 2.2.

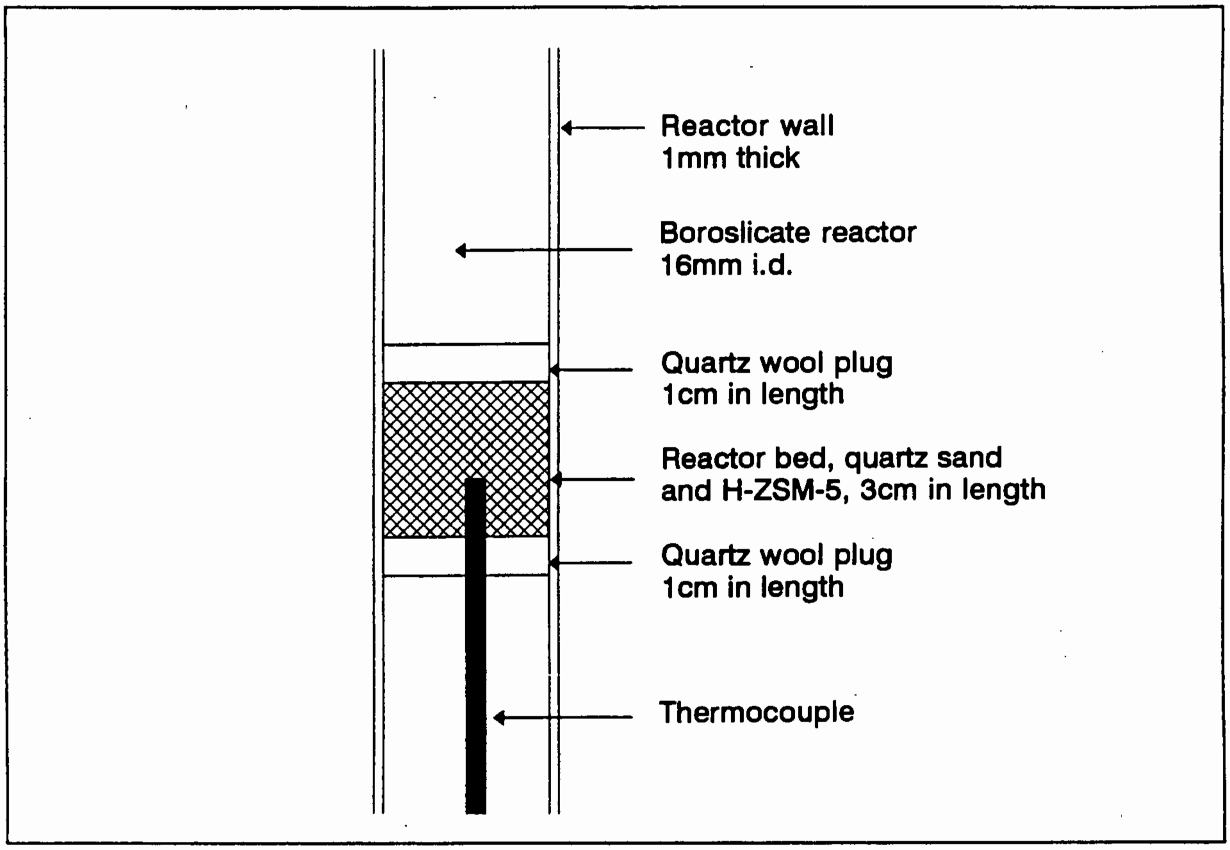

Figure 2.2 Schematic diagram of the catalyst bed

2.3.3. Run procedure

The following run procedure was used:

(i) ramp to 550°C in N_2 at 80ml/min at 5°C/min

(ii) calcine in air at 80ml/min at 550°C for two hours

(iii) flush with N_2 at 80 ml/min at 550°C for 15 minutes

(iv) reduce reactor temperature to the operating temperature

(v) bypass reactor and allow saturator and DME internal standard to equilibrate for 20 minutes

(vi) open valve to reactor to start run

Certain catalysts were pretreated with H_2 before they were tested. This involved two extra steps after (iii) above, namely:

(vii) reduction in hydrogen at 80ml/min at 550°C for two hours
(viii) flush with N_2 at 80ml/min at 550°C for 15 minutes

2.3.4. Gas analysis

On-line analysis of the gaseous product was carried out with a Hewlett Packard HP5890 GC with an on-line gas sampling valve. A Hewlett Packard PONA capillary column (50m length, 0.2mm i.d., 53μm film thickness) was used for resolution of the components, while detection was by FID. The lines leading from the reactor to the sampling valve were heated at 210°C by ribbon heating tape and insulated with quartz wool. The resolution of ethene\ethane and propane\propene could only be achieved by cooling the GC oven to -30°C using cryogenic operation with liquid nitrogen. The resolution of 1-butene and i-butene and p-xylene and m-xylene could not be achieved. The low temperature (-30°C) analysis of the gaseous product was performed only when it was deemed important to determine the relative ratios of C_2-C_3 alkanes and alkenes, due to the difficulty in performing the analysis by this method.

The compounds identified by on-line GC analysis are shown in Table 2.2. The heavy compounds are defined as those compounds heavier than the feedstock but not BTEX. Hence for 1-hexene aromatization C_7 and C_8 hydrocarbons are included in the heavies fraction. For 1-octene aromatization the C_7 hydrocarbons were grouped with the C_6 hydrocarbons

Repeatability between gas samples was good (less than 5% difference in total area) for blank runs, i.e. either when by-passing the reactor or when the reactor tube was empty (without catalyst). During actual experimental runs with catalyst there was a slightly greater variance between gas samples (*ca.* 10%).

Table 2.2 Compounds analyzed by online GC

Compound	Notation	Boiling Point	Response Factor
methane	C_1	-161°C	1.19
ethene	$C_2=$	-104°C	1.18
ethane	C_2	-88°C	1.07
propene	$C_3=$	-48°C	1.12
propane	C_3	-42°C	1.20
dimethyl ether	DME	-24.8°C	3.00
iso-butane	i-C_4	-11.8°C	1.14
iso-butene	i-$C_4=$	-7.0°C	1.19
1-butene	1-$C_4=$	-6.3°C	1.19
n-butane	n-C_4	-0.5°C	1.16
trans-2-butene	t-2-$C_4=$	1.7°C	1.26
cis-2-butene	c-2-$C_4=$	3.7°C	1.16
C_5's	C_5	30°C-35°C	1.00
1-hexene	1-$C_6=$	64°C	1.00
C_6's	C_6	64°C-69°C	1.00
benzene	B	80°C	1.15
toluene	T	110°C	1.11
C_8's	C_8	122°C-126°C	1.00
ethylbenzene	EtB	135°C	1.04
p-xylene	p-X	135°C	1.00
m-xylene	m-X	138°C	1.00
o-xylene	o-X	142°C	0.92
heavies	heavies	>feedstock	1.00

2.3.5. Liquid analysis

Off-line analysis of the liquid product trapped at 0°C was made with a Hewlett Packard HP5890 Series II GC using a Hewlett Packard HP5971A mass selective detector. A 50m PONA capillary column, as used for gas analysis, was used for component resolution.

2.3.6. Mass flow controller calibration

Two Brooks 5890TR mass flow controllers (MFC) were used. A 0-200sccm (standard cm^3/min) MFC was used as a controller for the carrier gas, nitrogen, as well as air and hydrogen, while a 0-5sccm MFC was used for the dimethyl ether (DME) internal standard. The MFC's were calibrated by different methods. The 0-200sccm MFC was calibrated for nitrogen, air and hydrogen using a bubble meter and the flows then converted to standard conditions (0°C, 1atm). Due to the solubility of DME in water, a bubble meter could not be used for the calibration of DME. The calibration of the DME MFC was accomplished by first calibrating the 0-200sccm MFC for propane using a bubble meter. Propane was then used as a carrier gas, while the flowrate of DME was determined from the relative ratios of DME and propane from GC analysis. The relative response factors of DME and propane were previously determined from calibration gases.

2.3.7. Calculations

The following section lists and explains the definitions used in describing catalyst performance.

2.3.7.1. Conversion

Conversion is defined as the percentage feed converted.

$$X = \frac{\text{mass of feed into system} - \text{mass of feed out of system}}{\text{mass of feed into system}}$$

2.3.7.2. Selectivity

Selectivity is the percentage converted carbon in the product species and is calculated on a carbon basis.

$$S_A = \frac{\text{carbon mass of } A}{\text{carbon mass of feed into system} - \text{carbon mass of feed out of system}}$$

2.3.7.3. Yields

The yield of a species is simply the conversion of the feed multiplied by the selectivity of the species.

$$Y_A = X \times S_A$$

2.3.7.4. WHSV

The weight hourly space velocity is the mass of feed per hour per mass of catalyst.

$$WHSV = \frac{\text{mass hourly flowrate of feed into the reactor}}{\text{mass of catalyst}}$$

2.3.7.5. Response factors

Response factors were determined for the compounds smaller than the C_5's as well as 1-hexene, DME, benzene, toluene, the xylenes and ethylbenzene. The response factors were calculated relative to 1-hexene, which was normalized to one. Response factors were determined by area normalization with standard calibration gases. During runs DME is added downstream of the reactor and is used as an internal standard . A carbon balance was performed.

$$R_{f_A} = \frac{Area_A \; Mass_{IS}}{Area_{IS} \; Mass_A}$$

R_{fA} is the response factor of species A relative to the internal standard

$Area_A$ is the area of species A on the GC trace

$Mass_A$ is the mass of species A injected into the GC

$Area_{IS}$ is the area of the internal standard on the GC trace

$Mass_{IS}$ is the mass of the internal standard

2.3.8. Catalyst treatments

Before the catalyst could be used for experimental runs, they were calcined. Two forms of calcination were employed, namely to convert NH_4-ZSM-5 to H-ZSM-5 and to reactivate (decoke) H-ZSM-5 after experimental runs. Several of the Ga/H-ZSM-5 catalysts were pretreated with hydrogen, after the initial calcination in air, to cause the reduction of the gallium oxide species.

2.3.8.1. Conversion of NH_4-ZSM-5 to H-ZSM-5

The catalyst was calcined in batches of 3g to 5g. The calcinations were made in the following manner in air at a flowrate of 160ml/min.

(i) Consecutive low temperature treatment at 80°C and 150°C for 2 hours at each temperature.

(ii) Temperature ramp up to 550°C at 25°C every 15 minutes

(iii) Held at 550°C for 12 hours

2.3.8.2. Decoking Calcinations

These were carried out in air with a flowrate of 80ml/min at 550°C for 2 hours. Some decoking calcinations were carried out overnight for 12 hours, however, all catalysts were treated for a least 2 hours before any reaction was carried out.

2.3.8.3. Hydrogen Pretreatment of Ga/H-ZSM-5

Certain Ga/H-ZSM-5 catalysts were pretreated before catalytic testing with H_2 at 550°C for 2 hours at a flowrate of 80ml/min. The H_2 pretreatment of catalysts was carried out after calcination in air.

Chapter 3

RESULTS

3. Results

3.1. Blank Runs

3.1.1. Temperature profile of the reactor

To accurately test catalytic performance it is necessary to ensure isothermal operating conditions over the catalyst bed. The catalyst bed was diluted with quartz sand, giving a bed *ca.* 3cm in length. It was thus necessary to determine whether isothermal operation was possible over the length of the catalyst bed. The temperature profile of the reactor bed was determined by moving the thermocouple along the inside of the reactor tube which was packed with quartz sand. The reactor temperature was set at 500°C with a N_2 carrier gas flow rate of 100ml/min. There was an isothermal range of *ca.* 7cm over the length of the reactor furnace, as shown in Figure 3.1, which was sufficient to ensure isothermal operation for a catalyst bed of the length used.

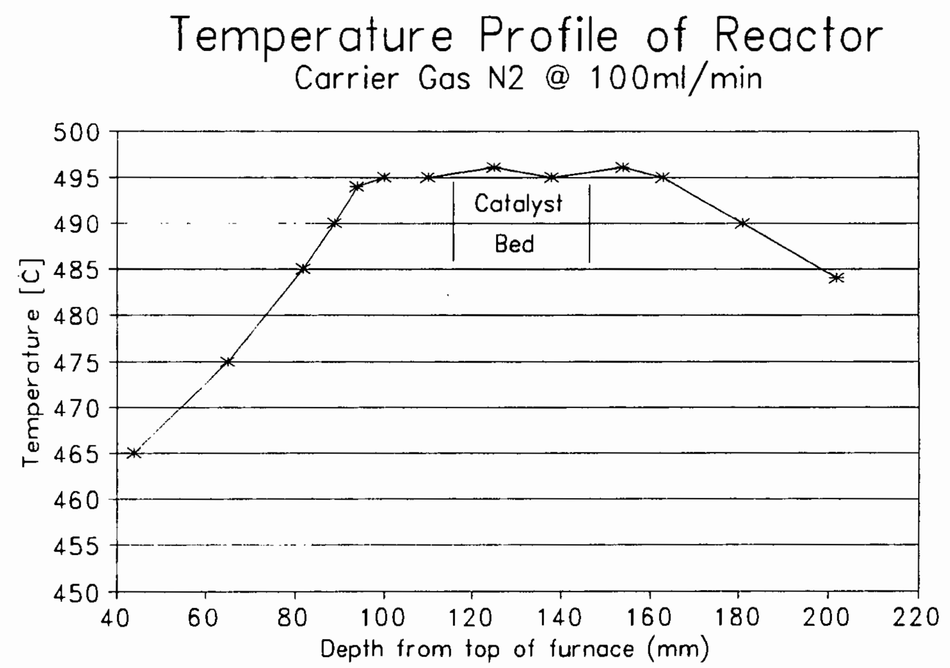

Figure 3.1 Temperature profile of the reactor bed

3.1.2. Blank runs with quartz sand

It was necessary to determine the catalytic activity, if any, of the quartz sand with which the catalyst bed was diluted. A series of blank runs were made to determine the inherent catalytic activity of the quartz sand, quartz wool plug and the borosilicate glass reactor with 1-hexene as feedstock. The results are shown in Table 3.1.

Table 3.1 Results of blank runs[a]

Reactor packing	Bed temp.	1-C_6=	1-C_6= X^b	other C_6= isomers	C_1	C_2	C_3	C_4	C_6
quartz	300°C	55	45	45	0	0	0	0	0
sand	400°C	22	88	78	0	0	0	0	0
(3cm)	500°C	18	88	78	0	1	1	1	1
	550°C	17	83	69	1	3	3	3	4
quartz wool	550°C	67	33	7	1	6	9	7	3
empty	300°C	100	0	0	0	0	0	0	0
	400°C	98	2	2	0	0	0	0	0
	500°C	93	7	3	0	1	2	1	0
	550°C	70	30	6	1	6	8	6	3

(a) selectivity (wt%), 1-hexene as feedstock at 0.01g/hr, N_2 flowrate of 20ml/min; (b) 1-hexene conversion

By comparing the products from the "empty" and "quartz sand" cases it can be seen that presence of quartz sand in the reactor causes an increase in the degree of isomerization of 1-hexene. This can be explained by the fact that the quartz sand, which was acid washed, may still have had residual acidity. It has been shown that washing the quartz sand with de-ionized water markedly lowered its isomerization activity towards 1-butene [Seally, private communication]. All quartz sand used in subsequent experimentation was washed with de-ionized water. The higher amount of cracked product in the "empty" and "quartz wool" reactors at 550°C than in the "quartz sand" reactor may perhaps be explained in terms of the differences in residence times of the feedstock through the reactor tube. The actual residence time in the packed reactor will be much lower than that of the empty reactor, hence allowing a greater degree of thermal cracking to take place in the empty reactor. Thermal treatment will yield little or no isomerization products as isomerization reactions proceed via carbenium ion intermediates and hence need acidic sites. Thermal cracking should yield large amounts of ethene while acidic cracking would produce propene as a primary product.

The large amount of isomerization products in the "quartz sand" reactor indicates that residual acidity was present on the quartz sand. Residence times through the bed were too low to enable thermal cracking of 1-hexene to occur to any extent. Thermal cracking does, however, become more prevalent at 550°C. In the "empty" and "quartz sand" packed reactors more thermal cracking of 1-hexene than isomerization occurs at high temperatures due to the higher residence times of the feed in the reactor and the lack of any acidic sites on which to form carbenium intermediates.

Double bond isomerization of 1-hexene is so prevalent at high temperatures with even a trace of acid [Brouwer, 1962] that it was decided to consider all hexene isomers as a single feedstock.

3.1.3. Catalytic runs at low residence times and high WHSV

In an attempt to lower the conversion of 1-hexene at 550°C to below 100%, the WHSV was increased from $2.9hr^{-1}$ to $21hr^{-1}$ and $44hr^{-1}$ and the residence time over the bed reduced from 1.5 seconds to 0.26 seconds. The catalyst used was H-ZSM-5. The increase in WHSV was achieved by increasing the temperature of the saturator from 0°C to 10°C and by increasing the nitrogen carrier flowrate through the saturator from 80ml/min and 160ml/min. To reduce the feed residence time over the catalyst bed, an auxiliary feed of nitrogen was installed after the saturator, but before the reactor. This allowed an extra 300ml/min of nitrogen to be fed through the system, hence lowering the residence time over the catalyst bed. The results of these experiments showed that while conversion of 1-hexene remained at 100%, the major reaction products were C_2 & $C_2=$, C_3 & $C_3=$ and butenes (Table 3.2).

Table 3.2 Runs at high WHSV and low bed residence times

Reactor temperature	550°C	550°C	550°C	550°C
WHSV	2.9hr^{-1}	2.9hr^{-1}	21.9hr^{-1}	43.9hr^{-1}
Residence time	1.5s	0.32s	0.32s	0.26s
Conversion	100%	100%	99.3%	100%
C_1	0.7	0.0	0.0	0.0
C_2= & C_2	25.5	11.1	7.6	8.9
C_3= & C_3	41.4	71.2	70.9	71.5
i-C_4	1.2	0.0	0.0	0.0
i-C_4= & 1-C_4=	8.6	7.1	9.0	8.9
n-C_4	1.3	0.0	0.1	0.4
t-2-C_4=	3.6	3.1	3.8	3.8
c-2-C_4=	2.6	2.1	2.6	2.7
C_5	2.7	2.1	1.2	1.8
B	1.9	1.1	0.3	0.3
T	4.9	1.8	0.8	0.5
EtB	0.2	0.0	0.0	0.0
p,m-X	3.1	0.0	0.4	0.0
o-X	0.9	0.0	0.0	0.0
Heavies	1.1	0.3	1.6	2.2

Negligible amounts of aromatics were present in the product spectrum at low residence times over the bed. It is obvious that aromatic compounds are not primary products as selectivity to aromatic products decreases with increase in WHSV and decrease in residence time. Similarly the C_2 and C_3 products display opposite trends in selectivity with decrease in residence time over the catalyst bed. Hence, the C_2 products are unlikely to be primary reaction products. The selectivity to butenes remained essentially constant with decrease in residence time while selectivity to butanes decreased. From the data it appears that C_1, C_2 , C_4 and C_5 cracked compounds are not primary reaction products. However, the C_3 cracked products could be considered to be the primary reaction products at this temperature (550°C). This would be expected from β-scission of hexene to form two propene molecules: $C_6H_{12} \rightarrow 2C_3H_6$. The usual acid catalyzed oligomerization, cracking and cyclization reactions result in the formation of all the observed products.

3.1.4. Film diffusion test

As the linear flowrates through the reactor were low (*ca.* 1cm/s), it was necessary to test whether film diffusional effects were present in the catalyst bed. The results of two runs made at the same WHSV and residence time but with a different mass of catalyst and at different linear velocities of carrier gas were compared. The experiments were carried out at temperatures of 250°C and at 270°C. It was necessary to work at these low temperatures in order to keep the conversion of 1-hexene below 100%. The catalyst used in this experiment was H-ZSM-5. The mass of catalyst was 0.10g and 0.20g. To keep a constant WHSV the temperature of the saturator was varied by an appropriate amount. The flowrate of the carrier gas was 50ml/min and 100ml/min for the two catalyst masses respectively. Thus the residence time over the catalyst bed was kept constant. The change in linear velocity of the carrier gas produced a substantial change in the feed conversion as shown in Table 3.3. The implications of this observed change in conversion with feedstock residence time over the catalyst bed is discussed in greater detail in Chapter 4.

Table 3.3 Film diffusion test

Reaction temperature	250°C	250°C	270°C	270°C
WHSV	11.3hr^{-1}	11.3hr^{-1}	11.3hr^{-1}	11.3hr^{-1}
Residence time	1.9s	1.9s	1.8s	1.8s
Linear velocity through bed	0.79cm/s	1.6cm/s	0.82cm/s	1.6cm/s
Conversion	24.1%	53.7%	61.3%	78.4%
N_2 flowrate	50cm^3/min	100cm^3/min	50cm^3/min	100cm^3/min
Catalyst mass	0.10g	0.20g	0.10g	0.20g
C_1	0.0	0.0	0.0	0.0
C_2= & C_2	0.0	0.0	0.0	0.0
C_3= & C_3	10.4	7.8	10.7	10.0
i-C_4	0.0	0.6	1.0	1.7
i-C_4= & 1-C_4=	14.5	15.3	19.1	21.4
n-C_4	0.0	0.0	0.3	0.8
t-2-C_4=	10.1	7.9	8.7	8.5
c-2-C_4=	5.6	4.6	5.1	4.9
C_5	30.2	28.8	31.2	34.3
B	0.0	0.0	0.0	0.0
T	0.0	0.0	0.0	0.0
EtB	0.0	0.0	0.0	0.0
p,m-X	0.0	0.0	0.0	0.0
o-X	0.0	0.0	0.0	0.0
heavies	28.9	35.2	24.3	18.4

3.1.5. Typical GC trace

A typical GC trace of the reaction products for the aromatization of 1-hexene is shown below to allow the reader to visualize the nature of the product spectrum (Figure 3.2).

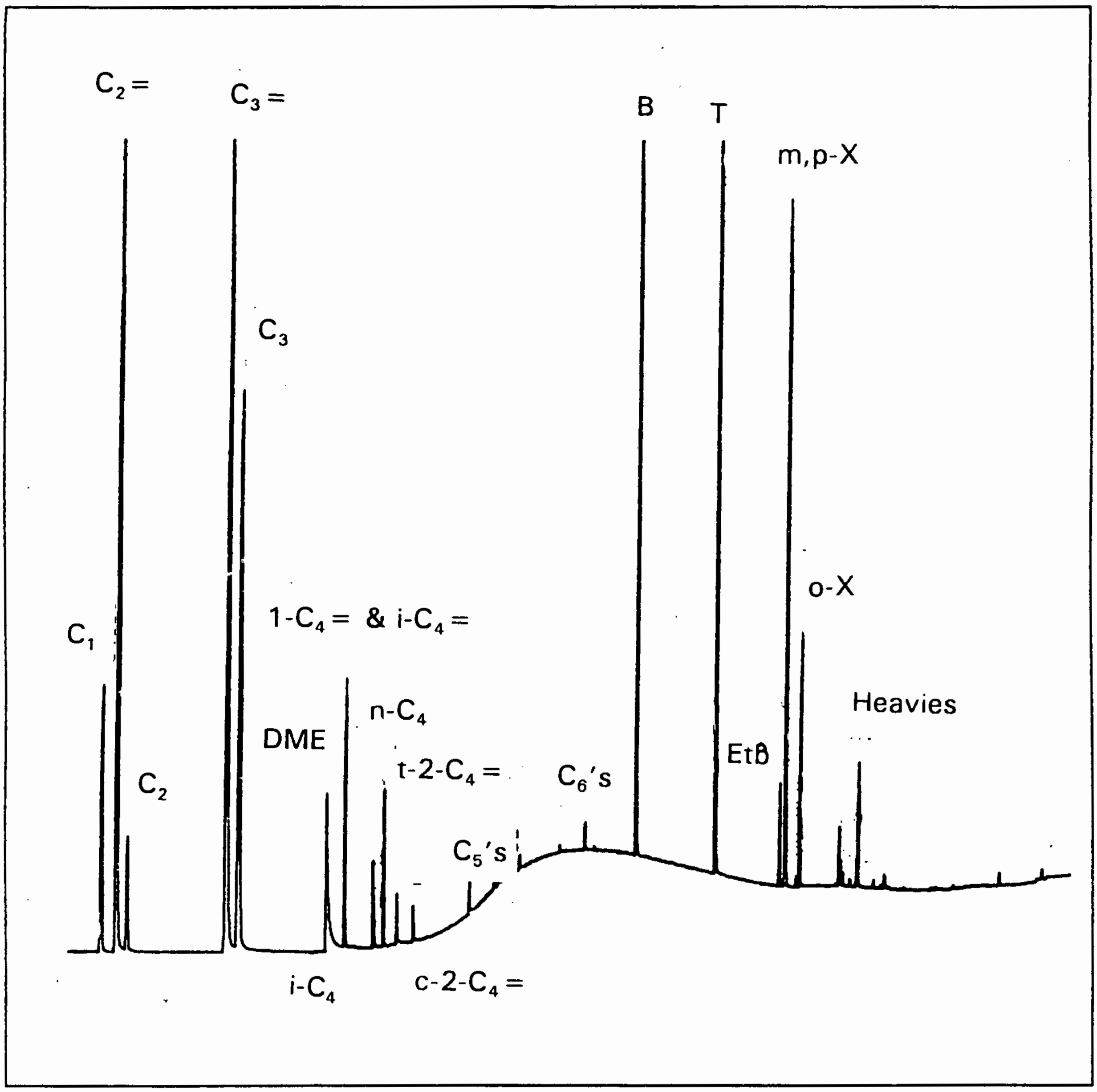

Figure 3.2 Typical GC trace for 1-hexene aromatization

3.2. Effect of Catalyst Preparation on Product Selectivity

Three methods were used to add gallium to H-ZSM-5:

i. physical mixing with β-Ga_2O_3;
ii. ion-exchange with $Ga(NO_3)_3.9H_2O$;
iii. impregnation with $Ga(NO_3)_3.9H_2O$.

Experimental runs were carried out at 500°C and 550°C using 1-hexene and 1-octene as feedstocks. At these high temperatures the conversion of the feedstock was always 100%. The Ga/H-ZSM-5 catalysts showed large changes in selectivity with time on stream. However, the H-ZSM-5 catalyst showed remarkable stability with regard to product selectivity with time on stream. No test of H-ZSM-5 was made using the catalyst bed packing described in section 2.3.2. However, prior testing using a shallow catalyst bed simply of H-ZSM-5 (no quartz sand dilution) showed no changes in product selectivity after 33 hours on stream at a reaction temperature of 550°C and a WHSV of hexene of $5hr^{-1}$. The conversion remained at 100% throughout. At high reaction temperatures (>400°C) it was not possible to reduce the feed conversion to below 100%, due to the high activity of H-ZSM-5 and the high reactivity of 1-hexene and 1-octene. At lower reaction temperatures (<350°C) only trace amounts of BTEX aromatics were present as product. At low reaction temperatures (<450°C) a large proportion of the product spectrum consisted of heavy oligimers (section 3.12) which complicated the GC analysis of the products.

The effect of the method of adding gallium (viz. mixing, ion-exchange, impregnation) to H-ZSM-5 as well as the effect of alkene feedstock (viz. 1-hexene and 1-octene) are shown in section 3.2.1. and section 3.2.2. The catalytic runs for Ga(mix)/H-ZSM-5 were made at a reaction temperature of 500°C, while Ga(impr)/H-ZSM-5 and Ga(ionx)/H-ZSM-5 were tested at 550°C.

3.2.1. 1-Hexene feedstock

3.2.1.1. C_1-C_3 light products

The Ga(mix)/H-ZSM-5 catalyst displayed stable product selectivity with time on stream. There was a slight decrease in selectivity to C_2 products. Ga(ionx)/H-ZSM-5 showed a large increase in selectivity to C_3 products and a decrease in selectivity to C_2 products. Ga(impr)/H-ZSM-5 displayed stable product selectivity with time on stream. The selectivity to methane was in all cases low (1% to 3%). The C_3 products were the major light products (25% to 35%) in for Ga(mix)/H-ZSM-5 and Ga(ionx)/H-ZSM-5.

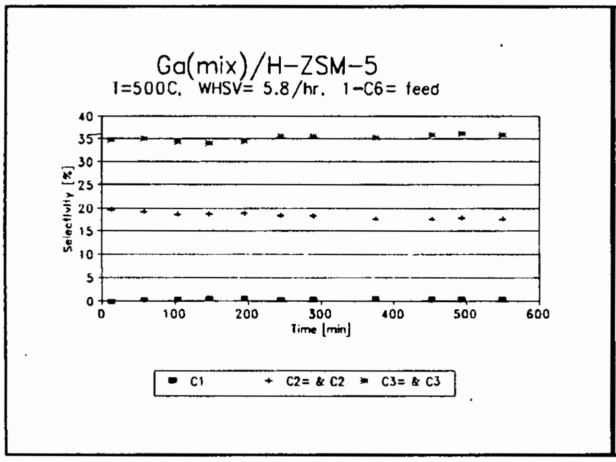

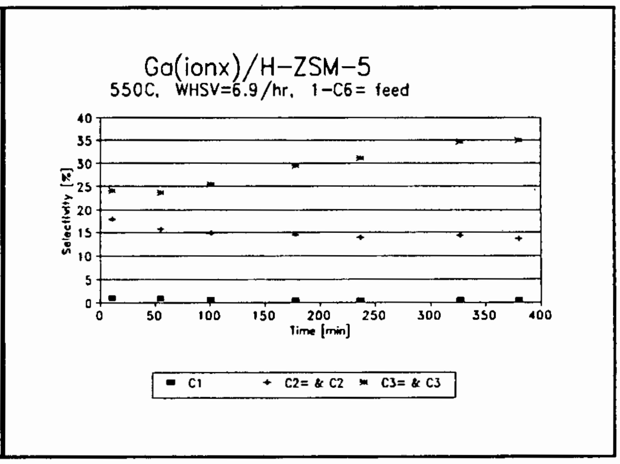

Figure 3.3 Ga(mix)/H-ZSM-5 (500°C) **Figure 3.4** Ga(ionx/)H-ZSM-5

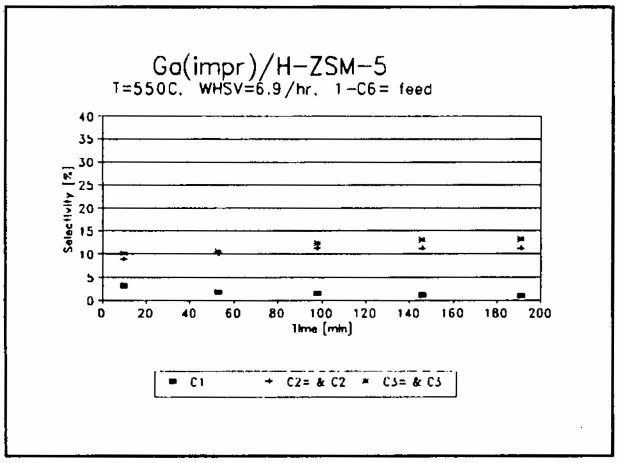

Figure 3.5 Ga(impr)/H-ZSM-5

3.2.1.2. C_4 products

With the Ga(mix)/H-ZSM-5 catalyst the selectivity to all the C_4 compounds remained stable. The selectivity to C_4 compounds increased in the case of Ga(impr)/H-ZSM-5 and Ga(ionx)/H-ZSM-5. In all cases 1-C_4=/i-C_4= was the major C_4 component and there was greater selectivity to trans-2-butene than cis-2-butene.

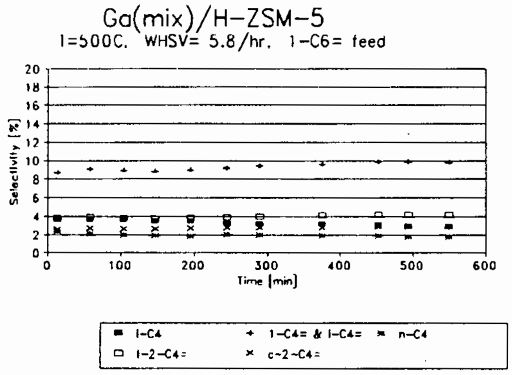

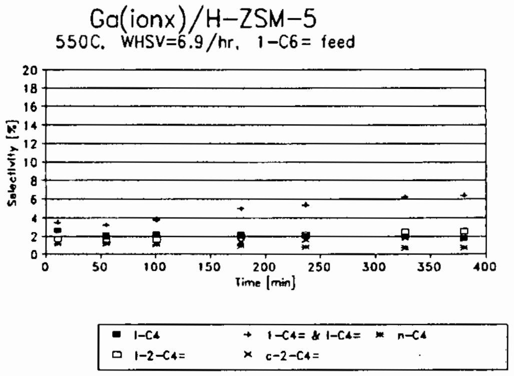

Figure 3.6 Ga(mix)/H-ZSM-5 (500°C) **Figure 3.7** Ga(ionx)/H-ZSM-5

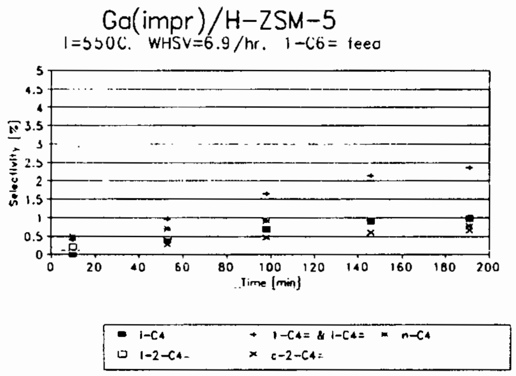

Figure 3.8 Ga(impr)/H-ZSM-5

3.2.1.3. Aromatic (BTEX) products

The selectivity to aromatic products remained constant for Ga(mix)/H-ZSM-5. A rapid decrease in selectivities to benzene and toluene was observed in the case of Ga(ionx)/H-ZSM-5 and Ga(impr)/H-ZSM-5, while the selectivity to xylenes remained constant. Toluene was the major aromatic component for all three catalysts. Selectivity to ethylbenzene and o-xylene was low (2%-3%).

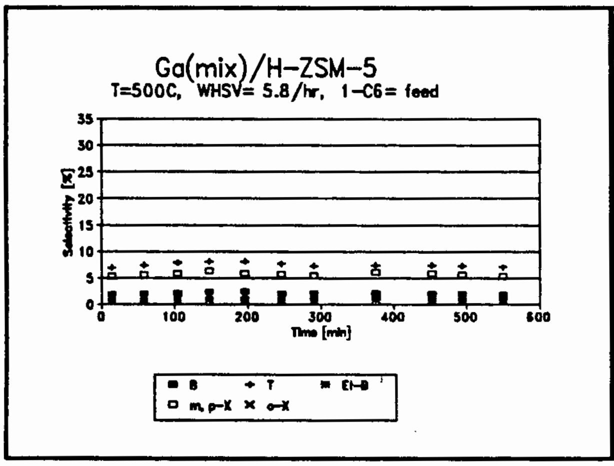

Figure 3.9 Ga(mix)/H-ZSM-5 (500°C)

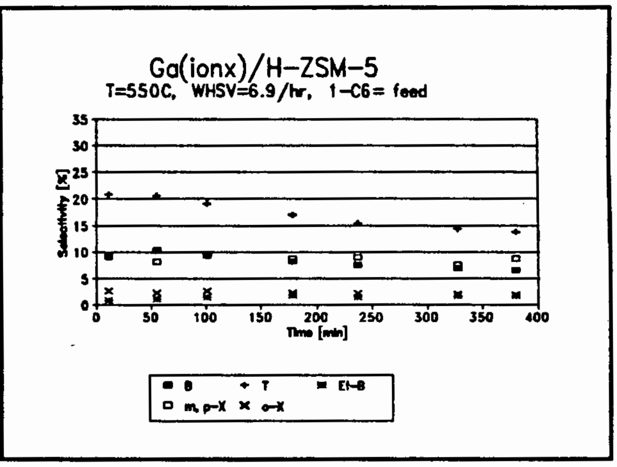

Figure 3.10 Ga(ionx)/H-ZSM-5

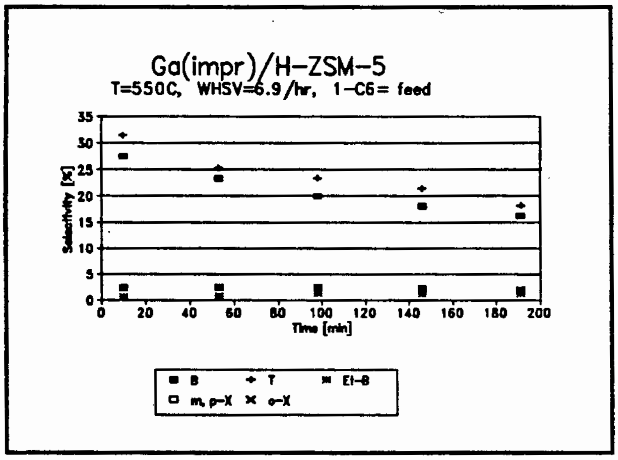

Figure 3.11 Ga(impr)/H-ZSM-5

3.2.1.4. C_5, heavy products and 1-hexene conversion

The conversion of 1-hexene remained at 100% for all three catalysts during the time on stream. With Ga(impr)/H-ZSM-5 the heavies increased from 5% to 20% while Ga(mix)/H-ZSM-5 and Ga(ionx)/H-ZSM-5 display stable selectivites of 5% to 7% for the heavy compounds.

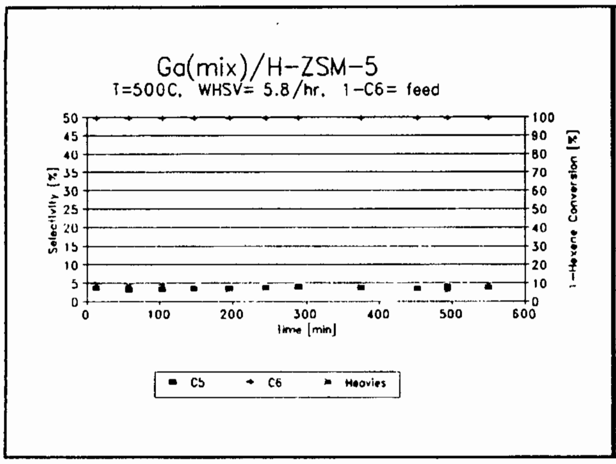

Figure 3.12 Ga(mix)/H-ZSM-5 (500°C)

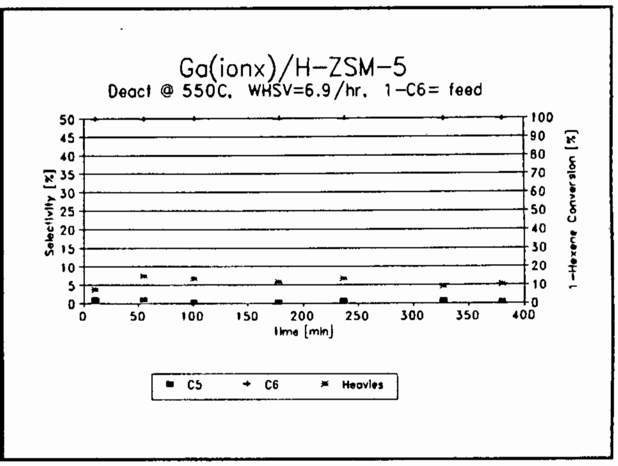

Figure 3.13 Ga(ionx)/H-ZSM-5

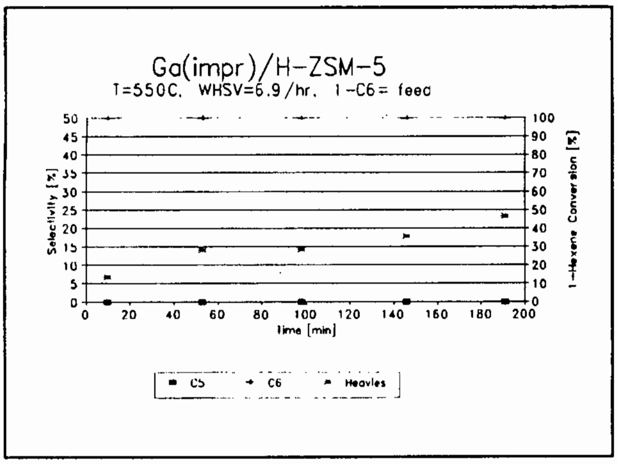

Figure 3.14 Ga(impr)/H-ZSM-5

3.2.2. 1-Octene feedstock

H-ZSM-5 and Ga(impr)/H-ZSM-5 were tested at a reaction temperature of 550°C. Ga(impr)/H-ZSM-5 was tested at two WHSV's (1.7hr^{-1} and 3.4hr^{-1}). The light products were resolved in the latter run by using the cryogenic GC method described in section 2.3.4.

3.2.2.1. C_1-C_3 light products

H-ZSM-5 showed stable selectivity to the C_1 to C_3 products with the C_3 products forming the major component of the light products (42%-44%). The selectivity to propene rapidly increases with time on stream for the Ga(impr)/H-ZSM-5 catalysts, while the C_2 compounds remain constant at 11%-14%. Selectivity to propane, ethane and methane decrease with time on stream. Ethene is the major component of the C_2 products.

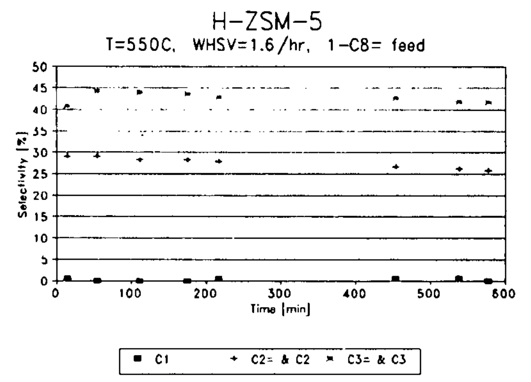

Figure 3.15 H-ZSM-5

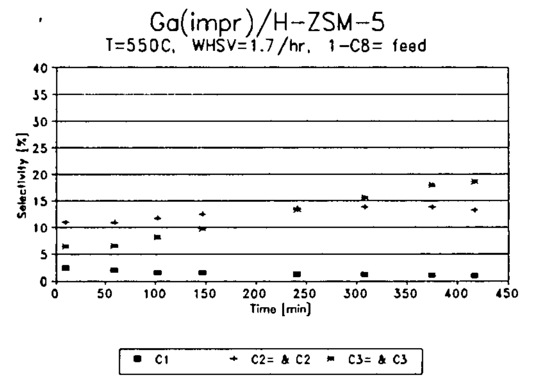

Figure 3.16 Ga(impr)/H-ZSM-5 (1.7hr^{-1})

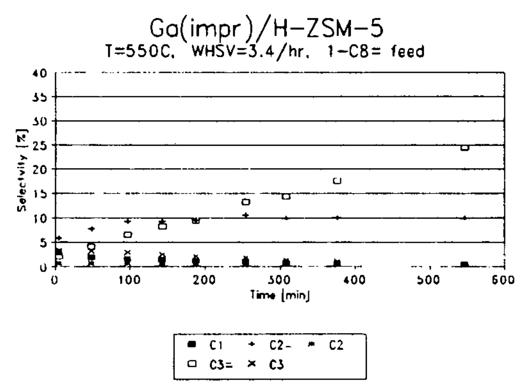

Figure 3.17 Ga(impr)/H-ZSM-5 (3.4hr^{-1})

3.2.2.2. C_4 products

The selectivity to all the C_4 compounds was stable for H-ZSM-5. The Ga(impr)/H-ZSM-5 catalysts showed an increase in selectivity to the C_4 products. The dominant C_4 component was 1-C_4=/i-C_4=. The C_4 alkanes were minor components (0% - 2%).

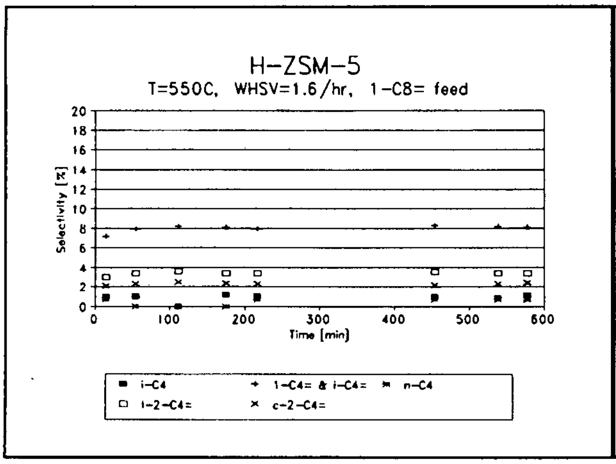

Figure 3.18 H-ZSM-5

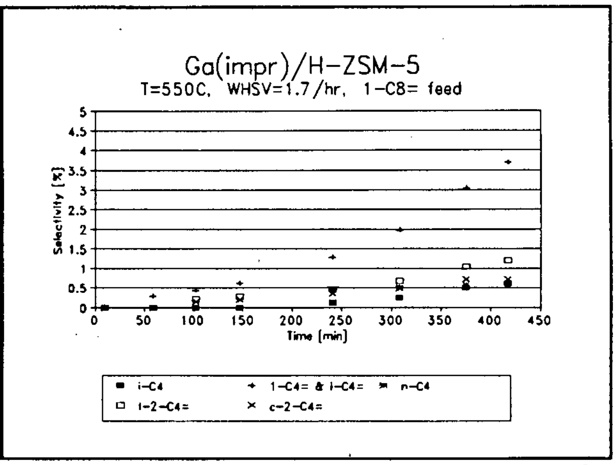

Figure 3.19 Ga(impr)/H-ZSM-5 (1.7hr^{-1})

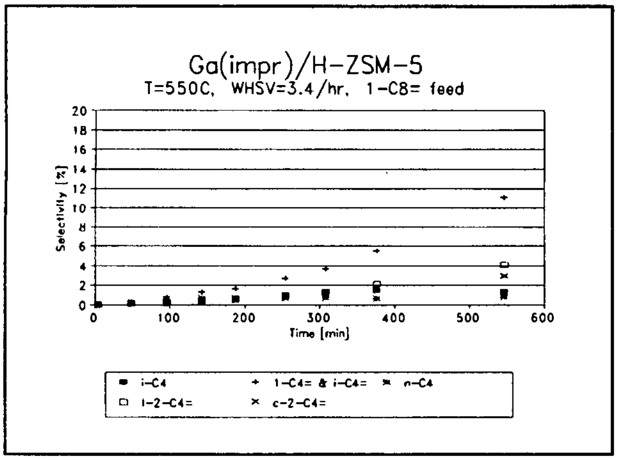

Figure 3.20 Ga(impr)/H-ZSM-5 (3.4hr^{-1})

3.2.2.3. Aromatic (BTEX) products

The selectivity to aromatic products was stable and low (15%) for H-ZSM-5. The selectivity to benzene and toluene decreased sharply with time on stream for Ga(impr)/H-ZSM-5. Toluene was the major initial aromatic compound (30%). The selectivity to the xylenes remained constant (10% for Ga(impr)/H-ZSM-5) for all catalysts.

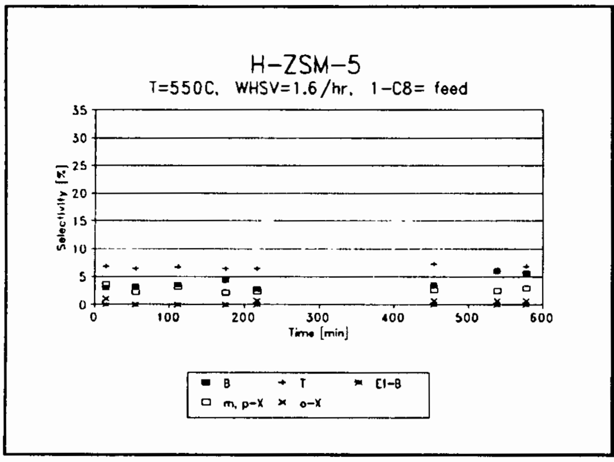

Figure 3.21 H-ZSM-5

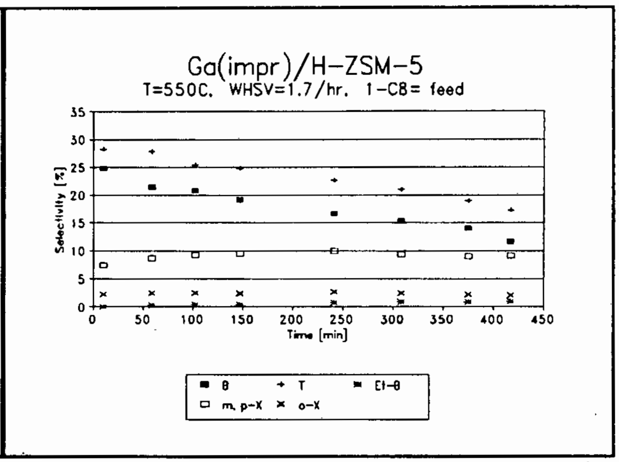

Figure 3.22 Ga(impr)/H-ZSM-5 (1.7hr^{-1})

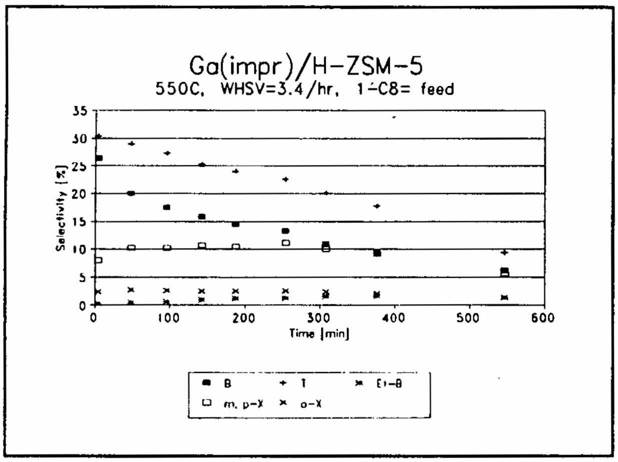

Figure 3.23 Ga(impr)/H-ZSM-5 (3.4hr^{-1})

3.2.2.4. C_5,C_6 heavy products and 1-octene conversion

For all catalysts, the conversion of the 1-octene feedstock remained at 100% during the time on stream. There were trace quantities of C_5, C_6 and heavy products present for H-ZSM-5. For the Ga(impr)/H-ZSM-5 catalyst, selectivities of 15% - 20% to heavy products were obtained, while selectivities to C_5 and C_6 products was low (0% to 2%).

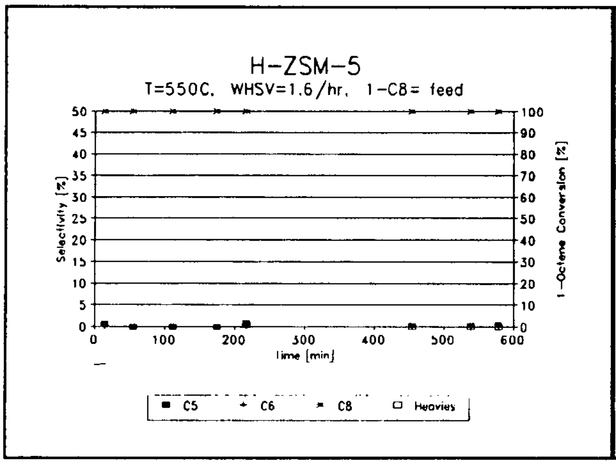

Figure 3.24 H-ZSM-5

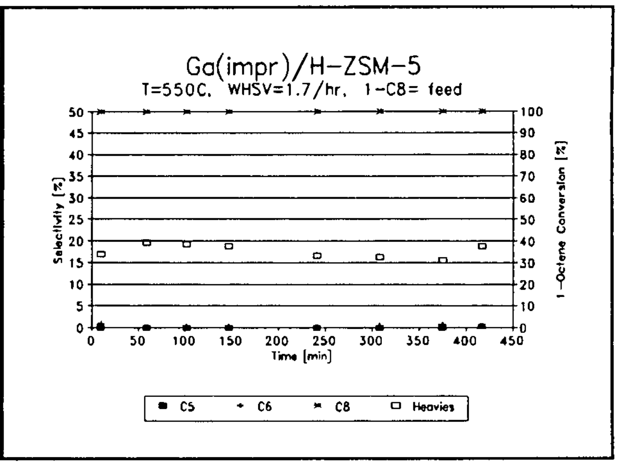

Figure 3.25 Ga(impr)/H-ZSM-5 (1.7hr^{-1})

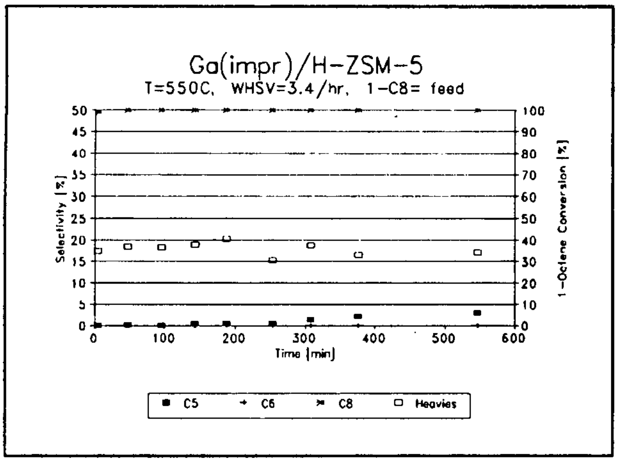

Figure 3.26 Ga(impr)/H-ZSM-5 (3.4hr^{-1})

3.3. Effect of Temperature

The effect of temperature on initial product selectivity was investigated (section 3.3.1. and section 3.3.2.). Some problems were encountered with the catalysts that displayed large changes in product selectivity with time on stream (Ga(impr)/H-ZSM-5 and Ga(ionx)/H-ZSM-5). Hence, the first sample was taken after 15 minutes on stream. The catalysts were regenerated (section 2.3.8.2) between each temperature increment. However, as repeated regeneration (redox) cycles are reported to increase gallium dispersion and hence increase catalyst activity [Changyu et al. 1988], this may have influenced the selectivity data.

At low reaction temperatures (<350°C) the appearance of large amounts of heavy oligomers (15%-25%) complicated the GC analysis as they masked the appearance of BTEX aromatics i.e. the C_9-C_{12} oligomers have similar retention times to the BTEX aromatic products. At higher reaction temperatures (>400°C) the conversion of the feed was typically 100%.

The light products were resolved by cryogenic GC analysis (section 2.3.3.) in most of the runs. However, 1-butene/i-butene and p-xylene/m-xylene could be resolved.

3.3.1. 1-Hexene feedstock

Ga(mix)/H-ZSM-5, Ga(ionx)/H-ZSM-5 and Ga(impr)/H-ZSM-5 were tested at reaction temperatures between 250°C and 550°C and WHSV's between 5hr^{-1} and 7hr^{-1}. H-ZSM-5 was tested between at reaction temperatures between 350°C and 500°C. There were difficulties with Ga(impr)/H-ZSM-5 and Ga(ionx)/H-ZSM-5 at high reaction temperatures (>500°C), as rapid changes in product selectivity occur (section 3.2.1.).

3.3.1.1. C_1-C_3 light products

Selectivity to all light products increased with increase in reaction temperature for H-ZSM-5 and Ga(mix)/H-ZSM-5. The C_3 products were the major components of the light products at all reaction temperatures. The selectivity to light products reached a maximum at 350°C for Ga(impr)/H-ZSM-5 and Ga(ionx)/H-ZSM-5 and then declined. Propene is the major light product at 350°C, but at higher reaction temperatures (550°C) ethene became the dominant component. Selectivity to methane increases with increase in reaction temperature.

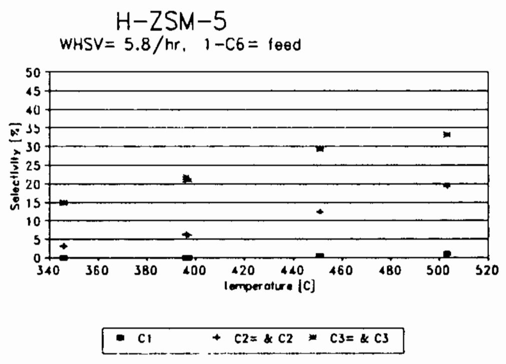

Figure 3.27 H-ZSM-5 (350°C-500°C)

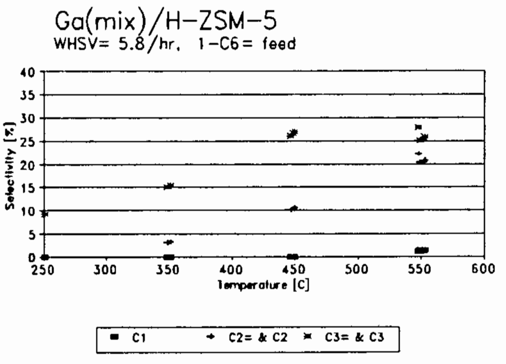

Figure 3.28 Ga(mix)/H-ZSM-5

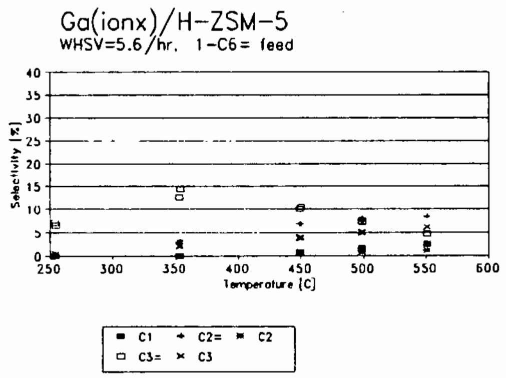

Figure 3.29 Ga(ionx)/H-ZSM-5

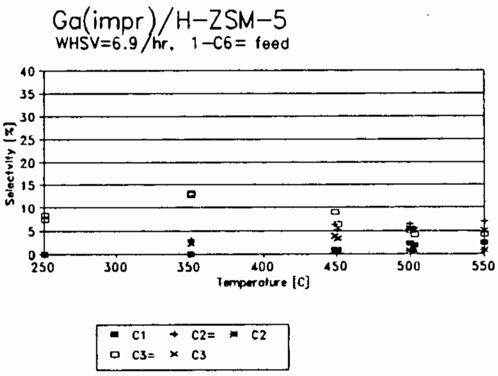

Figure 3.30 Ga(impr)/H-ZSM-5

3.3.1.2. C_4 products

The selectivity to iso-butane and n-butane decreased linearly with reaction temperature for H-ZSM-5. The C_4 alkenes showed stable selectivity over the temperature range. For Ga(mix)/H-ZSM-5, iso-butane was the dominant C_4 product between 350°C and 450°C. At 550°C 1-C_4=/i-C_4= was the dominant C_4 product. The selectivity to 1-C_4=/i-C_4= reaches a maximum between 350°C and 450°C for Ga(ionx)/H-ZSM-5 and Ga(ionx)/H-ZSM-5.

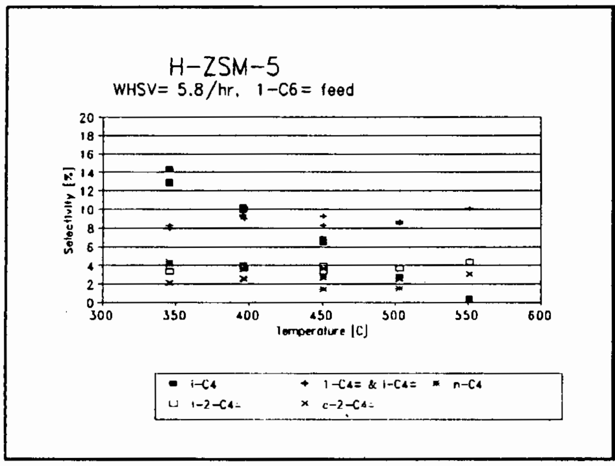

Figure 3.31 H-ZSM-5 (350°C-500°C)

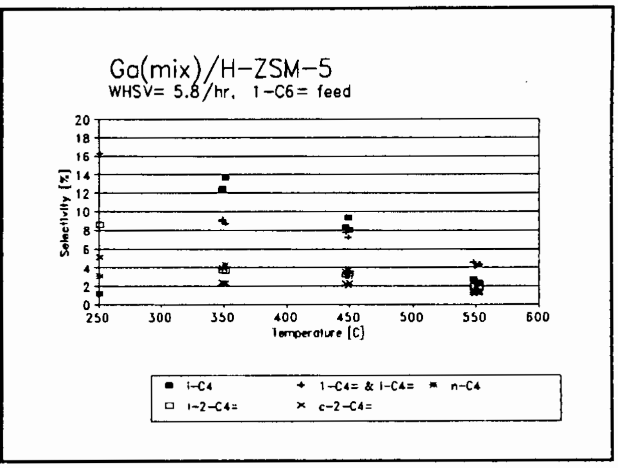

Figure 3.32 Ga(mix)H-ZSM-5

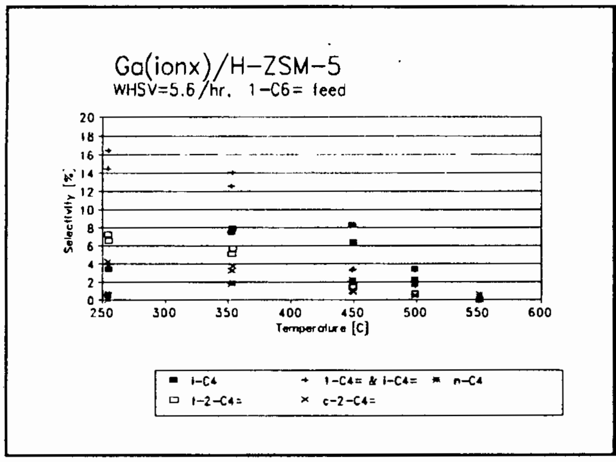

Figure 3.33 Ga(ionx)/H-ZSM-5

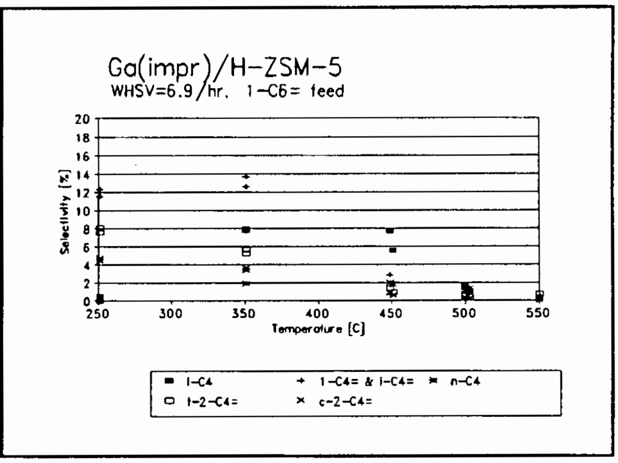

Figure 3.34 Ga(impr)/H-ZSM-5

3.3.1.2. C_4 products

The selectivity to iso-butane and n-butane decreased linearly with reaction temperature for H-ZSM-5. The C_4 alkenes showed stable selectivity over the temperature range. For Ga(mix)/H-ZSM-5, iso-butane was the dominant C_4 product between 350°C and 450°C. At 550°C 1-C_4=/i-C_4= was the dominant C_4 product. The selectivity to 1-C_4=/i-C_4= reaches a maximum between 350°C and 450°C for Ga(ionx)/H-ZSM-5 and Ga(impr)/H-ZSM-5.

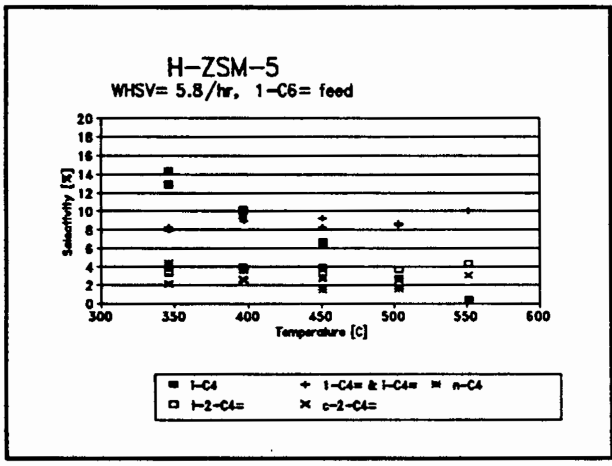

Figure 3.31 H-ZSM-5 (350°C-500°C)

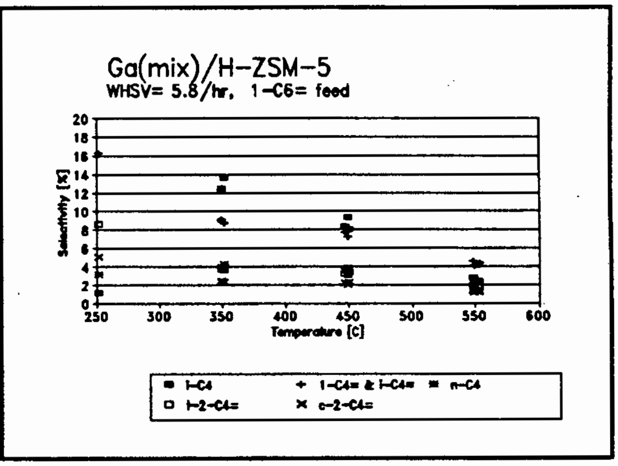

Figure 3.32 Ga(mix)H-ZSM-5

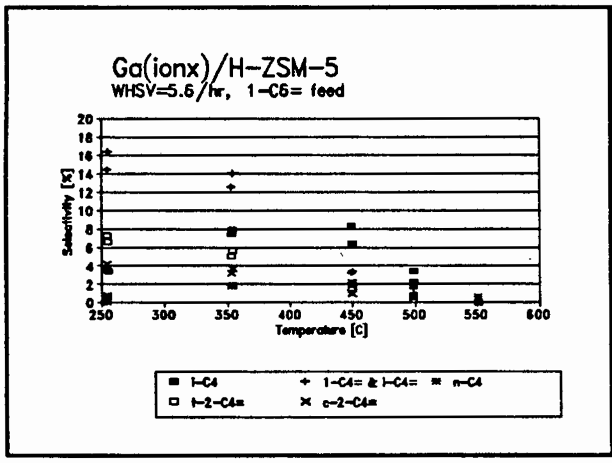

Figure 3.33 Ga(ionx)/H-ZSM-5

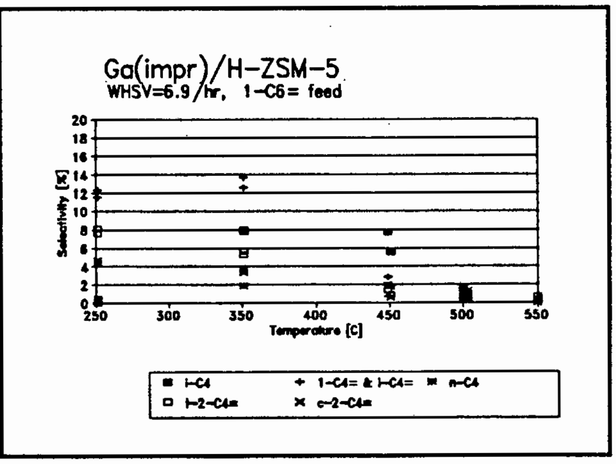

Figure 3.34 Ga(impr)/H-ZSM-5

3.3.1.3. Aromatic (BTEX) products

The selectivity to aromatic products remains constant over the temperature range for H-ZSM-5. The dominant aromatic products are toluene and p/m-xylene. The selectivity to benzene and toluene increases with reaction temperature for Ga(mix)/H-ZSM-5 while selectivity to the xylenes remains constant. There is an increase in selectivity to benzene with increase in reaction temperature for Ga(ionx)/H-ZSM-5 and Ga(impr)/H-ZSM-5. The selectivity to toluene and p/m-xylene reach a maximum at 500°C and 450°C respectively.

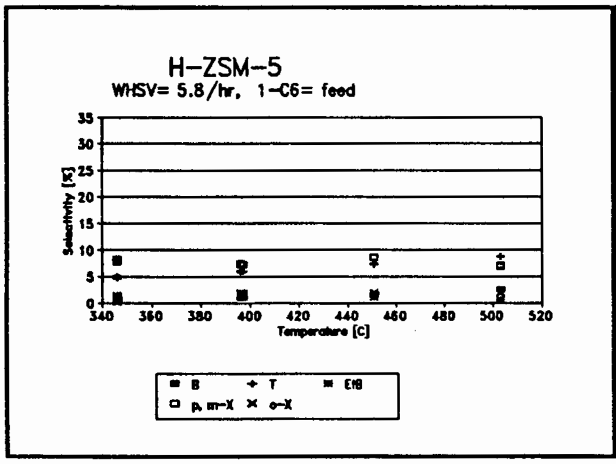

Figure 3.35 H-ZSM-5 (350°C-500°C)

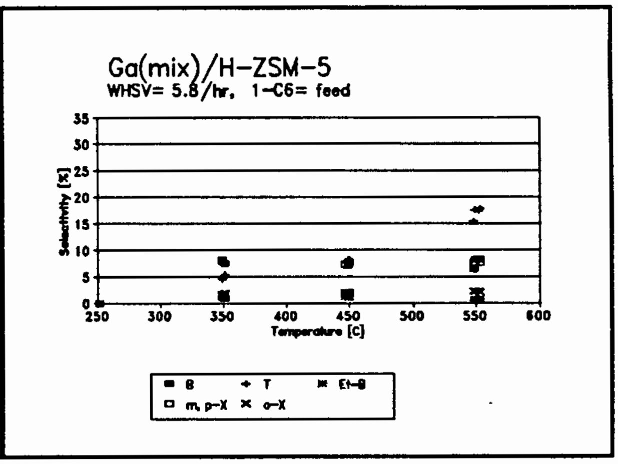

Figure 3.36 Ga(mix)/H-ZSM-5

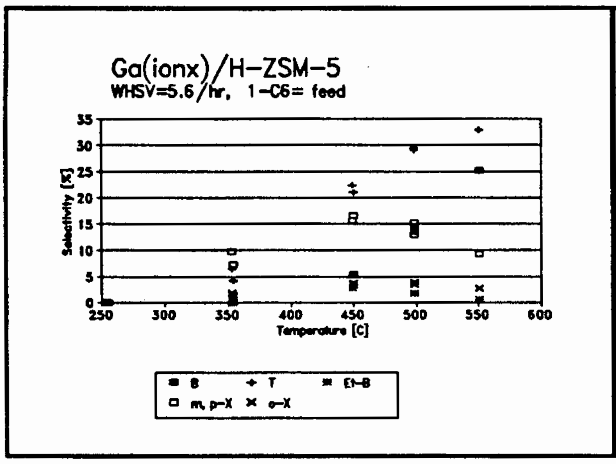

Figure 3.37 Ga(ionx)/H-ZSM-5

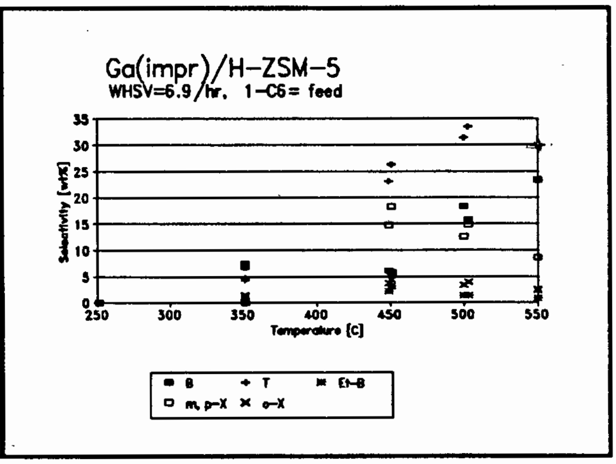

Figure 3.38 Ga(impr)/H-ZSM-5

3.3.1.4. C_5, heavy products and 1-hexene conversion

The conversion of 1-hexene reached 100% for all catalysts at reaction temperatures greater than 450°C and was at all times greater than 90%. The selectivity to C_5 and heavy products decreased with increase in reaction temperature.

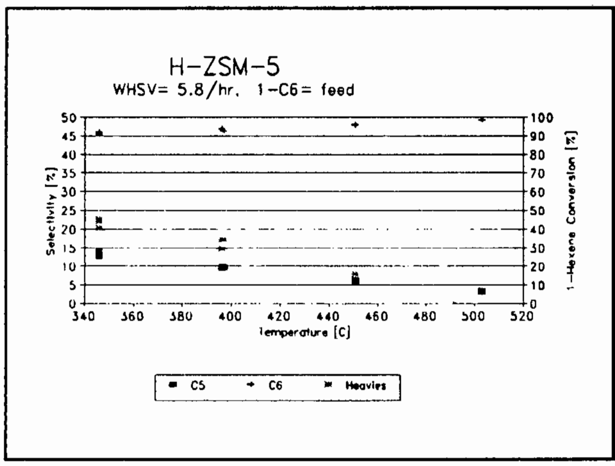

Figure 3.39 H-ZSM-5 (350°C - 500°C)

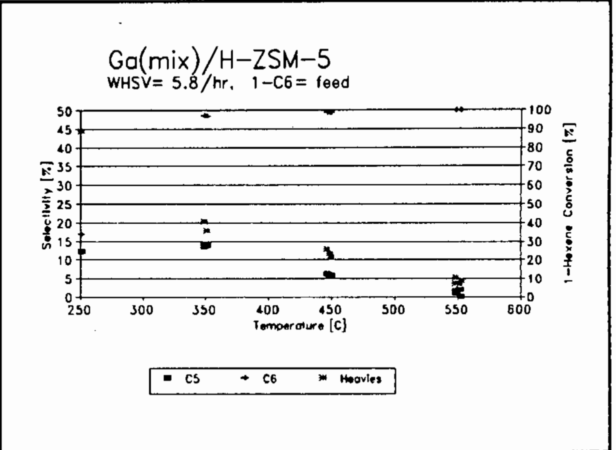

Figure 3.40 Ga(mix)/H-ZSM-5

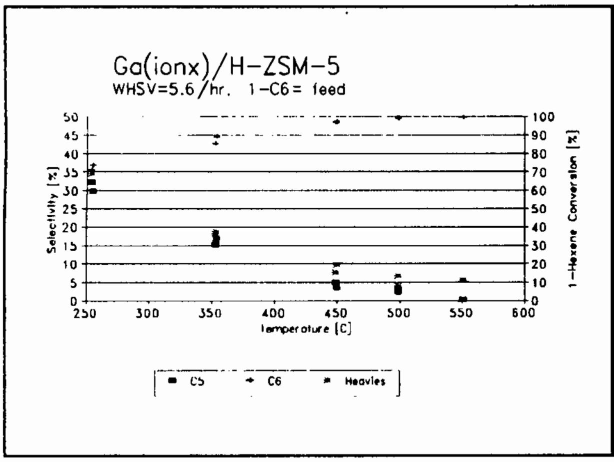

Figure 3.41 Ga(ionx)/H-ZSM-5

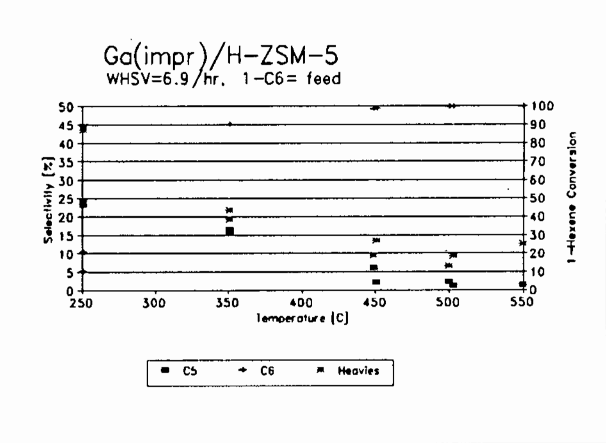

Figure 3.42 Ga(impr)/H-ZSM-5

3.3.2. 1-Octene feedstock

H-ZSM-5 and Ga(impr)/H-ZSM-5 were tested with 1-octene feed at temperatures between 250°C and 550°C and WHSV of 1.6hr^{-1} and 3.4hr^{-1} respectively. It was not possible to obtain higher WHSV's for 1-octene due to limitations of the double stage saturator, i.e. the vapour pressure of 1-octene could not be raised sufficiently.

3.3.2.1. C_1-C_3 light products

The selectivity to ethene and propene increased with increase in reaction temperature for H-ZSM-5 while selectivity to ethane and propane remain low. The selectivity to propene reached a maximum at 350°C for Ga(impr)/H-ZSM-5 and then declined.

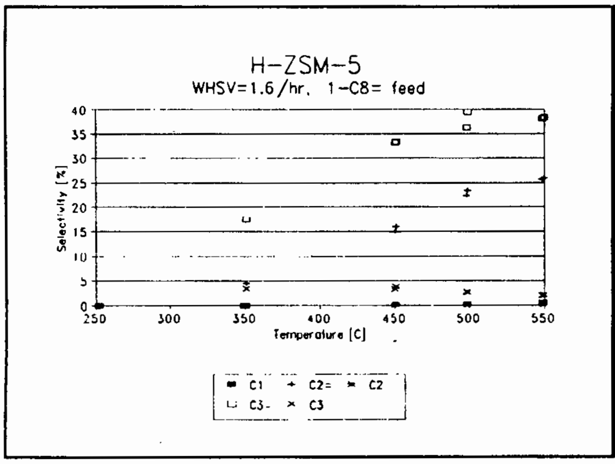

Figure 3.43 H-ZSM-5

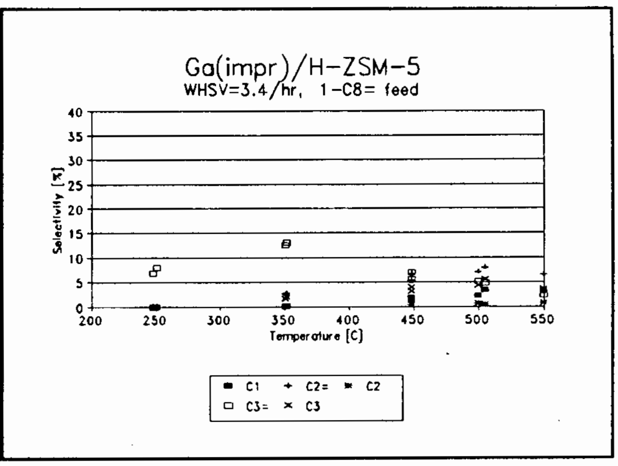

Figure 3.44 Ga(impr)/H-ZSM-5

3.3.2.2. C_4 products

The selectivity to C_4 products decreased with increase in reaction temperature. The selectivity to iso-butane reached a maximum at 350°C and the decreased. The dominant C_4 product is $1\text{-}C_4{=}/i\text{-}C_4{=}$ at reaction temperatures below 550°C.

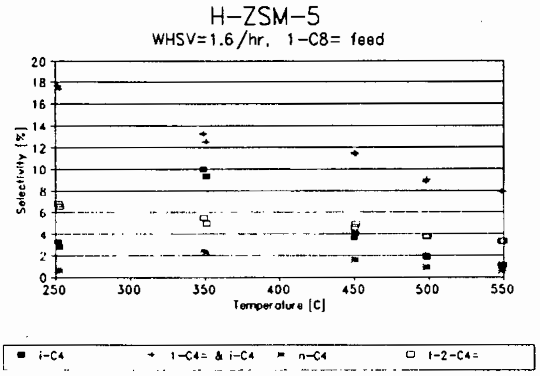

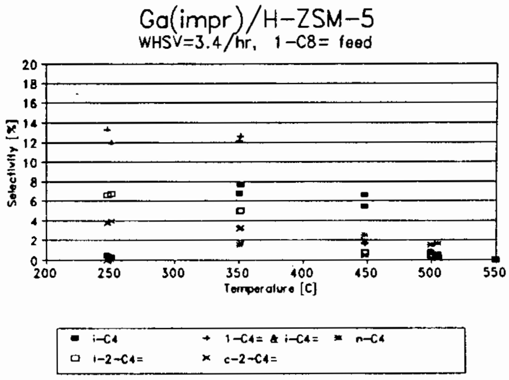

Figure 3.45 H-ZSM-5

Figure 3.46 Ga(impr)/H-ZSM-5

3.3.2.3. Aromatic (BTEX) products

The selectivity to aromatic products increased with increase in reaction temperature. The increase was most marked for Ga(impr)/H-ZSM-5. At high reaction temperatures (>500°C) toluene and benzene were the dominant aromatic compounds while at low reaction temperatures m/p-xylene is the major aromatic product. The selectivity to m/p-xylene reached a maximum at 450°C for Ga(impr)/H-ZSM-5.

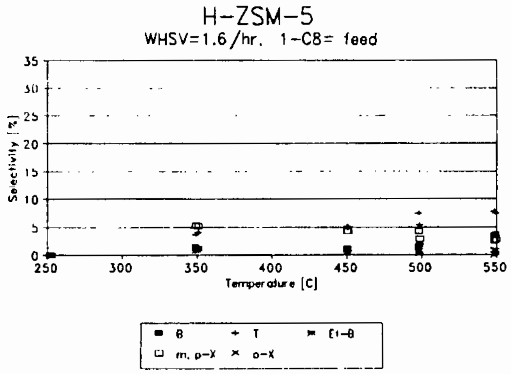

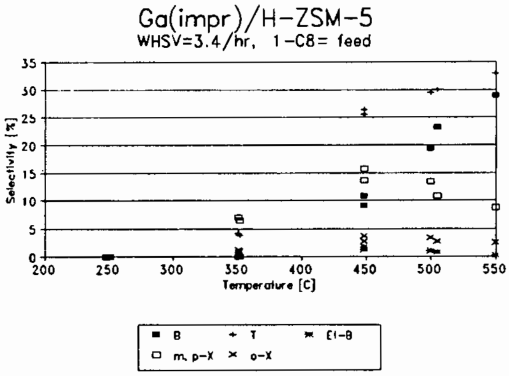

Figure 3.47 H-ZSM-5

Figure 3.48 Ga(impr)/H-ZSM-5

3.3.2.4. C_5,C_6 heavy products and 1-octene conversion

The conversion of 1-octene reached 100% at 450°C for H-ZSM-5. For Ga(impr)/H-ZSM-5 the conversion of 1-octene was 100% over the whole temperature range. Selectivity to C_5, C_6 and heavy products decreased with increase in reaction temperature.

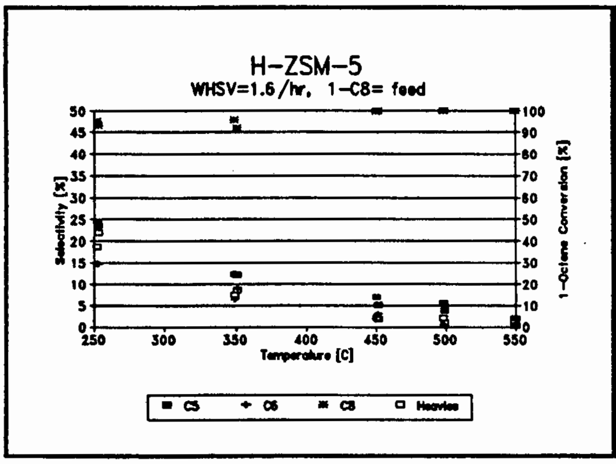

Figure 3.49 H-ZSM-5

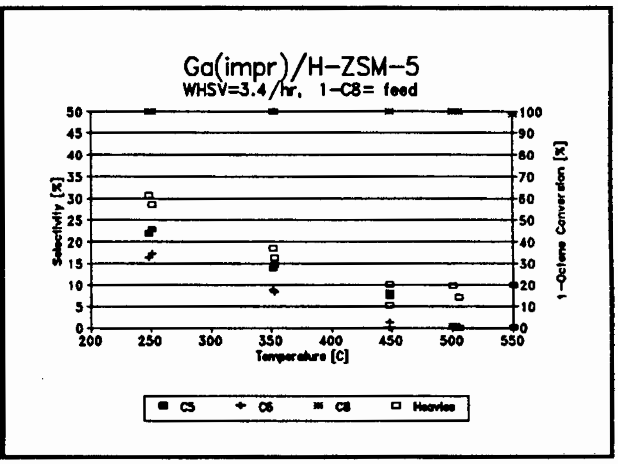

Figure 3.50 Ga(impr)/H-ZSM-5

3.4. Effect of Hydrogen Pretreatments

The effect of hydrogen pretreatments on Ga/H-ZSM-5 catalysts was investigated and is discussed further in section 4.7. The Ga/H-ZSM-5 catalysts were pretreated with hydrogen prior to catalytic testing (section 2.3.8.3). Unfortunately the run with Ga(impr)/H-ZSM-5 lasted less than 2 hours and hence trends are difficult to analyze with this catalyst.

In addition to catalytic testing at constant reaction temperatures, a temperature profile of Ga(mix)/H-ZSM-5 was carried out at reaction temperatures between 350°C and 550°C. The catalyst was regenerated (section 2.3.8.2) and hydrogen pretreated (section 2.3.8.3) before each temperature increment.

3.4.1. C_1-C_3 light products

There was an increase in selectivity to light products for Ga(mix)/H-ZSM-5 and Ga(ionx)/H-ZSM-5. Propane/propene was the dominant light product in both cases. The selectivity to light products remained constant for Ga(mix)/H-ZSM-5 (temperature profile) with C_3 compounds the major light product.

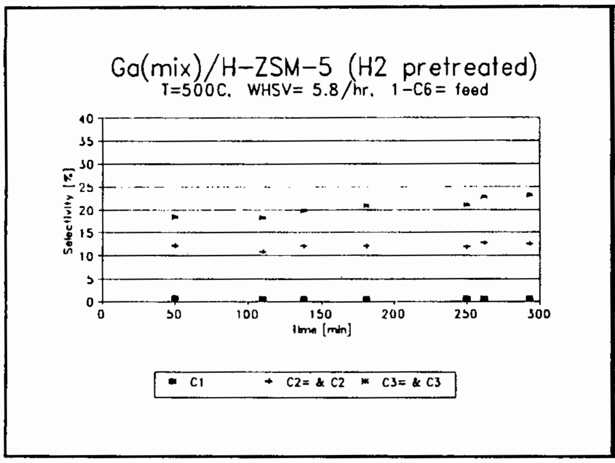

Figure 3.51 Ga(mix)/H-ZSM-5

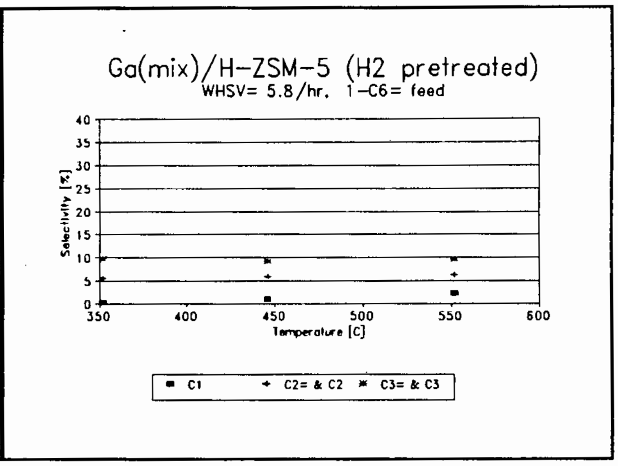

Figure 3.52 Ga(mix)/H-ZSM-5 (Temperature profile)

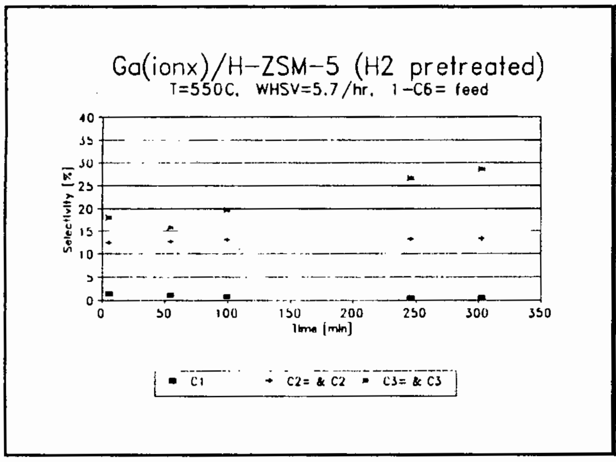

Figure 3.53 Ga(ionx)/H-ZSM-5

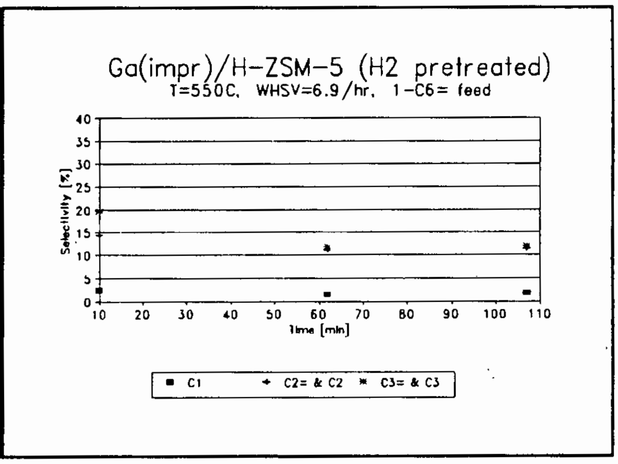

Figure 3.54 Ga(impr)/H-ZSM-5

3.4.2. C_4 products

The selectivity to C_4 compounds increased slightly with time on stream for Ga(mix)/H-ZSM-5 and Ga(ionx)/H-ZSM-5. The dominant C_4 product, with extended time on stream, was 1-C_4=/i-C_4=. The temperature profile of Ga(mix)/H-ZSM-5 shows a decrease in selectivity to C_4 products with increase in reaction temperature. The dominant C_4 product is n-butane for this catalyst.

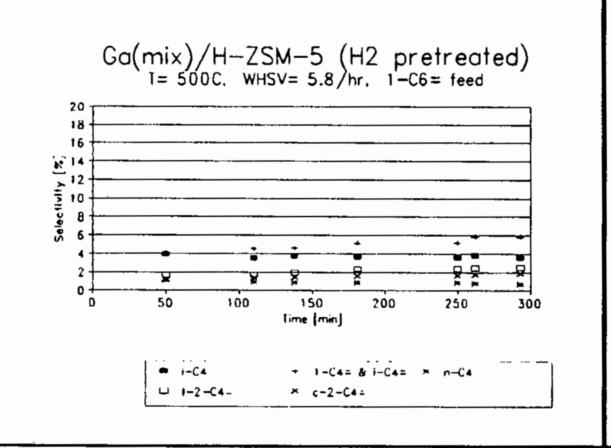

Figure 3.55 Ga(mix)/H-ZSM-5

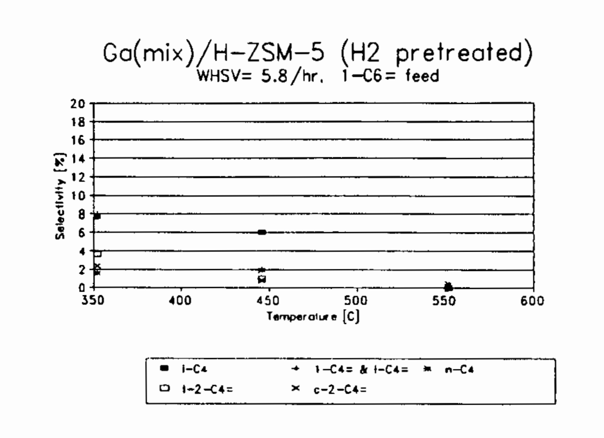

Figure 3.56 Ga(mix)/H-ZSM-5 (temperature profile)

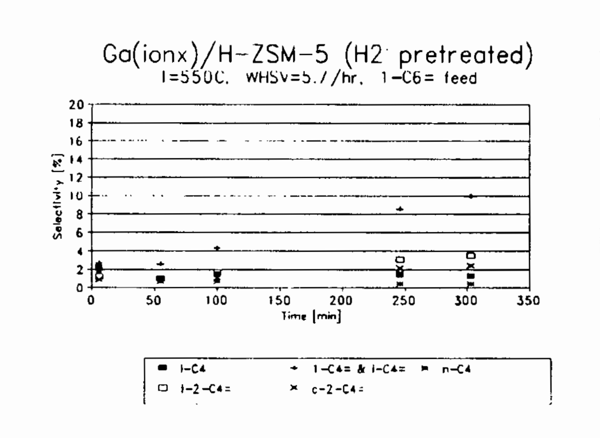

Figure 3.57 Ga(ionx)/H-ZSM-5

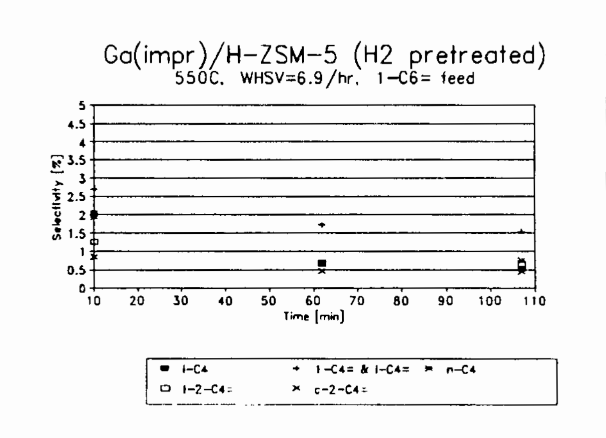

Figure 3.58 Ga(impr)/H-ZSM-5

3.4.3. Aromatic (BTEX) products

Toluene and m/p-xylene were the dominant aromatic products (18% and 11% respectively) for Ga(mix)/H-ZSM-5 at 500°C. The selectivity to benzene and toluene were similar for Ga(ionx)/H-ZSM-5 and Ga(impr)/H-ZSM-5 (15%-18%). There was a decline in selectivity to aromatic compounds for Ga(ionx)/H-ZSM-5 with time on stream. The temperature profile of Ga(mix)/H-ZSM-5 shows that selectivity to m/p-xylene reached a maximum at 450°C (and then declined) and that benzene and toluene are the dominant aromatic products at 550°C.

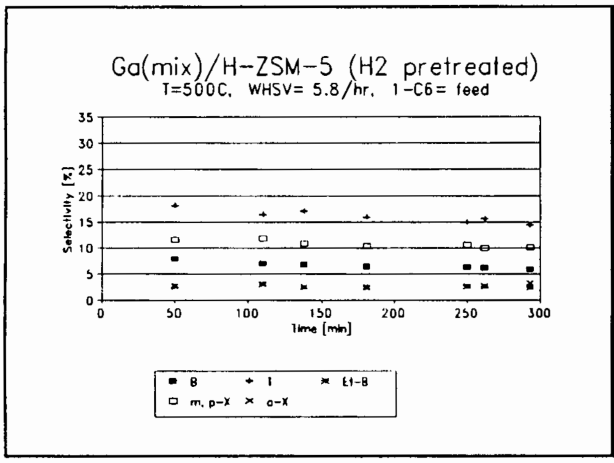

Figure 3.59 Ga(mix)/H-ZSM-5

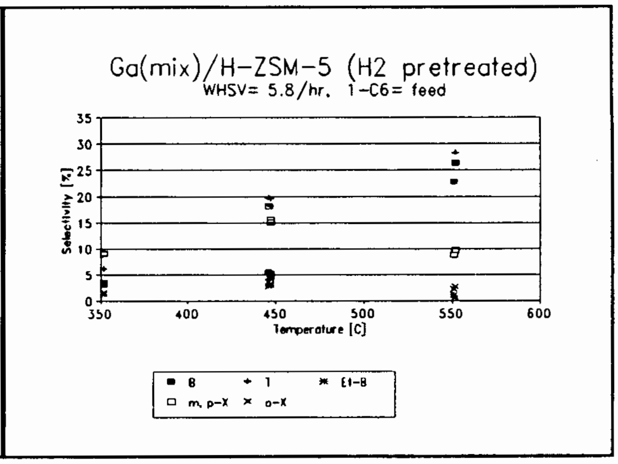

Figure 3.60 Ga(mix)/H-ZSM-5 (temperature profile)

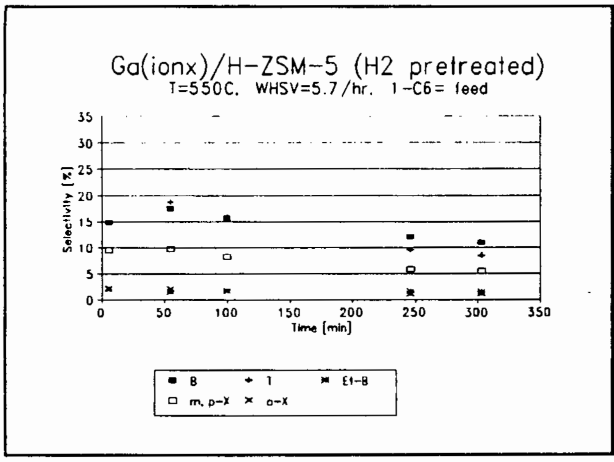

Figure 3.61 Ga(ionx)/H-ZSM-5

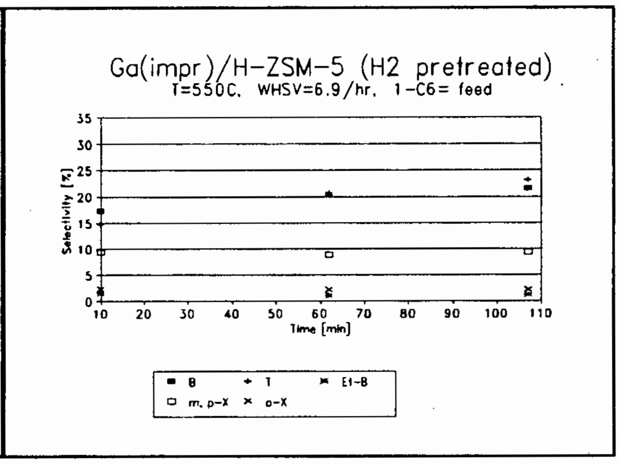

Figure 3.62 Ga(impr)/H-ZSM-5

3.4.4. C_5, heavy products and 1-hexene conversion

The conversion of 1-hexene was 100% in all cases (except for the temperature profile of Ga(mix)/H-ZSM-5 when the reaction temperature was below 350°C). The selectivity to C_5 and heavy products was constant during the time on stream for all catalysts. There was a decrease in selectivity to C_5 and heavy compounds with increase in reaction temperature for Ga(mix)/H-ZSM-5 (temperature profile).

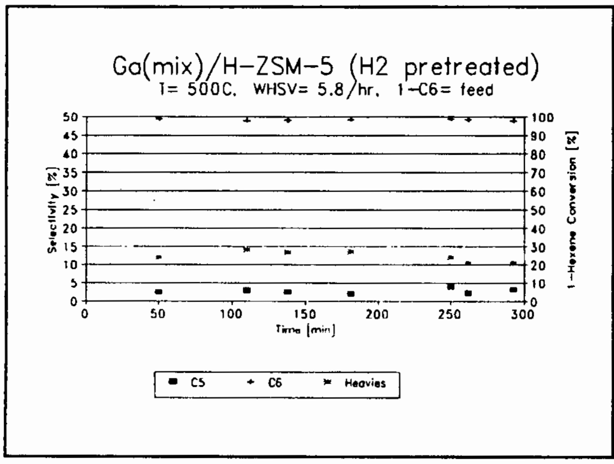

Figure 3.63 Ga(mix)/H-ZSM-5

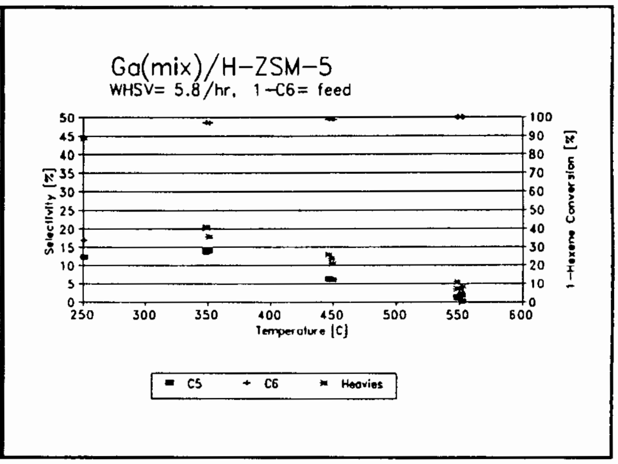

Figure 3.64 Ga(mix)/H-ZSM-5 (temperature profile)

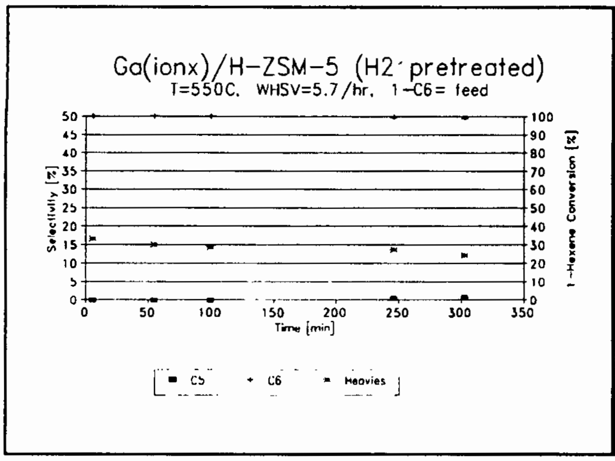

Figure 3.65 Ga(ionx)/H-ZSM-5

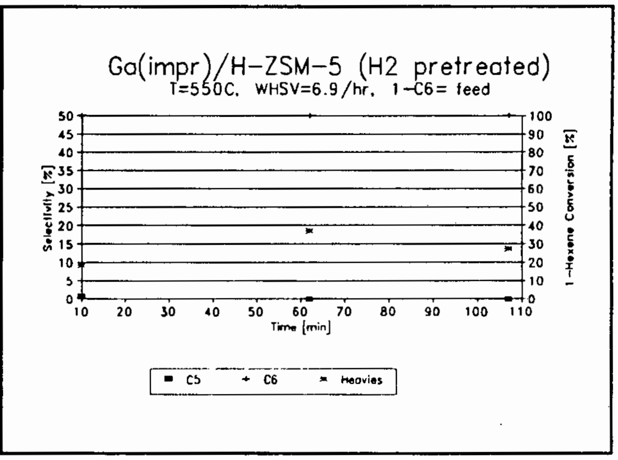

Figure 3.66 Ga(impr)/H-ZSM-5

3.5. Effect of WHSV

The effect of WHSV on product selectivity was carried out at different reaction temperatures for H-ZSM-5 (500°C) and Ga(mix)/H-ZSM-5 (250°C and 500°C). The WHSV range was from 5.2hr^{-1} to 27hr^{-1} for Ga(mix)/H-ZSM-5 at 500°C and 5.8hr^{-1} to 11hr^{-1} for Ga(mix)/H-ZSM-5 at 250°C and H-ZSM-5.

3.5.1. C_1-C_3 light products

In all cases a slight decrease in selectivity to light products was observed. Propene and ethene were the dominant light products at 500°C. At the reaction temperature of 250°C, propene was the only light product.

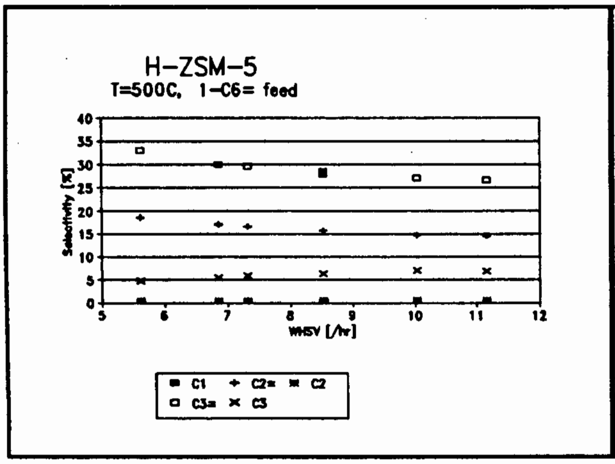

Figure 3.67 H-ZSM-5 (500°C)

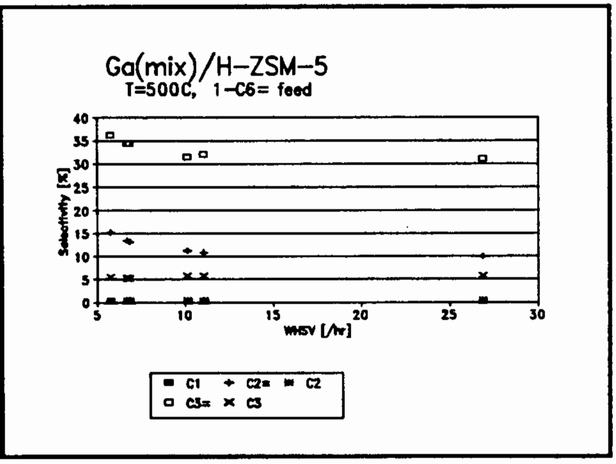

Figure 3.68 Ga(mix)/H-ZSM-5 (500°C)

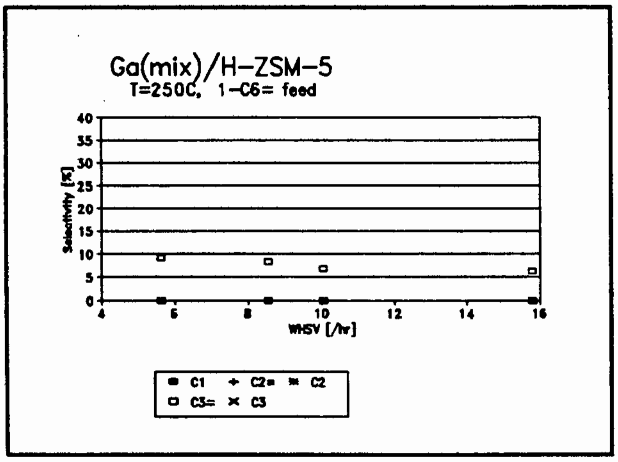

Figure 3.69 Ga(mix)/H-ZSM-5 (250°C)

3.5.2. C_4 products

The C_4 products remained constant over the WHSV range at the reaction temperature of 500°C for H-ZSM-5. There was a slight increase in selectivity to 1-C_4=/i-C_4= for Ga(mix)/H-ZSM-5 at 500°C. At the reaction temperature of 250°C a decrease in selectivity to C_4 products with increase in WHSV occured. At this reaction temperature the butenes were the dominant C_4 compounds.

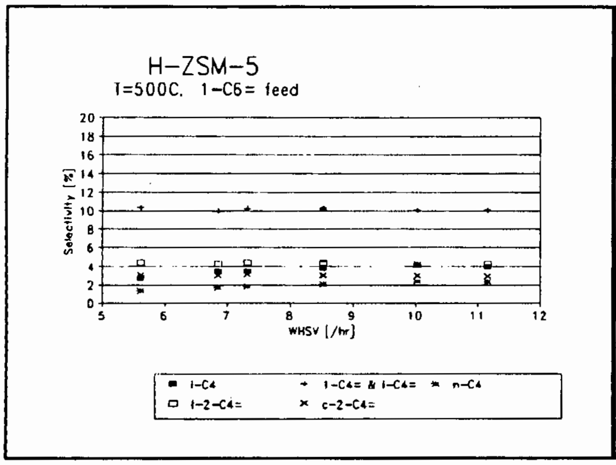

Figure 3.70 H-ZSM-5 (500°C)

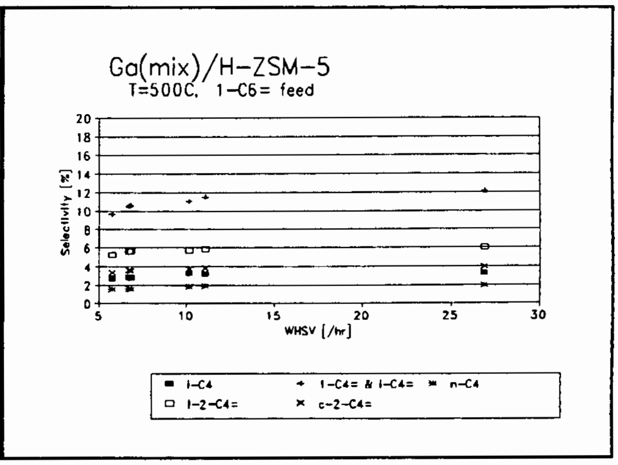

Figure 3.71 Ga(mix)/H-ZSM-5 (500°C)

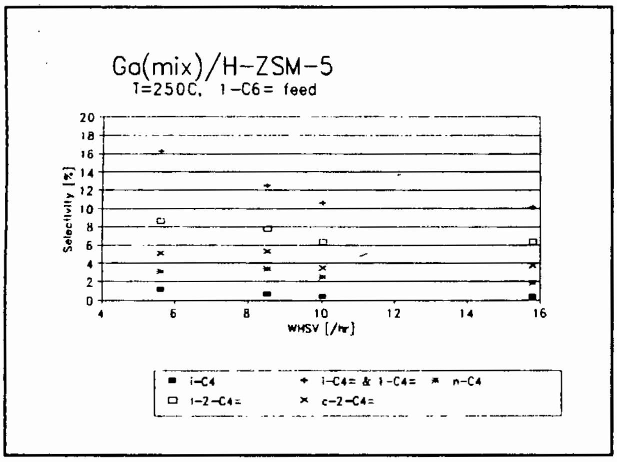

Figure 3.72 Ga(mix)/H-ZSM-5 (250°C)

3.5.3. Aromatic (BTEX) products

The selectivity to aromatic products remained constant over the WHSV range for all catalysts. There were no aromatic compounds present at the reaction temperature of 250°C (Ga(mix)/H-ZSM-5) and hence no graph is shown. Toluene and m/p-xylene were the dominant aromatic products at 500°C for H-ZSM-5 and Ga(mix)/H-ZSM-5 with similar selectivities of 5% - 8%.

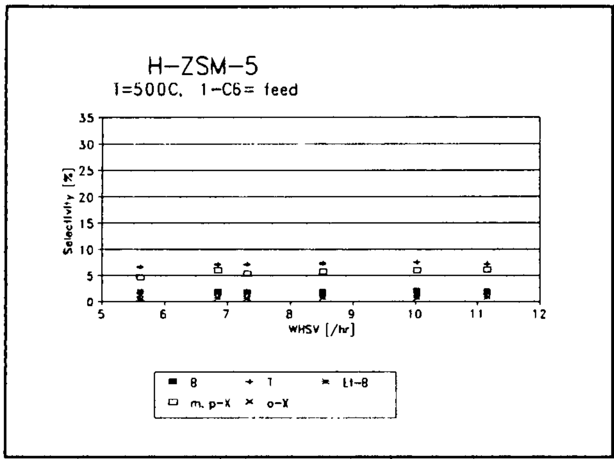

Figure 3.73 H-ZSM-5 (500°C)

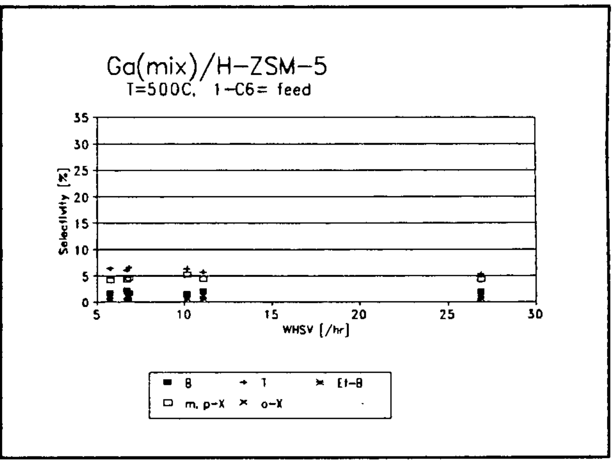

Figure 3.74 Ga(mix)/H-ZSM-5 (500°C)

3.5.4. C_5, heavy products and 1-hexene conversion

The conversion of 1-hexene declined for all the catalysts with increase in WHSV of the feed. The decline was greatest at low temperatures (250°C) for Ga(mix)/H-ZSM-5 where the conversion dropped from 35% to 18%. The selectivity to C_5 and heavy products remained constant over the WHSV range for H-ZSM-5 and Ga(mix)/H-ZSM-5 at 500°C.

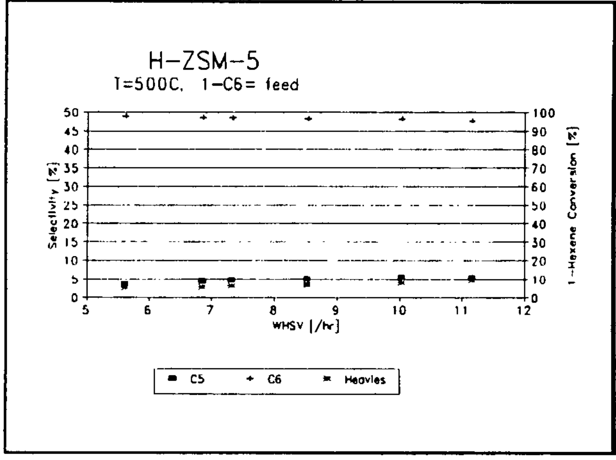

Figure 3.75 H-ZSM-5 (500°C)

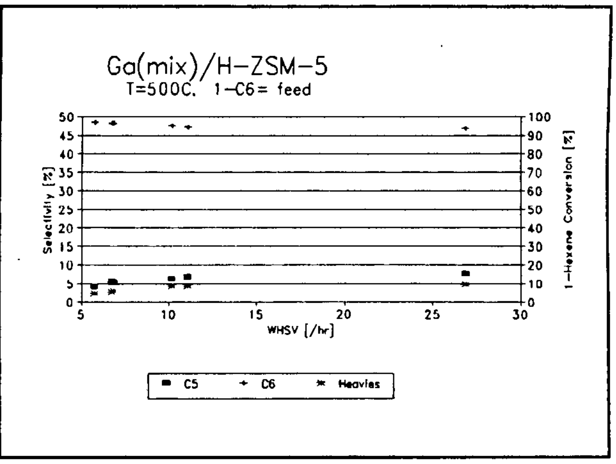

Figure 3.76 Ga(mix)/H-ZSM-5 (500°C)

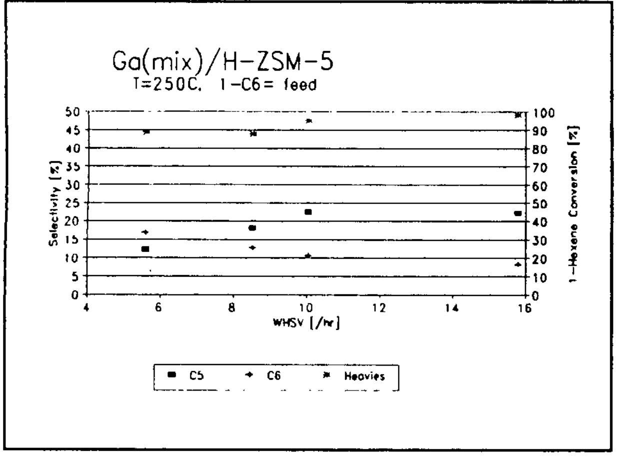

Figure 3.77 Ga(mix)/H-ZSM-5 (250°C)

3.6. Summary of Experimental Runs

3.6.1 Summary of runs at constant reaction temperature

These runs showed that H-ZSM-5 zeolite catalysts do not display any discernable change in product selectivity or reactant conversion during the time on stream (up to 10 hours). However, Ga/H-ZSM-5 catalysts showed large changes in product selectivity with time on stream. Hydrogen treatment of Ga(mix)/H-ZSM-5 catalysts caused an increase in selectivity to BTEX, but lowered selectivity to BTEX for Ga(impr)/H-ZSM-5. The results are summarized in Table 3.4 and Table 3.5. The values tabulated are from the first on-line GC sample taken for each run i.e. at a time on stream of 15 minutes.

3.6.1.1. C_1-C_6 products

Table 3.4 Summary of runs at constant reaction temperature

Catalyst	C_1	$C_2\&C_2=$	$C_3\&C_3=$	C_4	$C_4=$	C_6	ΣC_1-C_6
1-hexene feed							
Ga(mix)[a]	0	20	35	6	15	4	80
Ga(impr)[b]	3	7	10	1	1	0	22
Ga(ionx)[b]	1	18	24	4	6	0	53
1-octene feed at 550°C							
H-ZSM-5[c]	0	29	41	2	12	0	84
Ga(impr)[c]	2	10	6	0	0	0	18
Ga(impr)[d]	3	8	5	0	0	0	16
H_2 pretreated catalysts with 1-hexene feed							
Ga(mix)[a]	1	12	18	5	7	3	46
Ga(impr)[b]	2	11	12	1	3	0	29
Ga(ionx)[b]	1	12	18	3	4	0	38

(a) 500°C, WHSV 5.8hr^{-1}; (b) 550°C, WHSV 6.9hr^{-1}; (c) 550°C, WHSV 1.7hr^{-1}; (d) 550°C, WHSV 3.4hr^{-1};

3.6.1.2. Aromatic and heavy products

Table 3.5 Summary of runs at constant reaction temperature

Catalyst	B	T	m & p-X	o-X	EtB	H[e]	ΣBTEX
			1-hexene feed				
Ga(mix)[a]	2	7	5	1	1	5	16
Ga(impr)[b]	27	31	8	2	1	7	69
Ga(ionx)[b]	9	21	9	3	1	4	43
			1-octene feed at 550°C				
H-ZSM-5[c]	3	7	4	1	0	1	14
Ga(impr)[c]	25	28	7	2	0	17	62
Ga(impr)[d]	26	30	8	2	0	17	66
			H_2 pretreated catalysts with 1-hexene feed				
Ga(mix)[a]	8	18	12	3	3	12	44
Ga(impr)[b]	20	20	9	2	1	18	52
Ga(ionx)[b]	15	15	10	2	2	16	44

(a) 500°C, WHSV 5.8hr^{-1}; (b) 550°C, WHSV 6.9hr^{-1}; (c) 550°C, WHSV 1.7hr^{-1}; (d) 550°C, WHSV 3.4hr^{-1}; (e) Heavies

3.6.2. Summary of temperature profiles

The temperature profiles all show an increase in selectivity to BTEX and a decrease in selectivity to heavy products with increase in reaction temperature. The results of the temperature profiles, at reaction temperatures of 350°C and 550°C, are shown in Table 3.6 and Table 3.7.

3.6.2.1. C_1-C_5 products

Table 3.6 Summary of temperature profile runs

Catalyst	Temp [°C]	C_1	C_2&C_2=	C_3&C_3=	C_4	C_4=	C_6	ΣC_1-C_6
Temperature profiles with 1-hexene feed								
H-ZSM-5[a]	350	0	3	15	19	13	14	64
	500	1	19	33	4	15	3	75
Ga(mix)[a]	350	0	3	15	18	15	14	65
	550	1	20	25	4	7	0	57
Ga(impr)[b]	350	0	3	15	10	23	16	69
	550	2	6	9	2	1	1	21
Ga(ionx)[b]	350	0	3	15	9	21	15	63
	550	2	10	11	1	0	0	24
Temperature profiles with 1-octene feed								
H-ZSM-5[c]	350	0	5	22	12	22	12	72
	550	1	26	41	2	13	2	44
Ga(impr)[d]	350	0	3	15	9	21	15	66
	550	3	7	6	0	0	0	16
Temperature profiles of H_2 pretreated catalyst and 1-hexene feed								
Ga(mix)[a]	350	0	3	11	9	14	6	43
	550	2	8	7	0	0	0	17

(a) WHSV 5.8hr^{-1}; (b) WHSV 6.9hr^{-1}; (c) WHSV 1.7hr^{-1}; (d) WHSV 3.4hr^{-1};

3.6.2.2. Aromatic and heavy products

Table 3.7 Summary of temperature profile runs

Catalyst	Temp [°C]	B	T	m & p-X	o-X	EtB	H[e]	ΣBTEX
				Temperature ramps with 1-hexene feed				
H-ZSM-5[a]	350	1	5	8	0	1	20	15
	550	3	9	7	2	1	4	22
Ga(mix)[a]	350	1	5	7	2	1	18	16
	550	8	17	7	2	1	5	35
Ga(impr)[b]	350	0	4	7	1	1	19	13
	550	24	33	8	2	1	9	68
Ga(ionx)[b]	350	0	6	10	2	1	18	9
	550	25	33	9	3	1	6	71
				Temperature ramps with 1-octene feed				
H-ZSM-5[c]	350	1	4	5	1	1	7	12
	550	4	7	3	1	0	1	15
Ga(impr)[d]	350	0	4	7	1	1	16	13
	550	29	33	9	3	0	10	74
				Temperature ramp with H_2 pretreated catalyst and 1-hexene feed				
Ga(mix)[a]	350	3	6	9	2	1	37	21
	550	26	28	10	3	1	14	68

(a) WHSV 5.8hr^{-1}; (b) WHSV 6.9hr^{-1}; (c) WHSV 1.7hr^{-1}; (d) WHSV 3.4hr^{-1}; (e) Heavies;

3.7. TPR Data

3.7.1. β-Ga_2O_3

TPR spectra of β-Ga_2O_3 showed that no reduction of β-Ga_2O_3 took place up to a temperature of 1000°C. The TPR was repeated on three different occasions and gave the same results. It was, however, observed that a white-coloured compound was deposited on the cooler parts of the TPR tube. This proved to be highly resistant to chemical attack by concentrated nitric acid and even aqua-regia. It is speculated that sublimation of a gallium oxide was responsible. However, no analysis of the substance was made.

3.7.2. **Ga(mix)/H-ZSM-5** (Fig. 3.78 -3.79)

A Ga(mix)/H-ZSM-5 (10wt% Ga) ballmilled for 30 minutes showed only a small hydrogen adsorbance peak at *ca.* 700°C. Another sample that had been ballmilled for 4 hours with 10wt% gallium was tested under standard TPR conditions. This sample showed a similar hydrogen absorbance to the sample that had been ballmilled for 30 minutes. The peak maximum in hydrogen consumption occured at *ca.* 700°C as was the case of the sample ballmilled for 30 minutes. Hence, it is concluded that the length of time taken for physical mixing of Ga_2O_3 and H-ZSM-5 had a negligible effect on improving the degree of intimate mixing and dispersion of Ga_2O_3.

3.7.3. **Ga(ionx)/H-ZSM-5** (Fig. 3.80)

The TPR of Ga(ionx)/H-ZSM-5 (18 wt% Ga) showed a hydrogen consumption peak at ca. 600°C. This implies that the gallium is more intimately dispersed in the zeolite and hence easier to reduce as reduction of gallium requires the presence of acid sites [Price et al. 1990].

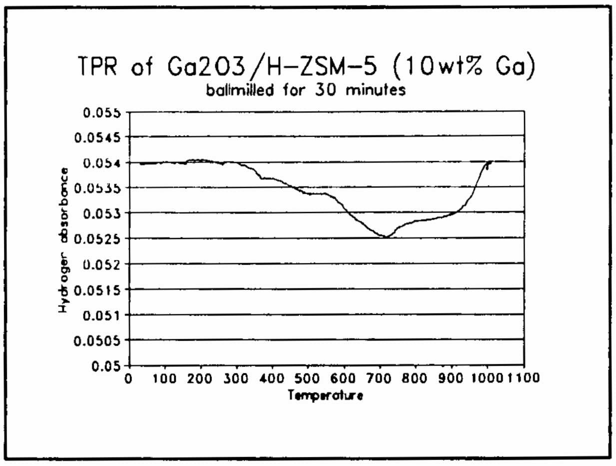

Figure 3.78 TPR of Ga(mix)/H-ZSM-5, mixed for 30 minutes

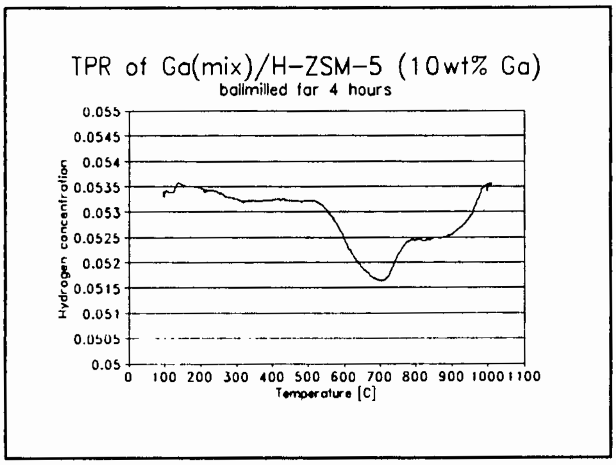

Figure 3.79 TPR of Ga(mix)/H-ZSM-5, mixed for 4 hours

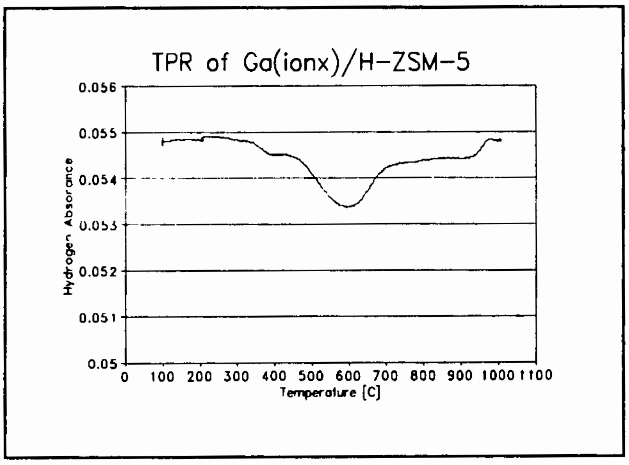

Figure 3.80 TPR of Ga(ionx)/H-ZSM-5 (18wt%Ga)

3.8. AA Analysis Of Gallium

3.8.1. Ga(ionx)/H-ZSM-5

AA analysis of the Ga(ionx)/H-ZSM-5 catalyst sample revealed that the gallium loading was 18.2wt%. This is a substantially greater gallium loading than any of the other Ga/H-ZSM-5 catalysts that were used. The level of gallium is far greater than would be expected for total ion exchange of the protonic sites. However, multivalent ions do not easily exchange univalent ions in ZSM-5. Hence the gallium was probably present as $[Ga(III)](OH)_3$ deposited in the zeolite channels. The catalyst was washed twice with 400ml deionized water after the two successive ion exchanges which was expected to remove any gallium species from the catalyst surface. However, the SEM micrographs clearly show Ga crystallite species deposited on the surface of the ZSM-5 substrate (section 3.9.5).

3.8.2. Ga(mix)/H-ZSM-5

AA analysis confirmed that the gallium loadings for these catalysts were between 4.9wt% and 5.1wt%.

3.8.3. Ga(impr)/H-ZSM-5

No AA analysis was performed on this catalyst. However, the catalyst was synthesized by incipient wetness to give a gallium loading of 5wt% and this is assumed to be correct.

3.9. SEM Results

Scanning electron microscopy (SEM) analysis was performed to detemine the morphology of the catalysts. It was hoped that it would be possible to observe the effects of physical mixing of β-Ga_2O_3 and H-ZSM-5 as well as any changes caused by impregnation and ion-exchange techniques.

3.9.1. H-ZSM-5

The SEM micrographs of H-ZSM-5 revealed that the crystallite size was between 1μm and 3μm. The crystallites seem to be of fairly uniform shape.

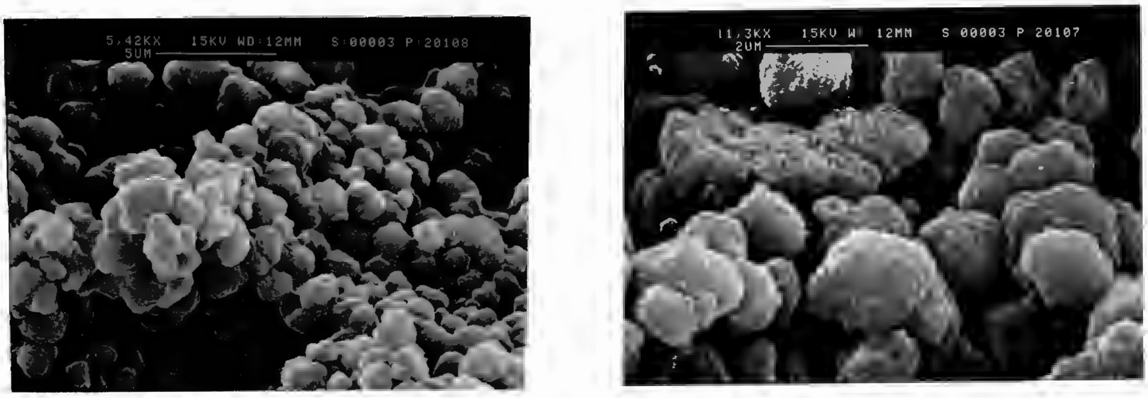

Figure 3.81 SEM micrographs of H-ZSM-5

3.9.2. β-Ga_2O_3

The SEM micrographs of Ga_2O_3 show that a large range of crystallite sizes were present. The crystallites were irregular in size and shape and are easily distinguishable from H-ZSM-5. It is important to note that the crystallites of Ga_2O_3 are much larger than that of H-ZSM-5. No increase in crystal size was observed after heating Ga_2O_3 to 1200°C for 24 hours in a muffle furnace (section 2.1.5) to convert it to β-Ga_2O_3.

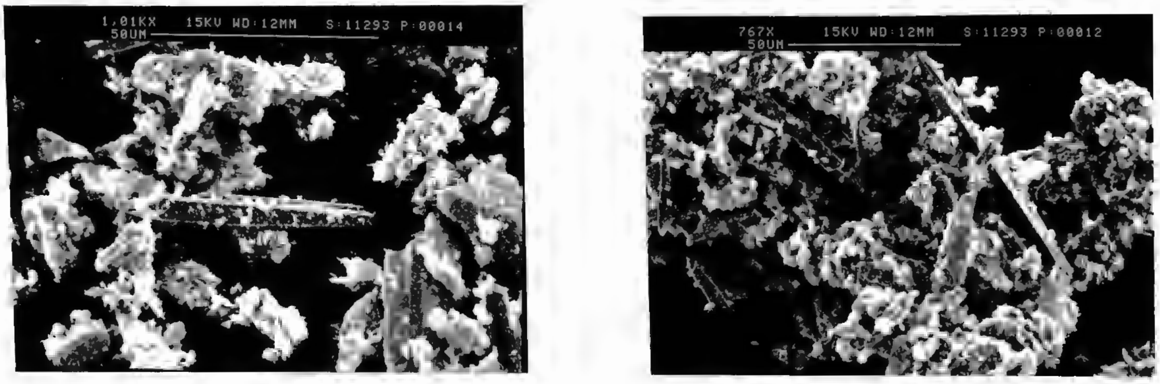

Ga_2O_3 β-Ga_2O_3

Figure 3.82 SEM micrographs of Ga_2O_3 and β-Ga_2O_3

3.9.3. Ga(mix)/H-ZSM-5

The SEM micrographs clearly show the small H-ZSM-5 crystallites on the larger Ga_2O_3 crystallites.

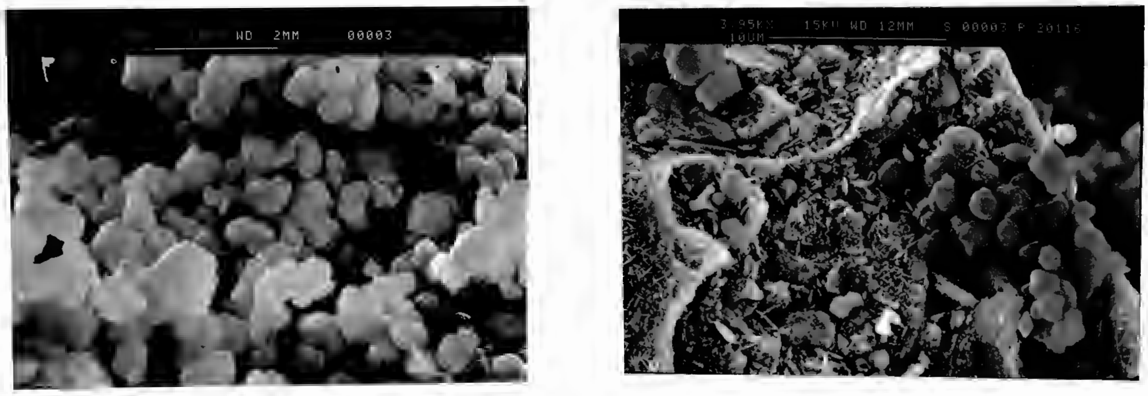

Figure 3.83 SEM micrographs of Ga(mix)/H-ZSM-5 (5wt% Ga)

3.9.4. Ga(mix)/H-ZSM-5 (H_2 pretreated)

The SEM micrographs of Ga(mix)/H-ZSM-5 (5wt% Ga) after hydrogen pretreatment do not reveal whether or not there has been a reduction in the size of the Ga_2O_3 crystallite size.

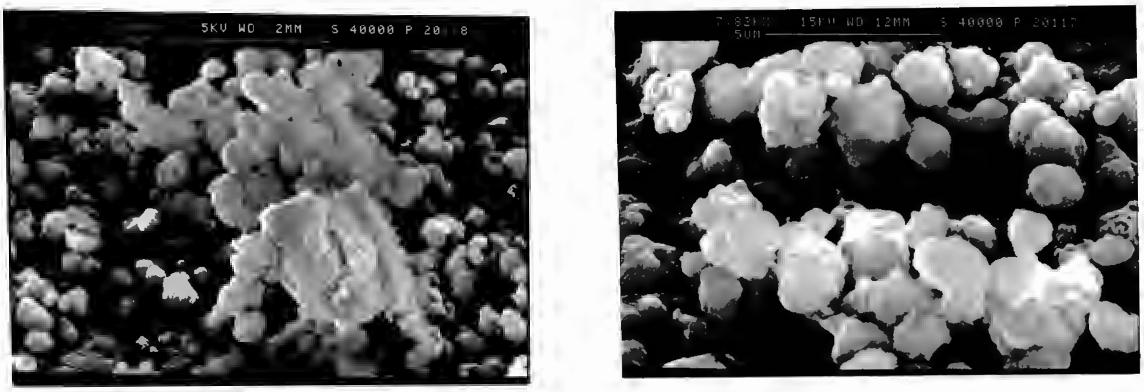

Figure 3.84 SEM micrographs of Ga(mix)/H-ZSM-5 (10wt% Ga) after hydrogen pretreatment

3.9.5 Ga(ionx)/H-ZSM-5

The SEM micrographs of Ga(ionx)/H-ZSM-5 shows clearly that gallium crystallites species are deposited on the surface of the H-ZSM-5 substrate. The SEM analysis was made after the catalyst had been dried overnight (section 2.1.3) but before calcination in N_2. Hence, it must be concluded that washing the catalyst with de-ionized water did not remove Ga^{+3} ions from the surface of H-ZSM-5. This explains the high mass loading of gallium obtained for this catalyst.

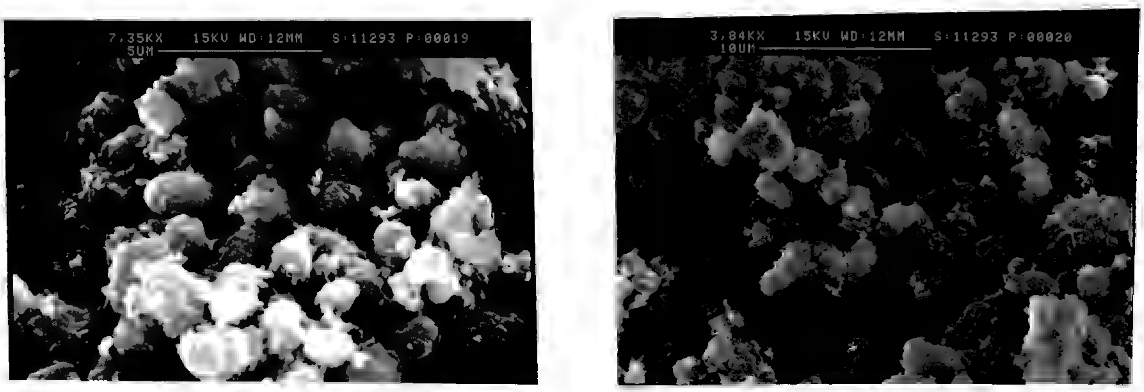

Figure 3.85 SEM micrograph of Ga(ionx)/H-ZSM-5 (18wt% Ga)

3.10. XRD Results

3.10.1. Ga_2O_3

The XRD spectra shown below are for Ga_2O_3 as obtained from the Aldrich Chemical Company as well as the same Ga_2O_3 after heating to 1200°C for 24 hours to convert it to β-Ga_2O_3. As can be seen from the second XRD spectrum, the treatment of Ga_2O_3 at 1200°C for 24 hours in a muffle furnace, dramatically improves the crystallinity of the compound. There is an increase in peak intensity and peak sharpness, indicative of an increase in crystal size. However, the SEM micrographs for Ga_2O_3 (Figure 3.82) show that no observable increase in crystal size occured.

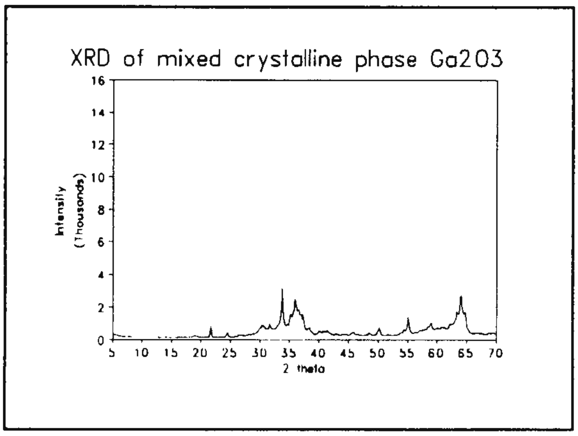

Figure 3.86 XRD spectrum of Ga_2O_3

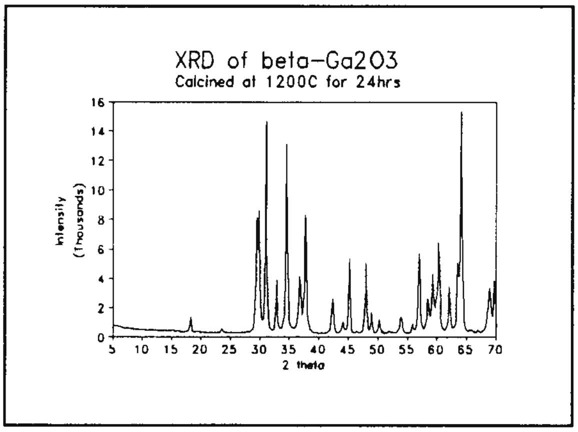

Figure 3.87 XRD spectrum of β-Ga_2O_3

3.10.2. H-ZSM-5

The XRD spectrum obtained for the H-ZSM-5 used in this project, as well as the published XRD pattern [van Koningsveld et al. 1987] are shown below and compare favourably.

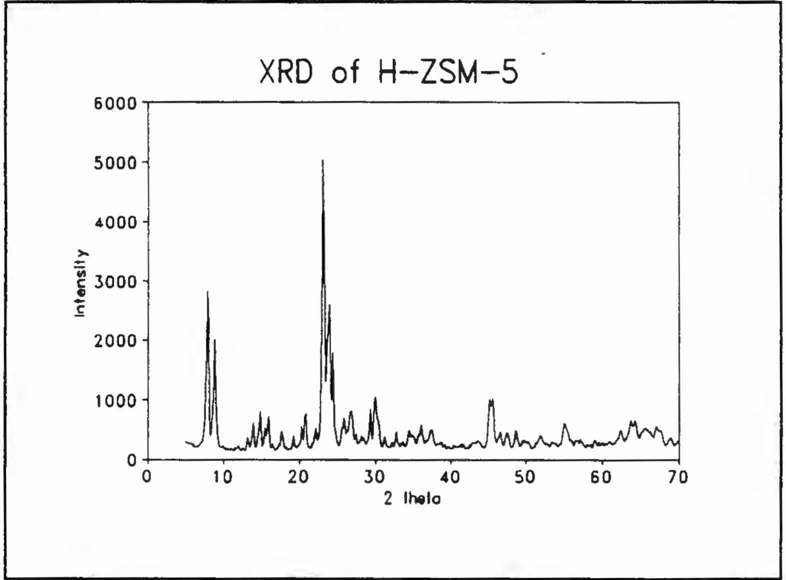

Figure 3.88 XRD spectrum of H-ZSM-5 used in catalytic testing

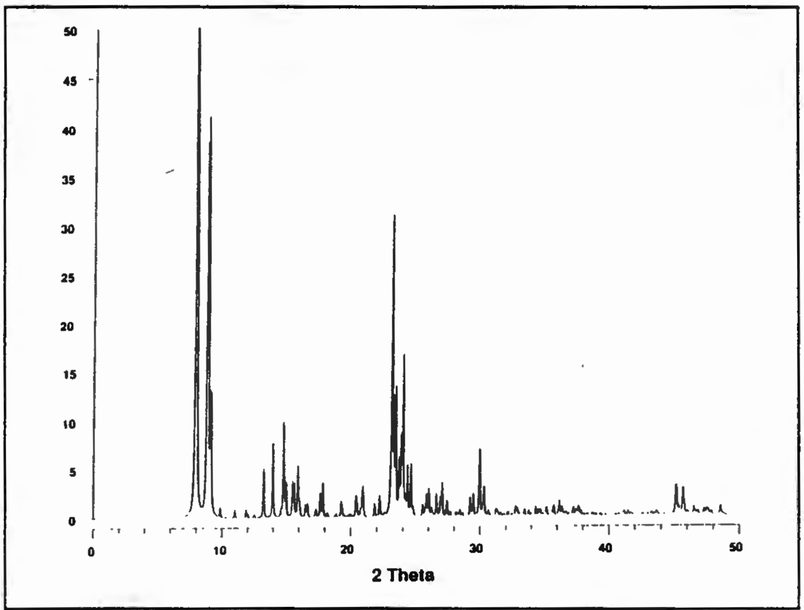

Figure 3.89 Published XRD pattern for H-ZSM-5 [van Koningveld et al. 1987]

3.10.3. The effect of hydrogen treatment on Ga(mix)/H-ZSM-5

XRD spectra of Ga(mix)/H-ZSM-5 before and after treatment with hydrogen at 550°C for 2 hours are shown below. The loading of gallium was 10% by mass and this relatively high loading was chosen to make the β-Ga_2O_3 more visible on the XRD spectra. As can be seen, hydrogen pretreatment decreases the intensity of the β-Ga_2O_3 peaks. This can be explained by the interaction between hydrogen and β-Ga_2O_3/H-ZSM-5 which causes migration of gallium within the zeolite pore structure and as such causes a decrease in the size of β-Ga_2O_3 crystallites, as well as the number of X-ray visible β-Ga_2O_3 crystallites.

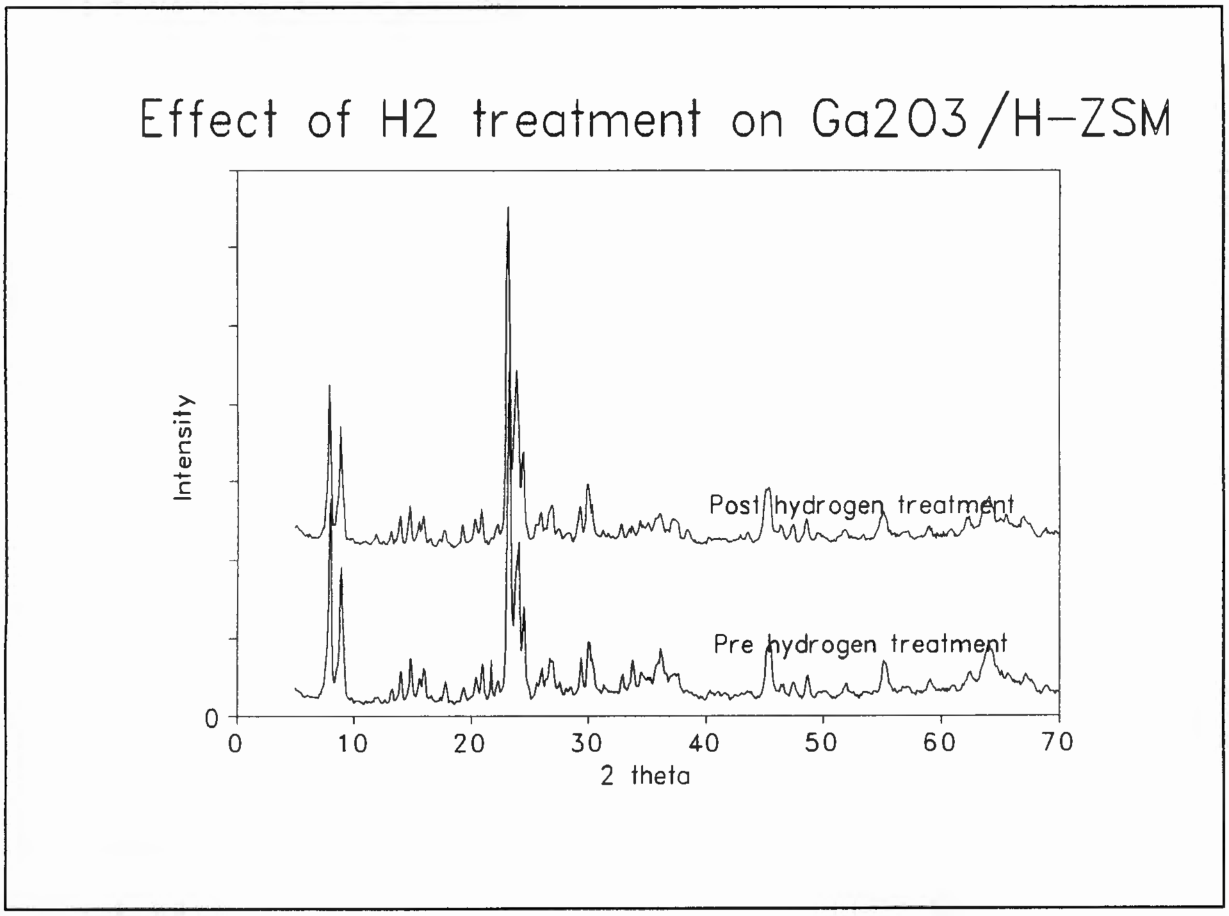

Figure 3.90 XRD patterns of Ga(mix)/H-ZSM-5 before and after hydrogen treatment

The figure below shows a close up of the above figure, better enabling the reader to see the effect of hydrogen treatment on Ga_2O_3/H-ZSM-5 physical mixtures. The arrows indicate the main Ga_2O_3 XRD peaks.

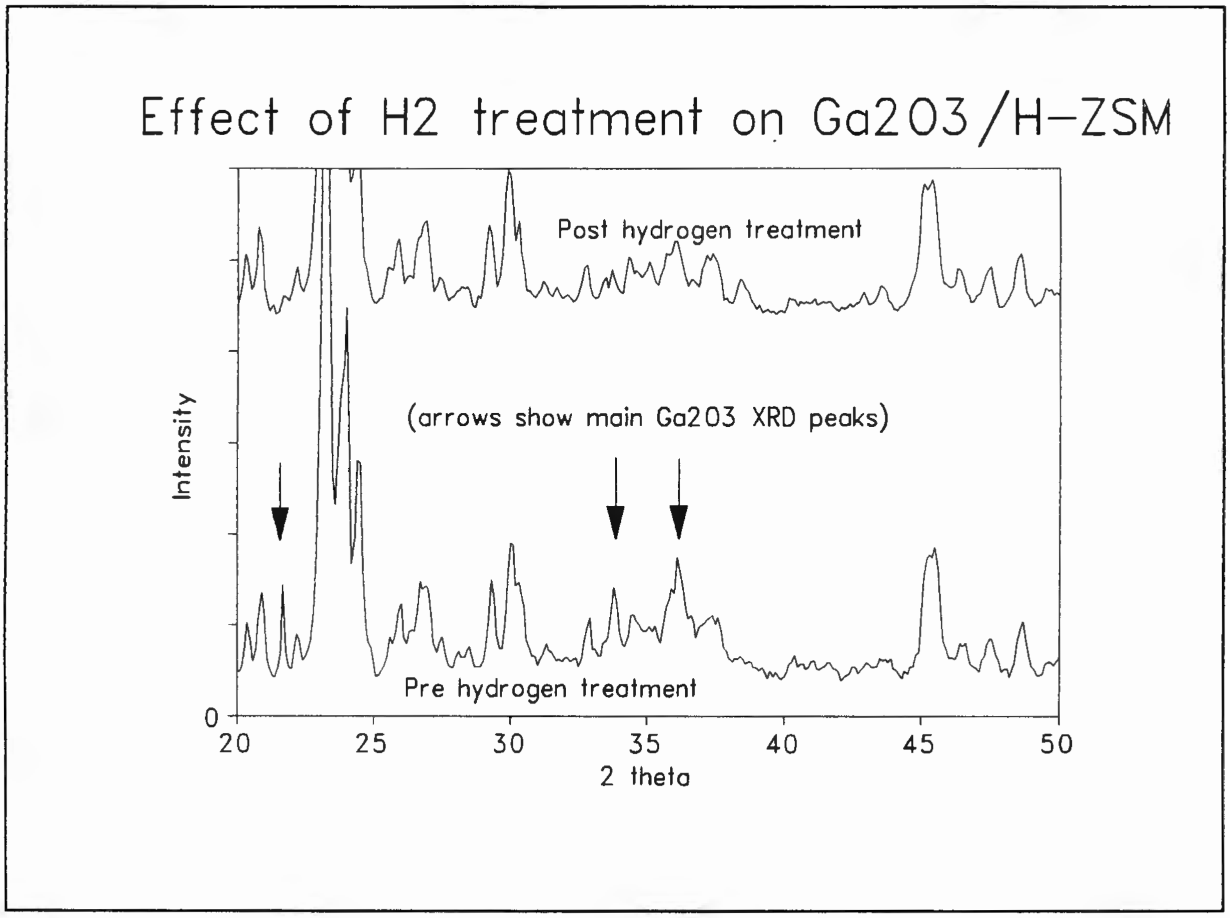

Figure 3.91 XRD patterns of Ga(mix)/H-ZSM-5 before and after hydrogen treatment

3.11. FTIR Results

3.11.1. β-Ga_2O_3

The FTIR spectra of Ga_2O_3 prior to calcination at 1200°C as well as β-Ga_2O_3 are shown below. The FTIR spectrum of β-Ga_2O_3 shows greater absorbance at *ca.* 700cm^{-1}, indicative of M-O (metal-oxygen) bond stretching, which corresponds well with the published value of 696cm^{-1}. The increase in absorbance is a result of β-Ga_2O_3 being more crystalline and hence having greater local order relative to amorphous Ga_2O_3 .

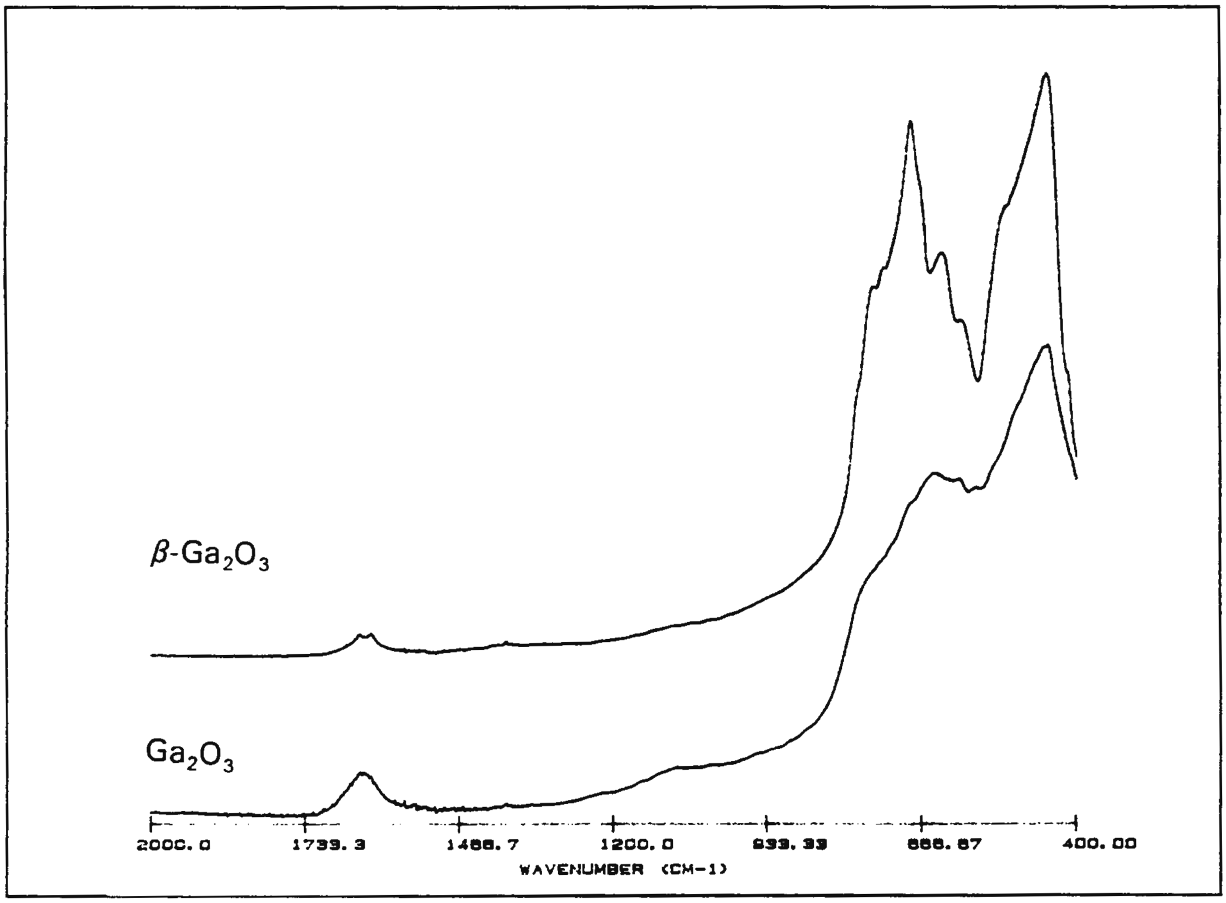

Figure 3.92 FTIR spectra of Ga_2O_3 and β-Ga_2O_3

3.11.2. FTIR of physical mixtures of H-ZSM-5 and β-Ga_2O_3

The FTIR of H-ZSM-5, Ga(mix)/H-ZSM-5 (10wt% Ga) and Ga(mix)/H-ZSM-5 (10wt% Ga) after H_2 treatment at 550°C for 2 hours is shown in Figure 3.93 and 3.94. The mixing of β-Ga_2O_3 with H-ZSM-5 causes an increase in absorbance at *ca.* 700cm^{-1}. Hydrogen treatment causes a decrease in absorbance in this region, indicating that there is a "decrease" in the amount of β-Ga_2O_3. Thus it can be concluded that hydrogen treatment of β-Ga_2O_3 and H-ZSM-5 mixtures causes an interaction to occur between the zeolite and β-Ga_2O_3 which leads to a "decrease" in the amount of β-Ga_2O_3 crystallites.

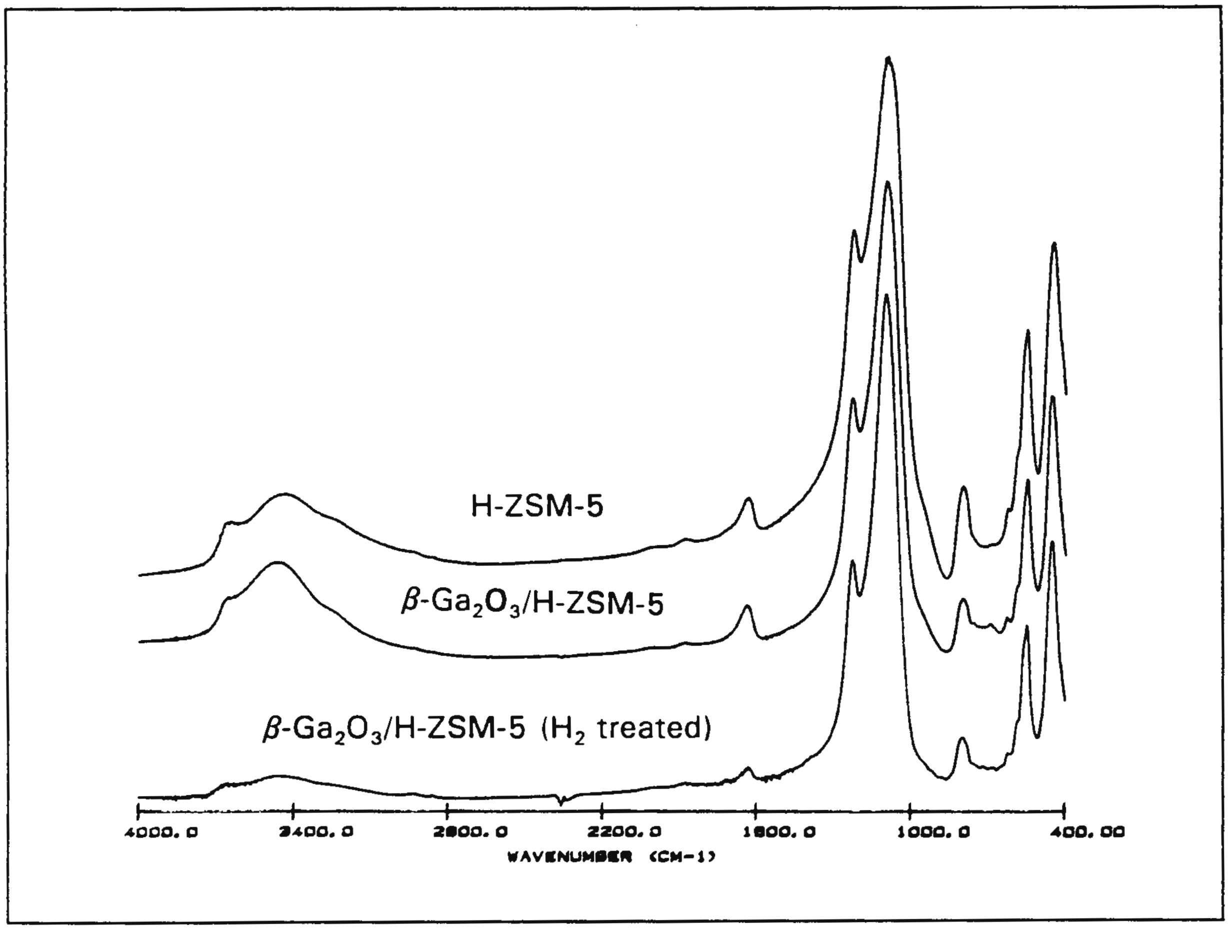

Figure 3.93 FTIR spectra of β-Ga_2O_3 and H-ZSM-5 physical mixtures

The above mentioned results are shown more clearly in Figure 3.94.

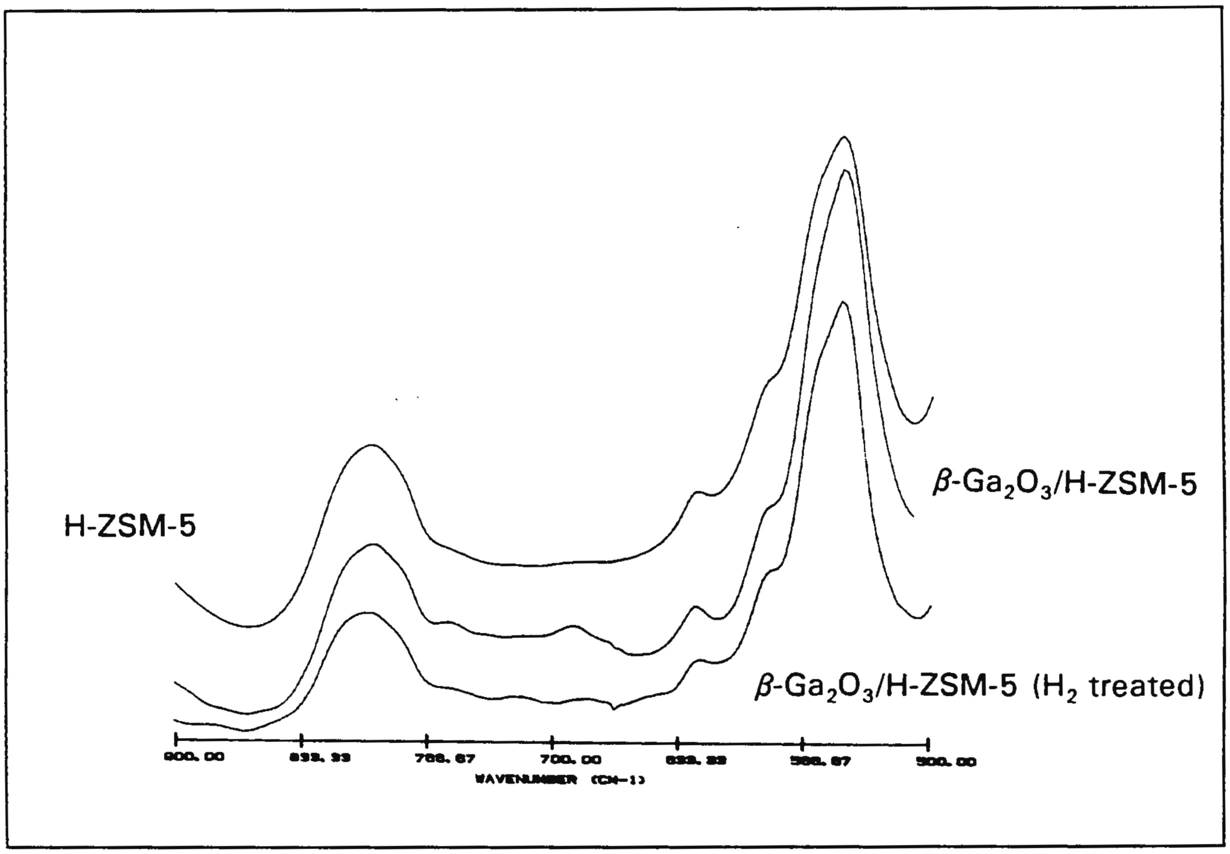

Figure 3.94 FTIR spectra of β-Ga_2O_3 and H-ZSM-5 physical mixtures

3.11.3. FTIR analysis of coked catalysts

FTIR analysis of coked samples of H-ZSM-5, Ga(mix)/H-ZSM-5 and Ga(impr)/H-ZSM-5 shows that both "hard" (graphitic) coke and "soft" (aliphatic) coke is present. All the samples posses multiple bands at 1360cm^{-1} to 1480cm^{-1}, which are indicitive of aliphatic and alkenyl compounds, as well as bands at 1520cm^{-1} to 1600cm^{-1}, which are indicitive of polynuclear aromatics. However, the low intensity of the CH_3 and CH_2 stretching modes (2900cm^{-1}) indicates only a low concentration of type I (''soft" coke) in comparison to type II ("hard" or aromatic) coke. This is consistent with current data on H-ZSM-5. The catalysts used were tested at 550°C, using 1-hexene as feedstock at a WHSV 5.8hr^{-1} for 3 hours prior to FTIR analysis. The spectra (Figure 3.95) show that Ga(impr)/H-ZSM-5 contained the most coke, followed by Ga(mix)/H-ZSM-5 and H-ZSM-5.

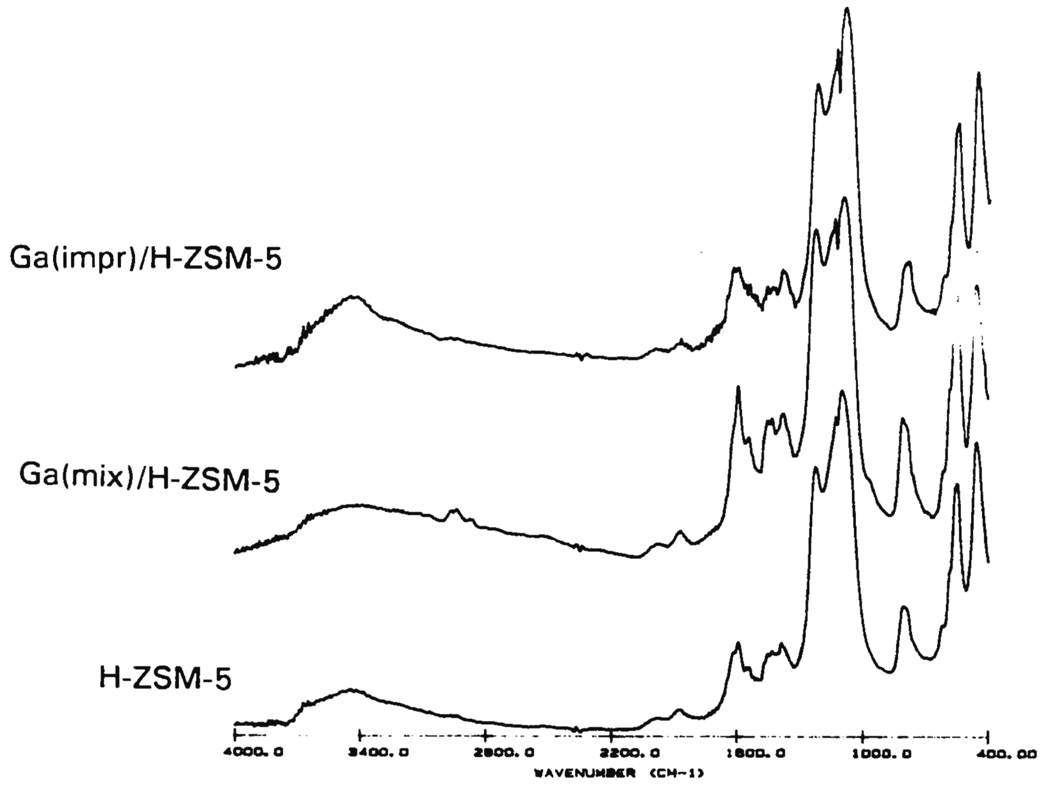

Figure 3.95 FTIR spectra of coked catalysts

3.12 Analysis Of Liquid Product

Offline analysis of the liquid product by GC/MS revealed that the heavy compounds produced at reaction temperatures of 500°C to 550°C were primarily alkylated polynuclear aromatics. Amongst the compounds identified were methylnapthalene, dimethylnapthalenes and anthracenes. The identification of the compounds was hampered by the low resolution which was obtained by the GC capillary column used for component separation.

At lower reaction temperatures (250°C to 350°C) it is reasonable to assume that the heavy compounds would be primarily oligomers of the feedstock and the cracked alkenes, as very small amounts of aromatic products were produced at these reaction temperatures. The retention times of the heavy peaks on the GC traces at low and high reaction temperatures were substantially different. Hence it is concluded that different heavy products were produced at low (250°C) and high (>350°C) reaction temperatures. There were no available means of identifying the heavy products produced at low reaction temperatures.

Chapter 4

DISCUSSION

4. Discussion

4.1. Experimental

The objective of this research was to determine whether long chain alkenes could be converted to BTEX aromatics over Ga/H-ZSM-5 catalysts. The following factors were investigated with regard to their effect on product selectivity:

(i) Effect of feedstock, 1-hexene and 1-octene;
(ii) Method of adding gallium to H-ZSM-5;
(iii) Effect of reaction temperature;
(iv) Effect of time on stream;
(v) Effect of hydrogen pretreatments;
(vi) Effect of WHSV.

The results from these experiments have been tabulated in various forms in this chapter to enable qualitative and quantitative assessments of the effect of gallium and H-ZSM-5 on alkene aromatization. The effect of temperature, time on stream will furthermore be discussed with regard to observed product selectivity and that expected from theoretical reaction pathways.

One of the major problems with this study is that the catalysts were tested at 100% conversion of the alkene feedstock. Conversion of the feedstocks was always 100% at reaction temperatures above 350°C. It proved impossible to reduce the feed conversion levels to below 100%. This was a result of the low linear velocities through the reactor bed, the high activity of H-ZSM-5 for acid catalyzed reactions and the the high reactivity of 1-hexene and 1-octene. At low reaction temperatures (<350°C) selectivity to BTEX aromatics was low and the GC analysis was complicated by the presence of heavy oligomers. Tests at high linear velocities (low catalyst bed contact times) resulted in high selectivity to propene, butene and ethene, with very few aromatic products (section 3.1.3.). Due to the high feed coversion (100%) care must taken in making direct comparisons between different catalysts.

4.1.1. Reproducibility

One the primary concerns, where limited time is available to repeat experiments, is reproducibility of catalyst performance. In general reproducibility between the same type of catalysts was good, as shown in the Table 4.1 for two Ga(mix)/H-ZSM-5 catalysts, synthesized separately under identical conditions. Due to time constraints, however, not all catalysts were tested to determine the reproducibility of the experimental method and catalyst synthesis. Table 4.1 shows that reproducibility with respect to selectivities to within 4% points was obtained. It was assumed that similar reproducibility was possible for all other catalysts. There were a number of factors that could affect catalyst performance. The most serious was film diffusion between the catalyst particles and carrier gas as will be discussed in section 4.1.3. Due to the low linear velocities in the reactor, *ca.* 0.66cm/second, this problem was quite severe. Hence, it was important to pack the bed in such a manner so as to reduce channelling and bypassing of the catalyst by the feedstock. Another factor is the effect of multiple regenerations on Ga/H-ZSM-5 catalysts, which are reported to enhance selectivity to aromatics [Price and Kanazirev, 1990]. This is discussed further in section 4.1.4. A factor affecting reproducibility between successive GC samples was the rate of change in product selectivity with time on stream. H-ZSM-5 and Ga(mix)/H-ZSM-5 (sections 3.2.1 - 3.2.2) displayed stable performance during the time on stream (10 hours). Ga(impr)/H-ZSM-5 and Ga(ionx)/H-ZSM-5 (sections 3.2.1 - 3.2.2.), however, showed large changes in product selectivity with time on stream (3 hours to 6 hours).

Table 4.1 Reproducibility between Ga(mix)/H-ZSM-5 catalysts (selectivities)

Catalyst	C_1	C_2^b	C_3^b	C_4	$C_4=$	B	T	X	Heavies	ΣBTX
Ga(mix)^a	2	11	10	1	1	25	25	10	14	60
Ga(mix)^a	1	11	11	0	0	23	23	10	17	56

(a) Ga(mix)/H-ZSM-5, H_2 pretreated, 550°C; (b) alkane and alkene;

4.1.2. Carbon mass balances

Carbon mass balances were made using dimethyl ether (DME) as an internal standard. The results of carbon balances from selected experiments are shown in Table 4.2. In general mass balances were out by as much as 20%, but at other times by even more. However, a variation of 20% from the ideal would be a fairly typical result. Carbon mass balances were made in the following fashion:

i. Calculate the DME flow rate (STP cm^3/hour) from the mass flow controller (MFC) readings and calibration chart for DME. The conversion to mass and molar flowrates is made by application of the ideal gas law (i.e. $PV = nRT$).

ii. Calculate the mass flow rate of the feed into the system by by-passing the reactor and measuring the area of feed relative to the DME internal standard. The mass flowrate of the feed relative to DME is calculated using response factors determined previously. Conversion to molar flowrates is made by application of the ideal gas law.

iii. The mass flowrates of products out of the system are calculated using the ratio of the area of each compound on the GC trace relative to the area of the DME internal standard, taking the appropriate response factors into account. The conversion to carbon molar flowrates was calculated for all of the identifiable product compounds (i.e. the molecular mass and number of carbon atoms were known).

iv. The carbon flowrate out of the system is made by the summation of the carbon flowrates of each individual product and is compared to the carbon flowrate into the system.

The greatest deviation was observed at low reaction temperatures, after substantial time on stream (all temperatures) and when using 1-octene as a feedstock. These factors as well as other factors affecting the accuracy with which mass balances tied are discussed below:

i. Ideal gas behaviour was assumed for the DME internal standard, the 1-hexene and 1-octene feedstocks. Neither 1-hexene nor 1-octene are commonly considered ideal gases which would result in a constant error in measuring the mass flow rate of the feedstock into the system (the Z (compressibility) factor at 100°C and 101.3kPa was 0.96 and 0.95 for 1-hexene and 1-octene respectively, as calculated by Hysim). However, the assumption could be justified due to the low vapour pressures of the feedstocks, typically 5kPa to 20kPa, at the temperatures at which they were used,

ii. At low reaction temperatures a large proportion of the product spectrum was constituted by unidentified heavy compounds, which were assumed to be oligomers of the feed. Neither the response factors, molecular masses nor carbon number were known for these compounds. Similarly at high reaction temperatures, especially on catalysts that underwent rapid changes in product selectivity with time on stream, a large proportion of the product spectrum consisted of heavy polynuclear aromatic compounds. Off-line analysis of these heavy compounds identified some as alkylated naphthalenes. The remainder were unidentified.

iii. A carbon number of 10 and molecular mass of 142.3g/mol was assumed for the heavy products in the product spectrum. The values chosen were made on the basis of ad-hoc assumptions and could certainly be subject to change should new information on the molecular formulae of the heavy compounds become available.The response factors of these compounds were set at unity, i.e. equal to that of the feed. This topic is discussed further in section 4.7.2.

Table 4.2 Carbon mass balances of selected experiments

Catalyst	Temp [°C]	Carbon mass in [mmol/hr]	Carbon mass out [mmol/hr]	Carbon balance
1-hexene feed				
H-ZSM-5[a]	350	80.7	85.5	106%
	400	80.7	92.4	114%
	450	80.7	92.9	115%
	500	80.7	93.1	115%
	550	80.7	87.6	108%
Ga(impr)[a]	250	98.4	53.4	54%
	350	98.4	72.7	74%
	450	98.4	120	122%
	500	98.4	104	105%
	550	98.4	123	127%
Ga(impr)[b]	550	98.4	88.3	90%
Ga(impr)[d]	550	98.4	106	108%
Ga(ionx)[b]	550	98.4	84.4	86%
Ga(ionx)[c]	550	98.4	91.6	93%
1-octene feed				
H-ZSM-5[a]	250	22.4	16.0	71%
	350	22.4	20.3	90%
	450	22.4	27.2	121%
	500	22.4	32.5	145%
	550	22.4	30.0	134%
H-ZSM-5[b]	550	22.4	21.3	95%
H-ZSM-5[c]	550	22.4	26.4	118%
Ga(impr)[b]	550	23.7	20.8	88%
Ga(impr)[c]	550	23.7	28.7	120%

(a) temperature profile; (b) initial time on stream; (c) 5 hours time on stream; (d) 3 hours on stream;

4.1.3. Film diffusion effects

The results of the experiments to determine the magnitude of film diffusion showed that gas velocity caused a marked change in 1-hexene conversion (section 3.1.4.). This indicates that film diffusion between the catalyst particles and the bulk gas are present and fairly severe. The test was made at low temperatures and hence was not indicative of actual operating conditions for optimal aromatics formation. All subsequent catalytic testing was made with a constant nitrogen carrier gas flowrate of 80ml/min. Hence, the catalysts were tested within the film diffusion domain. The effect of film diffusion on feed conversion and hence product selectivity is acknowledged but could not be overcome due to the low linear velocities of carrier gas through the reactor. Higher linear velocities resulted in high selectivities to ethene, propene and butene and very low selectivities to BTEX aromatics. The diameter of the reactor was wider than was needed and this resulted in low linear velocities through the catalyst bed. Using a reactor of smaller diameter would have enabled higher linear velocities to be attained through a long narrow catalyst bed which would have minimised the effect of film diffusion and channelling of the feedstock.

4.1.4. Effect of multiple regenerations

The effects of multiple regenerations on the selectivities of Ga/H-ZSM-5 zeolite catalysts are shown in Table 4.3. Regeneration of the catalysts by calcination in air at 550°C caused an increase in selectivity towards aromatic products. This is assumed to be the result of increased dispersion of Ga species within the zeolite pores [Price and Kanazirev, 1990]. Care must be taken in arbitrarily comparing catalysts from different runs as the rapid rate of deactivation of most Ga/H-ZSM-5 catalysts means that the time on stream at which the sample was taken will have a substantial effect on the product selectivities observed, i.e. a decrease in BTEX selectivity and increase in light alkene selectivity. The results shown in Table 4.3. are for the first on-line GC sample after 15 minutes time on stream.

Table 4.3 Effect of multiple regenerations on catalyst selectivity

Regen no.[a]	C_1	C_2&C_2=	C_3&C_3=	C_4	C_4=	B	T	X	ΣBTX
		Ga(impr)/H-ZSM-5, 1-octene feed, 550°C, WHSV 3.4hr^{-1}							
6	3	7	5	0	0	26	30	10	66
9	3	7	6	0	0	29	33	11	73
		Ga(ionx)/H-ZSM-5, 1-hexene feed, 550°C, WHSV 6.9hr^{-1}							
0	1	18	24	4	6	9	21	12	42
4	2	10	11	1	0	25	33	12	70

(a) number of regenerations, i.e. redox cycles;

4.2 Effect of Alkene Feedstock

Two alkene feedstocks were used in this project, *viz.* 1-hexene and 1-octene. 1-Hexene was used a feedstock for H-ZSM-5, Ga(mix)/H-ZSM-5, Ga(impr)/H-ZSM-5 and Ga(ionx)/H-ZSM-5. 1-Octene was only used as feed for H-ZSM-5 and Ga(impr)/H-ZSM-5. The results of the temperature profiles (section 3.3.) show that there is very little difference in product selectivity as a result of using different alkene feedstocks.

4.2.1. Light products

The selectivity to light products (C_1-C_5) are shown in Table 4.4 and Table 4.5 for H-ZSM-5 and Ga(impr)/H-ZSM-5 respectively.

4.2.1.1. H-ZSM-5

There is general agreement between the selectivities to light products for H-ZSM-5. However, the most noticeable deviation is observed for propane/propene and the butenes at low reaction temperatures (350°C). There is a large difference in WHSV's for the alkene feedstocks (5.8hr^{-1} and 1.7hr^{-1} for 1-hexene and 1-octene respectively). This may have resulted in the observed deviations.

Table 4.4 Selectivity to light products for H-ZSM-5

	1-hexene			1-octene		
	H-ZSM-5[a]			H-ZSM-5[b]		
	350°C	450°C	500°C	350°C	450°C	500°C
C_1	0	0	0	0	0	0
C_2 & $C_2=$	4	13	19	5	15	23
C_3 & $C_3=$	15	30	34	21	36	37
C_4	17	8	4	12	3	2
$C_4=$	14	15	15	20	15	14
C_6	12	6	3	12	6	2
ΣC_1-C_6	62	72	75	70	75	78

(a) WHSV 5.8hr^{-1}; (b) WHSV 1.7hr^{-1};

4.2.1.2. Ga(impr)/H-ZSM-5

The difference between the selectivities to light products for Ga(impr)/H-ZSM-5 is small. The greatest difference occurs at 550°C. The difference in WHSV's is not as great as for H-ZSM-5 (6.9hr^{-1} and 3.4hr^{-1} for 1-hexene and 1-octene respectively)

Table 4.5 Selectivity to light products for Ga(impr)/H-ZSM-5

	1-hexene			1-octene		
	Ga(impr)/H-ZSM-5[a]			Ga(impr)/H-ZSM-5[b]		
	350°C	450°C	550°C	350°C	450°C	550°C
C_1	0	1	2	0	2	3
C_2	0	0	1	0	0	1
$C_2=$	3	5	7	3	5	6
C_3	2	3	5	2	3	4
$C_3=$	13	6	4	13	6	2
C_4	10	7	0	8	8	0
$C_4=$	21	4	1	20	3	0
C_5	15	2	1	14	3	0
ΣC_1-C_5	64	28	21	60	30	16

(a) WHSV 6.9hr^{-1}; (b) WHSV 3.4hr^{-1};

4.2.2. BTEX aromatics

The effect of using 1-hexene and 1-octene as aromatization feedstocks on BTEX selectivity for H-ZSM-5 and Ga(impr)/H-ZSM-5 are shown in Table 4.6. and Table 4.7. There is a difference in WHSV's but this was shown to have only a small effect on product selectivity (section 4.8).

4.2.2.1. H-ZSM-5

Less BTEX is produced when using 1-octene than when using 1-hexene as feed. The greatest difference in selectivity occurs for p,m-xylene, which has much lower selectivity when using 1-octene as feedstock.

Table 4.6 Effect of alkene feedstock on BTEX selectivity for H-ZSM-5

	1-hexene			1-octene		
	H-ZSM-5[a]			H-ZSM-5[b]		
	350°C	450°C	500°C	350°C	450°C	500°C
B	1	2	3	1	1	4
T	5	7	8	4	7	7
p,m-X	8	8	7	5	4	3
o-X	1	2	2	1	1	1
EtB	1	1	0	1	0	0
ΣBTEX	16	20	20	12	13	15

(a) WHSV = $5.8 hr^{-1}$; (b) WHSV = $1.7 hr^{-1}$

4.2.2.2 Ga(impr)/H-ZSM-5

There is very little difference in selectivity to BTEX products for Ga(impr)/H-ZSM-5. Slightly more BTEX is produced when using 1-octene as a feedstock than when using 1-hexene.

Table 4.7 Effect of alkene feedstock on BTEX selectivity for Ga(impr)/H-ZSM-5

	1-hexene			1-octene		
	Ga(impr)/H-ZSM-5[a]			Ga(impr)/H-ZSM-5[b]		
	350°C	450°C	550°C	350°C	450°C	550°C
B	0	6	27	0	10	29
T	5	23	32	4	26	33
p,m-X	7	15	8	7	14	9
o-X	1	4	2	1	3	2
EtB	1	2	1	1	2	0
Heavies	20	13	12	17	10	10
ΣBTEX	14	50	70	13	55	73

(a) WHSV = $6.9 hr^{-1}$; (b) WHSV = $3.4 hr^{-1}$

4.2.2.3. Conclusion on effect of alkene feedstocks

Although there is general agreement between the selectivities to both light and aromatic products when using either 1-hexene or 1-octene as aromatization feedstock, some differences do occur. When 1-octene is used as feedstock it was observed that Ga(impr)/H-ZSM-5 produces slightly more BTEX while H-ZSM-5 produces less BTEX (than when using 1-hexene as feedstock). However the differences are quite small (less than 5% points) and hence could be attributed to experimental error.

4.3. Effect of Gallium on Selectivity to Aromatic Compounds

Gallium was added to H-ZSM-5 via three methods, viz:

i. physical mixing with Ga_2O_3;
ii. impregnation by incipient wetness with $Ga(NO_3)_3.9H_2O$;
iii. ion-exchange with $Ga(NO_3)_3.9H_2O$.

4.3.1. Effect of gallium on BTEX selectivity

Gallium, when added to H-ZSM-5, increases selectivity to aromatic compounds dramatically, as shown in the Table 4.8. Benzene is not the dominant aromatic compound when 1-hexene is used as feedstock, neither are C_8 aromatics the dominant BTX components when 1-octene is used as feedstock (Table 4.6, Table 4.7). This indicates that aromatization does not occur via direct cyclization of the alkene feedstock, but rather that a cracked mixture of light alkenes react to form the aromatic compounds.

Table 4.8 Aromatic yields at 550°C for 1-hexene feedstock

	H-ZSM5[a]	Ga(mix)/H-ZSM-5[b]	Ga(mix)/H-ZSM-5[c]	Ga(ionx)/H-ZSM-5[d]	Ga(impr)/H-ZSM-5[e]
B	2	8	26	25	27
T	5	17	28	33	32
p,m-X	4	8	10	10	8
o-X	1	2	3	3	2
EtB	1	1	1	1	1
ΣBTEX	13	36	68	72	70

(a) WHSV = 11.3hr^{-1}; (b) WHSV = 5.8hr^{-1}; (c) hydrogen pretreated, WHSV = 5.8hr^{-1}; (d) WHSV = 6.9hr^{-1}; (e) WHSV = 6.9hr^{-1};

As can be seen from Table 4.8, gallium enhances selectivity towards aromatic products for all Ga/H-ZSM-5 catalysts. The selectivities shown are for the first on-line GC sample (time on stream of 15 minutes). The order with regard BTEX selectivity is Ga(ionx) ≈ Ga(impr) ≈ Ga(mix, H_2 treated) > Ga(mix) > H-ZSM-5. Ga(mix)/H-ZSM-5 that has not been pretreated with hydrogen exhibits lower selectivity to BTEX aromatics. It is presumed that the mixing between bulk β-Ga_2O_3 crystallites and H-ZSM-5 was not intimate enough to create a catalyst active for aromatization. The TPR profiles (section 3.7.) show clearly that reduction of gallium occurs at a lower temperature for Ga(ionx)/H-ZSM-5 than for Ga(mix)/H-ZSM-5 (100°C difference in peak maximum). This a result of more intimate contact between gallium species for Ga(ionx)/H-ZSM-5 than for Ga(mix)/H-ZSM-5. Gallium oxide requires the presence of acid sites for reduction to take place [Price et al. 1990]. The effect of hydrogen pretreatments is discussed in section 4.7. The gallium loading for Ga(ionx)/H-ZSM-5 was 18wt% as opposed to 5wt% for the other Ga/H-ZSM-5 catalysts. The fact that Ga(ionx)/H-ZSM-5 exhibits similar BTEX selectivities to the other catalysts is in agreement with Kitagawa et al. [1986] who reports that selectivities to aromatics increase with increasing gallium loading until the gallium content reaches the value corresponding to 100% ion exchange. As both catalysts have gallium loadings above this limit they would be expected to show similar results with respect to product selectivity.

4.3.2. Xylene isomer distribution

The dominant xylene isomer is p/m-xylene. The reason for the lower selectivity to o-xylene can be explained by the shape selective effects of the ZSM-5 pore structure. The rate constants for xylene isomerization are influenced by diffusion and shape selective effects [Collins et al. 1983]. Xylene isomerization proceeds readily on ZSM-5 at temperatures above 250°C with some disproportination to toluene and 1,3,5-trimethylbenzene occuring [Collins et al. 1983]. Unfortunately it was not possible to resolve p-xylene and m-xylene, but it would be reasonable to conclude, from the point of view of shape selectivity, that p-xylene would be the dominant xylene species as ZSM-5 is reported to show greater selectivity to p-xylene than to m-yxlene or o-xylene [Collins et al. 1983]. Under the reaction conditions skeletal isomerization of o-xylene and m-xylene to p-xylene would account for the low selectivity to these compounds.

The xylene ratios obtained experimentally show remarkable consistency with o-X forming 20% and p,m-X the remaining 80%. The ratios do not agree with the thermodynamic equilibrium xylene isomer distribution (Table 4.9). This could indicate that the shape selective effects of the zeolite pore system and pore openings decrease selectivity to the more bulky o-xylene and by inference m-xylene as well. In the absence of shape selective effects, and as a result of the high reaction temperatures (550°C) and low linear velocities of the carrier gas over the catalyst bed, thermodynamic equilibrium should be reached between the xylene isomers. Thermodynamic equilibrium (between xylene isomers) occurs on large pore zeolite HY at high reaction temperatures [Davis 1983]. However, as this equilibrium distribution was not observed in the present study, it can be concluded that the unique three dimensional pore system of H-ZSM-5 sterically hinders the formation of o-xylene and m-xylene

Table 4.9 Equilibrium xylene isomer distribution at 550°C

Catalyst	o-X	p,m-X
Published [Stull et al. 1969]	48%	52%
	Feed 1-hexene	
H-ZSM-5[a]	20%	80%
Ga(mix)/H-ZSM-5[a]	22%	78%
Ga(impr)/H-ZSM-5[b]	23%	77%
Ga(ionx)/H-ZSM-5[b]	22%	78%
	Feed 1-octene	
H-ZSM-5[c]	22%	78%
Ga(impr)/H-ZSM-5[d]	22%	78%
	Feed 1-hexene, catalysts H_2 pretreated	
Ga(mix)/H-ZSM-5[a]	22%	78%
Ga(impr)/H-ZSM-5[b]	20%	80%
Ga(ionx)/H-ZSM-5[b]	19%	81%

(a) WHSV 5.8hr^{-1}; (b) WHSV 6.9hr^{-1}; (c) WHSV 1.7hr^{-1}; (d) WHSV 3.4hr^{-1};

4.4. Proposed Reaction Mechanism

The following reaction mechanism is proposed to account for the selectivity changes that occur as a result of temperature and time on stream. It is similar to the widely accepted mechanism for propane aromatization (section 1.8.3). It is proposed that the selectivity changes that occur with time on stream are a result of a moving "deactivation band" which travels down the catalyst bed. This phenomena commonly occurs in commercial reactors [Dry 1993]. Thus selectivity to primary reaction products will increase with time on stream. It must be emphasised that conversion did not change with time on stream, but remained at 100% throughout for all catalysts at reaction temperatures above 400°C.

4.4.1. Acid catalyzed primary reactions for 1-hexene

On H-ZSM-5, the dominant cracking path will be reaction (a) which will result in propene formation by β-scission of 1-hexene [Apre and Krambeck, 1991b]. Thermal cracking of 1-hexene will result in the formation of ethene and butenes, reaction (b). Reaction (c) will not easily occur due to inherent instability of the C_1 carbenium species. Reaction (d) will only be favoured at lower reaction temperatures. Double bond isomerization of 1-hexene will be extremely rapid [Apre and Krambeck, 1991a] and is not included in this scheme.

$C_6{=} \rightarrow C_3{=} + C_3{=}$ ... (a)

$C_6{=} \rightarrow C_4{=} + C_2{=}$ ... (b)

$C_6{=} \rightarrow C_5{=} + C_1$ ... (c)

$C_6{=} \rightarrow C_{12}{=}$ ... (d)

4.4.2. Alkene oligomerization/cracking reactions

The alkenes formed from reactions (a) and (b) will rapidly undergo isomerization, oligomerization and cracking reactions [Sapre and Krambeck, 1991a]. A distribution of alkenes will result which will be dependent on the reaction temperature.

$C_2{=}, C_3{=}, C_4{=} \rightleftarrows C_5{=}$ to $C_{12}{=}$ ... (e)

4.4.3. Aromatization reactions

4.4.3.1. H-ZSM-5

On H-ZSM-5 hydride transfer, as a result of dehydrocyclization, results in the formation of C_1-C_4 alkanes. No hydrogen gas is formed during aromatization with H-ZSM-5 as a catalyst [Guisnet and Gnep, 1992]. Reaction (f) will be slow as hydrogen transfer reactions are slow on H-ZSM-5 [Guisnet and Gnep, 1992].

$C_6{=}$ to $C_8{=}$ → B, T, p-X, m-X, o-X, EtB + C_1-C_4 alkanes ... (f)

4.4.3.2. Ga/H-ZSM-5

Aromatization on Ga/H-ZSM-5 catalysts will result in the formation of dihydrogen gas as well as formation of C_2-C_4 alkanes by hydride transfer [Guisnet and Gnep, 1992]. During this project no analysis of the product gases were made to determine hydrogen concentrations. Reaction (g) will be faster than reaction (f) as gallium increases the rate of hydrogen transfer, the rate limiting step for aromatization [Gnep 1987].

C_6= to C_8= → B, T, p-X, m-X, o-X, EtB + C_1-C_4 alkanes + H_2 ... (g)

4.4.4. Dealkylation reactions

Dealkylation, reaction (h), of the xylene isomers result in the formation of methane and toluene. Similarly toluene dealkylation, reaction (i), will result in the formation of benzene and methane. Side-chain cracking of ethylbenzene, reaction (j), will form toluene and methane while dealkylation of ethylbenzene, reaction (k), will form benzene and ethane.

p-X, m-X, o-X → T + C_1 ... (h)
T → B + C_1 ... (i)
EtB → T + C_1 ... (j)
EtB → B + C_2 ... (k)

4.5. Effect of Temperature on Selectivity

4.5.1. Light alkene products

The catalytic testing of H-ZSM-5 with 1-hexene at high temperature and low residence times over the catalyst bed indicate that the major products are propene, ethene and iso-butene/1-butene (section 3.1.3.). Increasing the residence time over the catalyst bed results in less propene and more ethene and aromatics being formed. This indicates that propene is the primary reaction product (formed from β-scission of 1-hexene) and that it is extremely reactive under the operating conditions. The formation of alkenes from cracking reactions of 1-hexene on H-ZSM-5 would give rise to the primary products observed in the product spectrum. These alkenes would oligomerize to form C_5-C_8 alkenes which would then crack back to the smaller alkenes. The reactivity of larger alkenes will be greater than that of the smaller alkenes and hence less heavy alkenes would be expected to be observed in the product spectrum with increase in reaction temperature. At low temperatures there would be a thermodynamic shift towards larger oligomers and hence greater amounts of heavy compounds will be observed. As aromatic compounds are formed via a slow rate-determining dehydrogenation step, they would not be expected to be observed at low residence times over the catalyst bed or at low temperatures. The distribution of alkenes depend greatly on the reaction temperature. Significant cracking occurs even at 250°C with C_4, C_5 and heavier hydrocarbons being the dominant products (section 3.3.). The smaller cracked products, C_1, C_2, $C_2=$, C_3 and $C_3=$ are minor products at low temperatures but are the dominant cracked products at high temperatures. The results of published thermodynamic data for butene isomerization [Stull et al. 1969] and that obtained in the present experiments are shown in Table 4.10. The data shows that thermodynamic equilibrium for the butene products is obtained when using 1-hexene as a feedstock as well as when 1-octene is used as feedstock.

Table 4.10 Molar distribution of butene products (percent)

Catalyst	Temperature [°C]	i-C_4= & 1-C_4=	t-2-C_4=	c-2-C_4=
Published[a]	250	57	28	15
	350	54	28	18
	450	55	25	20
	500	55	27	18
Feed : 1-hexene				
H-ZSM-5[b]	350	59	25	16
	450	58	25	17
	500	58	25	17
Ga(ionx)[c]	250	62	24	14
	350	60	24	16
	450	57	25	18
	500	56	26	18
Ga(impr)[c]	250	49	32	19
	350	59	25	16
	450	55	27	18
	500	54	28	18
Feed : 1-octene				
H-ZSM-5[d]	250	62	24	14
	350	60	24	16
	450	58	25	17
	500	58	24	18
Ga(impr)[e]	250	56	28	16
	350	60	24	16
	450	58	25	17
	500	59	24	17

(a) Stull et al. 1969; (b) WHSV 5.8hr^{-1}; (c) WHSV 6.9 hr^{-1}; (d) WHSV 1.7hr^{-1};
(e) WHSV 3.4hr^{-1}

4.5.2. Light alkane product selectivity

On H-ZSM-5, aromatization reactions (at high temperatures) result in hydride transfer to carbenium species to form alkanes, which are relatively unreactive compared to alkenes. Thus an increase in selectivity to alkanes with increase in selectivity to aromatic compounds would be expected. However, increased selectivity to aromatics was always observed at high temperatures which would also result in a greater conversion of the light hydrocarbons (by dehydrogenation reactions) back to alkenes and then to BTEX aromatic products. Gallium is reported to increase the rate of hydrogen transfer by hydrogen back spillover (section 1.8.2.). This would result in the formation of dihydrogen gas rather than hydrogen transfer to carbenium ion species to form alkanes. Hence the selectivity ratio of alkanes to aromatics should be less over Ga/H-ZSM-5 catalysts than over H-ZSM-5. There is, however, a complicating factor in that gallium is reported to increase the rate of reaction of alkanes. If the primary effect of gallium was hydrogen back spillover then a decrease in the alkane/aromatics ratio of Ga/H-ZSM-5 catalysts as compared with H-ZSM-5 would be expected. This was observed (see Table 4.11) for all Ga/H-ZSM-5 catalysts. The only exception was Ga(mix)/H-ZSM-5 (not H_2 pretreated) which shows alkane/aromatic ratios very similar to that of H-ZSM-5 (Table 4.. However, both Ga(impr)/H-ZSM-5 and Ga(ionx)/H-ZSM-5 show reduced alkane/aromatic ratios relative to H-ZSM-5. There are two mechanisms whereby gallium functions to reduce the alkane/aromatic ratios, i.e. by hydrogen back spillover to form H_2 and by activating the alkanes to form more reactive alkenes. It is probable that both these mechanisms are present. No measure was made of the amount of hydrogen evolved by the reaction and hence it is not possible to make a definitive statement in this regard. Ga(impr)/H-ZSM-5 and Ga(ionx)/H-ZSM-5 catalysts appear to be the most active for hydrogen transfer as they have the lowest alkane/aromatics ratios.

Table 4.11 Effect of reaction temperature on alkane/aromatic ratios

Catalyst	Temp [°C]	C_2/BTX	C_3/BTX	n-C_4/BTX	i-C_4/BTX
		Feed 1-octene			
H-ZSM-5[a]	350	0.00	0.31	0.21	0.88
	450	0.013	0.25	0.14	0.33
	500	0.018	0.13	0.039	0.074
Ga(impr)[b]	350	0.00	0.13	0.11	0.50
	450	0.014	0.15	0.10	0.26
	500	0.014	0.16	0.046	0.014
	550	0.010	0.050	0.00	0.00
		Feed 1-hexene			
H-ZSM-5[d]	350	*	*	0.31	1.02
	450	*	*	0.14	0.33
	500	*	*	0.15	0.29
Ga(mix)[d]	350	*	*	0.27	0.87
	450	*	*	0.11	0.26
	500	*	*	0.16	0.32
Ga(impr)[c]	350	0.00	0.16	0.14	0.58
	450	0.00	0.079	0.039	0.16
	500	0.010	0.084	0.026	0.023
	550	0.012	0.078	0.00	0.00
Ga(ionx)[c]	350	0.00	0.11	0.098	0.42
	450	0.011	0.082	0.047	0.18
	500	0.011	0.087	0.033	0.057
	550	0.016	0.087	0.00	0.00

(a) WHSV 1.7hr^{-1}; (b) WHSV 3.4hr^{-1}; (c) WHSV6.9hr^{-1}; (d) WHSV 5.8hr^{-1}; (*) alkanes/alkenes not resolved by GC;

The effect of temperature on alkane/aromatic ratios are shown in Table 4.11. On H-ZSM-5 an increase in selectivity to alkanes would be expected with an increase in reaction temperature as a result of hydride transfer to carbenium species explained in section 4.3.1. However increasing the reaction temperature would also cause increased reaction of these alkanes to form alkenes and aromatics. The results of temperature profile runs (section 3.3) show that there is a corresponding decrease in selectivity to alkanes with an increase in selectivity to aromatic products for Ga/H-ZSM-5 catalysts. As can been in Table 4.11, increasing the reaction temperature causes an increase in C_2/BTX ratios and a decrease in C_3/BTX and C_4/BTX ratios. This indicates that propane and butane are being converted to alkenes and then to aromatics at higher reaction temperatures, but that ethane, which is relatively unreactive, does not react further to form aromatic compounds. Once again it can be seen that gallium decreases the alkanes/aromatics ratio relative to H-ZSM-5 at corresponding reaction temperatures. This occurs as gallium enhances the rate limiting step for aromatics formation, by increasing hydrogen transfer through the formation of hydrogen gas and is also active for light alkane activation to more reactive alkenes.

4.5.3. Aromatic (BTEX) selectivities

As the reaction temperature increases, the selectivity to BTEX increases. However, there is also a change in the relative BTEX selectivities. At reaction temperatures of 350°C, m,p-xylene is the dominant BTEX product. At high reaction temperatures (450°C to 550°C), toluene and benzene are the dominant BTEX products. Table 4.12 shows the change in individual BTEX products with temperature as a ratio of the total BTEX for that temperature. Relative selectivity to ethylbenzene declines as the reaction temperature increases. This is most likely a result of cracking reactions to form toluene and methane and dealkylation to form benzene and ethane. The relative selectivity to o-xylene and p,m-xylene also decrease with increase in reaction temperature similarly to ethylbenzene. The relative selectivity to benzene and toluene increase with increase in reaction temperature. The relative BTEX selectivities for Ga(ionx)/H-ZSM-5 and Ga(impr)/H-ZSM-5 are remarkably similar at all reaction temperatures.

Table 4.12 BTEX as a ratio of the total BTEX selectivity (1-hexene feed)

Catalyst	Temp [°C]	B	T	m,p-X	o-X	EtB
H-ZSM-5[a]	350	0.07	0.30	0.53	0.09	0.09
	450	0.08	0.37	0.44	0.10	0.05
	500	0.13	0.43	0.34	0.09	0.03
Ga(mix)[a]	350	0.06	0.29	0.47	0.11	0.06
	450	0.10	0.40	0.35	0.10	0.05
	550	0.22	0.47	0.22	0.06	0.03
Ga(impr)[b]	350	0.00	0.34	0.56	0.09	0.09
	450	0.13	0.48	0.31	0.08	0.04
	550	0.36	0.46	0.13	0.04	0.01
Ga(ionx)[b]	350	0.00	0.35	0.55	0.09	0.07
	450	0.11	0.45	0.35	0.08	0.07
	550	0.35	0.47	0.13	0.03	0.01

(a) WHSV 5.8hr^{-1}; (b) WHSV 6.9hr^{-1};

The selectivity to m,p-xylene reached a maximum at reaction temperatures of 350°C to 450°C for Ga(impr)/H-ZSM-5, Ga(ionx)/H-ZSM-5 and Ga(mix)/H-ZSM-5 (hydrogen pretreated). It may be reasonably assumed that dealkylation of C_8 aromatics to toluene and subsequent dealkylation of toluene to benzene may cause the increase in selectivity to toluene and benzene at higher reaction temperatures. There was an increase in selectivity towards methane, with a parallel decrease in selectivity to C_8 aromatics. Methane can only be formed by dealkylation reactions. Steric effects cannot explain the low selectivity to ethylbenzene. However, selectivity to ethylbenzene reaches a maximum at reaction temperatures of *ca.* 350°C. At higher reaction temperatures cracking of ethylbenzene to toluene results in a decline in selectivity to ethylbenzene. It must also be emphasized that the maximum yield of C_8 aromatics at 450°C is not observed for H-ZSM-5 and Ga(mix)/H-ZSM-5 (no H_2 pretreatment). As the activities of these two catalysts are lower than the other Ga/H-ZSM-5 catalysts, the peak in C_8 aromatics would most likely be found at a higher reaction temperatures. However, no peak was found at higher reaction temperatures (> 500°C) as dealkylation on H-ZSM-5 is fast relative to aromatization at these temperatures [Collins et al. 1983] and hence the C_8 aromatics would be dealkylated to toluene and benzene as soon as they were formed.

4.5.3.1. Primary aromatic products

On a mole-for-mole basis (for the feedstock), more hydrogen is liberated in the formation of benzene relative to toluene or xylene. If the rate determing step of aromatization is hydrogen transfer then xylenes will form faster than toluene or benzene.

$$28C_6H_{12} \rightarrow 28C_6H_6 + 84H_2$$

$$28C_6H_{12} \rightarrow 24C_7H_8 + 72H_2$$

$$28C_6H_{12} \rightarrow 21C_8H_{10} + 63H_2$$

Thus it is postulated that the C_8 aromatics (xylenes and ethylbenzene) are the primary aromatic products as they are the dominant aromatic compounds at low temperatures and become the dominant aromatic compounds with time on stream (section 4.6). The introduction of gallium, which increases the rate of hydrogen transfer, causes increased selectivity towards benzene and toluene rather than C_8 aromatics. As previously stated (section 4.2), the alkene feedstock caused very little change in product selectivity. Hence the interchange between oligomers and cracked products must be rapid relative to their conversion to aromatic compounds.

4.6 Effect of Time on Stream

Deactivation is defined as a decrease in catalyst activity, resulting in a decrease in feed conversion. No change in conversion of 1-hexene or 1-octene was observed in any of the runs (over a period of up to 10 hours). However, large changes in product selectivity did occur for the Ga/H-ZSM-5 catalysts, which indicate that some form of deactivation mechanism was present. At high reaction temperatures (>350°C) most of the heavy compounds were identified as polynuclear aromatics (section 3.12). Evidence for the formation of polynuclear aromatics at high reaction temperatures comes from off-line GC/MS analysis of the liquid product. At low reaction temperatures (<350°C) no BTX is formed and hence it is unlikely that polynuclear aromatics could constitute any portion of the heavy compounds. The presence of polynuclear compounds, increases the probability that condensation to form coke will occur. The mechanism of deactivation could be a result of a deactivation zone moving through the catalyst bed. As the deactivation zone moves down the catalyst bed less aromatics are formed (due to decreased contact time in the remainder of the catalyst bed) and conversely greater selectivity to cracked products are observed. This form of catalyst bed deactivation is commonly found in industrial reactors [Dry 1993] and it is probable that it could occur even in a small bench scale reactor. The moving deactivation zone would explain the changes in product selectivity observed with time on stream. There would be a decrease in selectivity to aromatic products, which are formed via a slow step, as the effective contact time with the active part of the catalyst bed decreases. As a consequence increased selectivity to the primary products (ethene, propene and butene), formed via fast cracking and oligomerization reactions, would be observed with time on stream. The formation of aromatic products is the only method for their permanent conversion. The decrease in selectivity to aromatic compounds should also be accompanied by a decrease in light alkane selectivity as these light products are formed from hydrogen transfer as a result of aromatization reactions. This was found to occur and is shown in Table 4.14 and section 3.2. These changes in selectivity can be used as a measure of the extent of "deactivation" of the catalyst.

4.6.1. Effect of different catalysts on product selectivity

4.6.1.1 H-ZSM-5

H-ZSM-5 is known to have exceptional stability towards deactivation by coke formation [Holderich and van Bekkum, 1991]. This is a result of the size of the three dimensional catalyst pore system which inhibits the formation of polynuclear aromatics, which are commonly referred to as "hard" coke precursors. During catalytic testing it was observed that H-ZSM-5 was exceptionally stable with regard to feed conversion and product selectivity (section 3.2). Coke formation caused the catalyst to turn a grey colour after 2 hours onstream and an intense matt black after *ca.* 6 hours onstream. FTIR analysis shows the formation of mainly polynuclear coke (section 3.11.3). This coke did not appear to cause any change in product selectivity. The rate of coke formation, if formed by ring fusion of polynuclear aromatic compounds, would be expected to be low as selectivity to aromatic compounds (BTX), the precursors of polynuclear aromatics, is low. The FTIR analysis shows H-ZSM-5 had a lower coke loading than Ga(mix)/H-ZSM-5 and Ga(impr)/H-ZSM-5. Hence, although coke formation did occur, it was not present in sufficient quantities to cause catalyst deactivation.

4.6.1.2. Ga(mix)/H-ZSM-5

These catalysts displayed a stability similar to H-ZSM-5. No change in product selectivity for 1-hexene conversion was observed over a period of 10 hours (section 3.2). The catalysts also turned a matt black colour after several hours on-stream. Thus it can be concluded that the β-Ga_2O_3 crystallites did not cause any observable decrease in BTEX formation as a result of coke formation. FTIR analysis shows that the coke is mainly polynuclear and that a greater amount of coke is present than for H-ZSM-5. Thus, the addition of β-Ga_2O_3 improves yields of aromatic compounds and causes an observable increase in the rate of coke formation over the time period that the catalyst was tested.

4.6.1.3. Ga(mix)/H-ZSM-5 pretreated with hydrogen

Pretreating Ga(mix)/H-ZSM-5 catalysts with hydrogen effectively doubled the initial yields of aromatic compounds but caused a rapid decrease in selectivity to BTEX over 5 hours time on stream (section 3.4). An increase in selectivity to C_3 and C_2 alkenes was observed, as well as to C_4 alkenes. Hence, the rate of coke formation on this catalyst must be greater than on the untreated Ga(mix)/H-ZSM-5.

4.6.1.4. Ga(impr)/H-ZSM-5

This catalyst was more selective towards aromatics than the physically mixed catalysts (sections 3.2.) over 7 hours time on stream. An increase in selectivity to the primary reaction products of propene, ethene and butenes was observed with time on stream, while a dramatic decrease in aromatics selectivity occurred concurrently. The selectivity towards heavy compounds increased with time on stream.

4.6.1.5. Ga(ionx)/H-ZSM-5

The ion-exchanged catalysts displayed product selectivities similar to the catalysts prepared by impregnation (sections 3.2.). No increase in selectivity towards heavy compounds with time onstream was observed (a slight decline in heavy compounds was noted). Hydrogen treatment of these catalysts resulted in similar overall trends in product selectivity as for the untreated catalysts, with the exception being a lower selectivity towards aromatics.

4.6.1.6. Conclusions on changes in selectivities

The change in product selectivities can be explained by a deactivated zone moving down the catalyst bed. However, the physical cause of deactivation of the zeolite is "hard" coke formation as confirmed by FTIR analysis. The activity of various catalysts, normalized to their initial toluene selectivity, is shown in Table 4.13. The gradient of the slope of toluene selectivity and the slope of the sum of $1\text{-}C_4=$ and $i\text{-}C_4=$ selectivity versus time on stream is also shown and serves as a measure of the rate of deactivation.

Table 4.13 Toluene and $1\text{-}C_4{=}/i\text{-}C_4{=}$ selectivity gradient at 550°C

Catalyst	Feed	Toluene selectivity gradient[g]	$1\text{-}C_4{=}/i\text{-}C_4{=}$ selectivity gradient[h]
Ga(mix)/H-ZSM-5[a]	$1\text{-}C_6{=}$	0	0
Ga(impr)/H-ZSM-5[b]	$1\text{-}C_6{=}$	-60	10
Ga(ionx)/H-ZSM-5[b]	$1\text{-}C_6{=}$	-25	9
H-ZSM-5[d]	$1\text{-}C_8{=}$	0	0
Ga(impr)/H-ZSM-5[d]	$1\text{-}C_8{=}$	-36	20
Ga(impr)/H-ZSM-5[c]	$1\text{-}C_8{=}$	-33	8
Ga(mix)/H-ZSM-5[e]	$1\text{-}C_6{=}$	-10	0
Ga(ionx)/H-ZSM-5[f]	$1\text{-}C_6{=}$	-40	8

(a) WHSV 5.8hr^{-1}, 500°C; (b) WHSV 6.9hr^{-1}; (c) WHSV 3.4hr^{-1}; (d) WHSV 1.7hr^{-1}; (e) WHSV 5.8hr^{-1}; 500°C, H_2 pretreated; (f) WHSV 5.7hr^{-1}, H_2 pretreated; (g) Gradient from linear regression of toluene selectivity; (h) Gradient from linear regression of $1\text{-}C_4{=}/i\text{-}C_4{=}$ selectivity;

The data in the table shows that Ga(impr)/H-ZSM-5 catalysts exhibited the greatest change in toluene selectivity, followed by Ga(ionx)/H-ZSM-5 and H_2 pretreated Ga(mix)/H-ZSM-5. Hydrogen pretreatment of Ga(ionx)/H-ZSM-5 caused this catalyst to deactivate more rapidly. The effect of WHSV on toluene selectivity for Ga(impr)/H-ZSM-5 catalysts (1-octene feed) is small. However, greater changes in selectivity for the butene products are observed.

The rate of deactivation does appear to be affected by a change in feedstock from 1-hexene to 1-octene, with 1-hexene causing a greater decline in toluene selectivity (section 3.2.). However, these results may be misleading as the WHSV of the two feedstocks were different. Changes in selectivity are most likely a result of either pore mouth blocking or deactivation of strong acid sites by polynuclear aromatics, as confirmed by FTIR analysis (section 3.11.3). Pore mouth blocking would increase diffusional constraints of the larger product molecules and hence a decline in selectivity towards the aromatic and heavy compounds would be expected. Deactivation of strong acid sites would cause a decrease in aromatic compounds as strong acid sites are needed for cyclization and hydrogen transfer reactions. However, an increase in heavy oligomers would also be expected as there would be fewer strong acid sites needed for cracking reactions. A decrease in the conversion of the primary products of propene, ethene and butenes indicates that the rate of aromatization had decreased as the formation of aromatics is the only reaction pathway to permanently remove these compounds. The greater the rate at which a catalyst produces aromatic compounds the greater the rate of change in product selectivity with time on stream and the greater the coke loading (section 3.10.3). It is probable, therefore, that the mechanism of deactivation is the same in all the catalysts, but that the rate differs significantly.

4.6.3. Changes in alkane/BTEX ratios

Unfortunately, the propane/propene and ethane/ethene hydrocarbons were only resolved in a few of the runs. Most of the runs took place at high reaction temperatures and thus the selectivity to C_4 alkanes was low as they are more easily converted to BTEX aromatics than ethane or propane [Guisnet and Gnep, 1992]. Gallium catalyzes the dehydrogenation of butane to butene [Gnep 1987]. However, Table 4.14 shows that the butane/BTEX ratios for Ga/H-ZSM-5 catalysts are quite stable, with a slight decrease observed with time on stream On H-ZSM-5 the butane/BTEX ratio is constant, as would be expected, as this catalyst showed no change in product selectivity with time on stream. In general the alkane/BTEX ratio should remain constant with time on stream because as less aromatics are produced there should be a corresponding decrease in alkane formation. On Ga/H-ZSM-5 overall selectivity to C_4 alkanes decreases with time on stream, thus indicating that some butane is dehydrogenated to butene and is hence recycled. As the "deactivation band" moves down the catalyst bed, a decrease in the amount of aromatics produced will occur, but a decrease in the alkanes/BTEX ratio will be observed as the dehydrogenation reaction of butane to butene still takes place and is more rapid than aromatization [Gnep 1987] .

Table 4.14 Change in alkane to BTEX ratios with time on stream

Catalyst	T.o.S.[e] [min]	Temp [°C]	C_2/BTX	C_3/BTX	n-C_4/BTX	i-C_4/BTX
			Feed 1-hexene			
Ga(mix)[a]	15	500	*	*	0.14	0.24
	420	500	*	*	0.11	0.18
Ga(impr)[b]	15	550	*	*	0.00	0.00
	190	550	*	*	0.01	0.01
Ga(ionx)[b]	15	550	*	*	0.03	0.06
	420	550	*	*	0.02	0.06
			Feed 1-octene			
H-ZSM-5[c]	15	550	*	*	0.07	0.06
	420	550	*	*	0.05	0.07
Ga(impr)[d]	15	550	0.01	0.05	0.00	0.00
	420	550	0.01	0.03	0.01	0.02
			H_2 pretreated catalysts, feed 1-hexene			
Ga(mix)[a]	15	500	*	*	0.025	0.098
	290	500	*	*	0.020	0.10
Ga(ionx)[f]	15	550	*	*	0.039	0.053
	300	550	*	*	0.013	0.051

* alkene/alkanes not resolved by GC; (a) WHSV 5.8hr^{-1}; (b) WHSV 6.9hr^{-1}; (c) WHSV 1.7hr^{-1}; (d) WHSV 3.4hr^{-1}; (e) time on stream; (f) WHSV 5.7hr^{-1};

4.6.4. Summary of selectivity changes with time on stream

4.6.4.1. Light products

There is an increase in selectivity to light alkenes with time on stream and a decrease in selectivity to light alkanes (Table 4.15).

Table 4.15 Effect of time on stream on light product selectivity

Catalyst	T.o.S.[d] [min]	C_1	C_2	C_3	$C_2=$	$C_3=$	$1\text{-}C_4=/i\text{-}C_4=$	$i\text{-}C_4$
				1-hexene feed, 550°C				
Ga(impr)[e]	15	3	*	*	9	10	0	0
	190	1	*	*	11	13	2	1
Ga(ionx)[e]	15	1	*	*	18	24	3	3
	380	0	*	*	14	35	6	2
Ga(mix)[a]	15	1	*	*	12	18	4	4
	290	0	*	*	12	23	6	4
				1-octene feed, 550°C				
Ga(impr)[b]	15	2	*	*	10	6	0	0
	380	1	*	*	14	18	3	0
Ga(impr)[c]	15	3	1	3	6	2	0	0
	380	1	0	1	10	18	5	1

(*) compounds not resolved, $C_2=$ and $C_3=$ are the sum of the alkanes and akenes in this case; (a) WHSV 5.8hr^{-1}, H_2 pretreated, 500°C; (b) WHSV 1.7hr^{-1}; (c) WHSV 3.4hr^{-1}; (d) time on stream; (e) WHSV 6.9hr^{-1};

This is in agreement with the proposed "deactivation zone" moving down the catalyst bed. As less catalyst is available for aromatization reactions, the primary alkene products will increase in selectivity and the alkanes, which are formed from hydrogen transfer, will decrease. The alkane/alkene ratios which were resolved for Ga(impr)/H-ZSM-5 with 1-octene feed show that a decrease in selectivity to ethane and propane and increase in light alkenes occurs with time on stream. Selectivity to methane decreases with time on stream in all cases. The greatest selectivity to methane (Table 4.15) is observed with high selectivity to benzene and toluene (Table 4.16). Hence it can be concluded that methane is formed primarily through dealkylation reactions of C_8 aromatics.

4.6.4.2. Selectivity to BTEX aromatic products

The selectivity to benzene and toluene decrease with time on stream while selectivity to xylene remains constant or only decreases slightly.

Table 4.16 Effect of time on stream on BTEX selectivity

Catalyst	T.o.S.[d] [min]	B	T	m,p-X	o-X	EtB	ΣBTEX
			1-hexene feed, 550°C				
Ga(impr)[e]	15	27	31	8	2	1	71
	190	22	25	8	2	1	60
Ga(ionx)[e]	15	9	21	9	3	1	43
	380	6	14	9	2	2	33
Ga(mix)[a]	15	8	18	12	3	3	44
	290	6	14	10	3	2	35
			1-octene feed, 550°C				
Ga(impr)[b]	15	25	29	7	2	0	63
	380	12	19	9	2	1	43
Ga(impr) [c]	15	26	30	8	2	0	66
	380	10	18	9	2	1	40

(a) WHSV 5.8hr^{-1}, H_2 pretreated, 500°C; (b) WHSV 1.7hr^{-1}; (c) WHSV 3.4hr^{-1}; (d) time on stream; (e) WHSV 6.9hr^{-1};

Hence, it can be postulated that C_8 aromatics are the primary aromatic compounds and they are dealkylated to benzene and toluene at high reaction temperatures and on highly active catalysts (short time on stream). With time on stream, selectivity to benzene and toluene will decrease if these compounds are formed via C_8 aromatic dealkylation. This is supported by a decrease in methane selectivity with time on stream (Table 4.15). Methane should be formed mainly by dealkylation reactions.

4.7. Effect of Hydrogen Pretreatments

Hydrogen pretreatment of Ga/H-ZSM-5 catalysts are widely reported to increase selectivity towards aromatics [Changyu et al. 1988; Price and Kanazirev 1990]. However, the gallium species most active for aromatization, as reported in recent literature, is not the reduced Ga^+ ion, but a dispersed Ga^{+3} species [Dooley et al. 1992, 1993].

4.7.1. Ga(mix)/H-ZSM-5

The effect of hydrogen pretreatment on the Ga(mix)/H-ZSM-5 catalyst is shown in Table 4.17. Hydrogen pretreatment of Ga(mix)/H-ZSM-5 dramatically improves the selectivity to aromatic compounds. The phenomenon noted earlier with regard to the change in selectivity to C_8 aromatics with increasing reaction temperature is clearly visible in the table above. The Ga(mix)/H-ZSM-5 catalyst pretreated with hydrogen shows a maximum in the yield of C_8 aromatics at *ca.* 450°C, which is not observed in the untreated Ga(mix)/H-ZSM-5. The selectivity towards $C_2/C_2=$ and $C_3/C_3=$ cracked products remains more constant over the entire temperature range when the catalyst was pretreated with hydrogen. This indicates that the hydrogen pretreated catalyst is more active for aromatization (as aromatization reactions convert these compounds into BTEX).

XRD data for Ga(mix)/H-ZSM-5 (section 3.10.2) shows a reduction in the number and probably size of β-Ga_2O_3 crystallites. It may be reasonably assumed that hydrogen pretreatment of β-Ga_2O_3/H-ZSM-5 physically mixed catalysts causes reduction of the β-Ga_2O_3 bulk crystallites to form a gallium suboxide which interacts strongly with anionic sites present in ZSM-5. These gallium suboxides are labile and hence are dispersed throughout the zeolite channels [Price and Kanazirev, 1990]. When reoxidized to Ga^{+3}, they constitute the active species for hydrogen transfer [Dooley et al. 1992, 1993].

Table 4.17 Result of hydrogen pretreatment at 550°C

	Ga(mix)/H-ZSM-5[a]			Ga(mix)/H-ZSM-5 (H_2 pretreated)[a]		
	350°C	450°C	550°C	350°C	450°C	550°C
C_2= & C_2	3	10	22	3	7	8
C_3= & C_3	15	27	28	10	10	7
C_4=	15	12	8	14	4	0
C_4	18	13	4	9	8	1
B	1	2	8	3	5	26
T	5	8	17	6	20	28
p,m-X	8	7	8	9	18	10
o-X	2	2	2	2	3	3
EtB	1	1	1	1	3	1
Heavies	20	12	5	30	18	14
ΣBTEX	17	20	36	21	49	68

(a)1-hexene feed, WHSV 5.8hr^{-1};

4.7.2. Ga(ionx)/H-ZSM-5 and Ga(impr)/H-ZSM-5 catalysts

When these catalysts were pretreated with hydrogen, a decrease in selectivity to aromatic compounds was observed. The results are shown in Table 4.18. The table shows the similarity in product spectrum for Ga(impr)/H-ZSM-5 and Ga(ionx)/H-ZSM-5 catalysts. The effect of hydrogen pretreatment on both catalysts is similar with selectivity to toluene reduced most markedly and that of benzene to a lesser degree. The selectivity to C_2 and C_3 cracked products increased, but selectivity to C_8 aromatics remains essentially unchanged for the hydrogen treated catalysts. However, the xylenes contribution as a percent of the total BTEX increases. Due to the high degree of dispersion of gallium within these catalysts, it is postulated that hydrogen treatment reduces the gallium to a Ga(I) species which is not active for aromatization reactions [Dooley et al. 1992, 1993]. Reduction of Ga_2O_3 requires acid sites [Price et al. 1990] and hence a highly dispersed gallium species will be easier to reduce as it will be in close proximity to acid sites. Bulk β-Ga_2O_3 crystallites will not be easily reduced as only a small part of the crystallite will be in contact with acid sites. This is confirmed by the TPR results (section 3.7) which show that Ga(impr)/H-ZSM-5 has a lower peak maximum for hydrogen consumption than Ga(mix)/H-ZSM-5. This reduced gallium species is most likely not as active for hydrogen transfer as the partially or unreduced gallium species [Dooley et al. 1992,1993]. Unfortunately no analytical instruments were available to determine the oxidation state of the gallium species. However, it is clear that pretreatment of these catalysts with hydrogen results in a less active aromatization catalyst.

Table 4.18 Effect of H_2 pretreatment at 550°C, 1-hexene feedstock

	Ga(impr)/H-ZSM-5[a]	Ga(impr)/H-ZSM-5[b]	Ga(ionx)/H-ZSM-5[c]	Ga(ionx)/H-ZSM-5[d]
C_2= & C_2	8	11	10	12
C_3= & C_3	10	12	11	16
C_4=	2	3	1	2
C_4	1	1	1	4
B	27	20	25	17
T	31	20	33	19
p,m-X	8	9	9	10
o-X	2	2	3	2
EtB	1	1	1	2
Heavies	7	18	8	17
ΣBTEX	69	52	71	50

(a) WHSV = 6.9hr^{-1}, no H_2 treatment; (b) WHSV = 6.9hr^{-1}, H_2 pretreated; (c) WHSV = 6.9hr^{-1}, no H_2 treatment; (d) WHSV = 5.7hr^{-1}, H_2 pretreated

There is an increase in selectivity to heavy compounds after hydrogen pretreatment. The reason for this phenomena is unclear as a less active catalyst will produce less aromatics and hence less heavy polynuclear aromatic compounds. However, an increase in the carbon mass balances with time on stream was observed (Table 4.2). Initially the carbon mass balances are below 100%, but they increase with time on stream to *ca.* 120%. Hence, it is postulated that the heavy compounds (alkylated naphthalenes) diffuse slowly from the catalyst pore system and thus appear in low concentrations in the initial GC samples. They appear in increasing amounts with time on stream as the coke build up on the catalyst increases. No GC/MS identification of heavy compounds from the experiments with hydrogen pretreated catalysts was made. However, the heavy compounds from these experiments show similar retention times to those of the naphthalenes which were identified by GC/MS. Hence it is assumed that they are polynuclear aromatics (naphthalenes) as well.

4.8. Effect Of WHSV on Product Selectivity

The effect of different WHSV on product selectivity at 500°C was slight (section 3.5.) An increase in the WHSV of the feed for H-ZSM-5 and Ga(mix)/H-ZSM-5 caused a slight decrease in selectivity towards propene and ethene. The linear velocity of the carrier gas over the catalyst bed was at all times kept constant at 0.66cm/s. Residence time over the catalyst bed was a more important factor in determining product selectivity (section 3.13 and section 4.1.3) as a result of operating in the diffusion controlled regime. Two experimental runs at different WHSV's, with Ga(impr)/H-ZSM-5 as the catalyst and 1-octene as the feedstock, showed that WHSV had a negligible effect on product selectivity with time on stream (section 3.2.2.).

At low temperatures (250°C) the effect of WHSV is more marked with a decrease in selectivity to propene and the C_4 butenes and a noticeable increase in selectivity towards C_5 and heavy compounds (section 3.5). The heavy compounds at this temperature are likely to be oligomers of 1-hexene and hence the C_5 products observed are a result of cracking of these oligomers. Conversion of 1-hexene decreases with increasing WHSV at this temperature.

Chapter 5

CONCLUSION

5. Conclusions

The purpose of this investigation was to research the feasibility of producing aromatics, mainly BTX, from Ga/H-ZSM-5 zeolite catalysts. It was found that H-ZSM-5, without gallium, could produce aromatics from C_6 and C_8 alkene feedstocks (13% BTEX), but that this was accompanied by the formation of large amounts of C_2-C_4 cracked products (75%). The introduction of gallium onto the zeolite dramatically enhanced yields of aromatic products (70% BTEX) and there was a corresponding decrease in selectivity towards light cracked products (17%). However, Ga/H-ZSM-5 catalysts displayed greater changes in product selectivity with time on stream than H-ZSM-5. This change in product selectivity was accompanied by an increase in light alkene yields and a decrease in selectivity to BTEX and light alkanes. Reactant conversion was always 100% at reaction temperatures above 400°C and did not decrease with time on stream.

The selectivity to BTEX was strongly influenced by the reaction temperature and contact times with the catalyst bed. Greatest selectivity to BTEX was observed at high reaction temperatures (>450°C) and long contact times (*ca.* 2 seconds) with the catalyst bed. The alkene feedstock (1-hexene or 1-octene) had a negligible effect on BTEX product selectivity.

The method of adding gallium did not result in large changes in product selectivity, providing that a high dispersion of gallium within the zeolite was achieved. The highest aromatic selectivities were obtained for Ga(impr)/H-ZSM-5, Ga(ionx)/H-ZSM-5 and Ga(mix)/H-ZSM-5 (H_2 pretreated). Hydrogen treatment improved selectivity to aromatics only for catalysts prepared by physical mixing of β-Ga_2O_3 and H-ZSM-5, i.e. Ga(mix)/H-ZSM-5. This improvement in selectivity is caused by the interaction of a labile gallium suboxide species and the zeolite framework which results in dispersion of gallium within the zeolite channels. Catalysts prepared by ion-exchange and impregnation techniques do not exhibit increased selectivity to aromatics after being subjected to hydrogen treatment. This is in agreement with recent literature [Dooley et al. 1992, 1993] and is a result of reducing the already highly dispersed gallium to the univalent state (a stabilized Ga^{+1} species). Hence the most active state of gallium for hydrogen transfer is a highly dispersed species in a bivalent or trivalent state.

The optimal conditions for BTX products would depend on the selectivity towards each BTX component that is required. Benzene and toluene became the dominant aromatic products at reaction temperatures above 500°C, while at low temperatures (350°C) the dominant aromatic compounds were p-and-m-xylene. It is proposed that C_8 aromatics are the primary aromatic compounds and that dealkylation of these compounds to benzene and toluene occur at high temperatures. Methane, which would be formed in dealkylation reactions, shows increased selectivity with increase in reaction temperature.

A major disadvantage with Ga/H-ZSM-5 catalysts is the rapid decrease in BTEX selectivity with time on stream. However, they can be regenerated repeatedly by calcination in air, with no observed loss in catalytic activity. Recycle of the non-aromatic compounds would have to be performed for this catalyst to be used efficiently in industrial processes. This occurs in the Cyclar process for propane and butane aromatization.

Further work in this field could include investigating the effect of the gallium precursor (β-Ga_2O_3 and other phases thereof) on product selectivity. There is much scope for research in determining the mechanism of deactivation as well as characterization of the heavy reaction products. The effect that oxygenates in the feedstock would have on product selectivity and catalyst deactivation would be interesting from the point of view of SASOL as the products from the Fischer-Tropsch process contain a substantial amount of oxygenates. Furthermore, the addition of hydrogen transfer agents like Zr_2Fe to Ga/H-ZSM-5 [Chetina et al. 1992] could also be researched.

REFERENCES

6. References

Anderson,J.R., Chang,Y.F., Western,R.J., *J. Catal.*, **118**, p.406, (1989)

Anderson,J.R., *Appl. Catal.*, **75**, p.87, (1991)

Arguer,R.J., Landolt,G.R., *US Patent 3702,886*, (1972)

Arroyo, P.A., Sousa-Aguiar, E.F., Monteiro, J.L.F., *Symposium on Alkylation, Aromatization, Isomerization of Short Chain Hydrocarbons over Heterogeneous Catalysis, American Chemical Society*, New York, August 25-30, (1991), p.685

Bailar,J., Comprehensive Inorganic Chemistry, I, Pergamon Press Ltd., Oxford, (1973)

Bandiera,J., Ben Taarit,Y., *Appl. Catal.*, **62**, p.309, (1990)

Bayense,C.R., Damen, H.A.M., van Hooff, J.H.C., *Symposium on Alkylation, Aromatization, Isomerization of Short Chain Hydrocarbons over Heterogeneous Catalysis, American Chemical Society*, New York, August 25-30, (1991), p.651

Bayense,C.R., van der Pal, A.J.H.P., van Hooff,J.H.C., *Appl. Catal.*, **72**, p.81, (1991)

Bhatia, T.K., Phillips, M.J., *J. Catal.*, **110**, p.150, (1988)

Brouwer,D.M., *J. Catal.*, **1**, p.22, (1962)

Buckles,G., Hutching, G.H., Williams, C.D., *Catal. Lett.*, **11**, p.69, (1991)

Carli,R., Bianchi,C.L., Giannantonio,R., Ragaini,R., *J. Mol. Catal.*, **83**, p.379, (1993)

Changyu,T., Changrui,C., Lixin,Z., Shaoryi,P., *Proc. 9th Int. Congr. Catal., Calgary,* The Chem. Inst. Canada, Ottawa, (1988), p.445

Chetina,O.V., Vasina,T.V., Lunin,V.V., *Catal. Lett.*, **14**, p.101, (1992)

Collins,D.J., Medina,R.J., Davis,B., *Canadian J. Chem. Eng.*, **61**, p.29, February, (1983)

Cosimo,R., Burrington,J.D., Grasselli,R.K., *J. Catal.*, **102**, p.234, (1986)

Doolan,P.C., Pujada P.R., *Hydrocarbon Processing*, September, p.72, (1989) Dooley,K.M., Chang,C., Kanazirev,K., Price,G.L., *New Frontiers in Catalysis, Proc. 10th Int. Conf. Catal.*, 19-24 July, (1992), Budapest, Hungary, p.2415

Dooley,K.M., Chang,C., Price,G.L., *Appl. Catal. A General*, **84**, p.17, (1992)

Dry,M., private communication, (1993)

Edmonds, T., Catalysis and Catalytic Processes, Blackie and Sons, Ltd., Glasgow, (1981), p.88

Engelhardt,J., Hall,W.K., *J. Catal.*, **125**, p.475, (1990)

Gianetto,G., Perez, J.A., Sciamanna,R., Garcia,L., Gallasso,R., Monque,R., *Symposium on Alkylation, Aromatization, Isomerization of Short Chain Hydrocarbons over Heterogeneous Catalysis, American Chemical Society*, New York, August 25-30, (1991), p.659

Gianetto,G., Sansare,S., Guisnet,M., *J. Chem. Soc. Commun.*, p.1302, (1986)

Gnep,N.S., Doyemet, J.Y., Seco, A.M., Ribero,F.R., Guisnet,M., *Appl. Catal.*, **35**, p.93, (1987)

Gnep,N.S., Doyemet,J.Y., Guisnet,M., *J. Mol. Catal.*, **45**, p.281, (1988)

Gnep, N.S., Doyemet,J.Y., Guisnet, M., *Studies in Surface Science and Catalysis*, **46**, p.153, Elsevier Ltd., Amsterdam, (1989)

Gosling, C.D., Wilcher, F.P., Sullivan,L., Mountford,R.A., *Hydrocarbon Processing*, December, p.69, (1991)

Grunert,W., Saffert,W., Feldhaus,R., Anders,K., *J. Catal.*, **99**, p.149, (1986)

Guczi, L., Kemeny, G., Matusek, K., Mink, J., *J. Chem. Soc. Faraday Trans. I*, **76**, p.782, (1980)

Guisnet, M., Gnep, N.S., *Appl. Catal.*, **89**, p.1, (1992)

Haag,W.O., Dessau,R.M., *Proc. 8th Int. Congress on Catalysis*, Berlin, vol.2, Verlag Chemie, Weinheim, (1984), p.305

Holderich,W.F., van Bekkum,H., *Studies in Surface Science and Catalysis*, **58**, p.631, Elsevier Ltd., Amsterdam, (1991)

Hungenburg, K.D., *J. Catal.*, **68**, p.200, (1981)

Hutchings,C.J., Scurrell,M.S., *Catal. Today*, **6(3)**, p.351, (1990) Inui,T., *Studies in Surface Science and Catalysis*, **44**, p.189, Elsevier Ltd., Amsterdam, (1989)

Inui,T., Ishihara,I., Kamachi,K., Matsuda,H., *Studies in Surface Science and Catalysis*, **49B**, p.1183, Elsevier Ltd., Amsterdam, (1989)

Joly,J.F., Ajot,H., Merlen,E., Raatz,F., Alasio,F., *Appl. Catal. A*, **79**, p.249, (1991)

Joly,J.F., Ajot,H., Alario,F., Aittaleb,D., Gnep,N.S., Guisnet,M., *Int. Zeolite Conference*, Montreal, July 1992, in press

Kanai,J., Katawa,N., *Appl. Catal.*, **55**, p.115, (1989)

Kanai,J., Katawa,N., *Appl. Catal.*, **62**, p.141, (1990)

Kanai,J., Kawata,N., *J. Catal.*, **114**, p.284, (1988)

Karge,H.G., Boldingh,E., *Catal. Today*, **3**, p.379, (1988)

Kitagawa,K., Sendoda,Y., Ono,Y., *J.Catal.*, **101**, p.12, (1986)

Kanazirev,V., Price,G.L., Dooley,K.M., *J. Chem. Soc. Commun.*, p.712, (1990)

Kanazirev,V., Price,G.L., Dooley,K.M., *Studies in Surface Science and Catalysis*, **69**, p.277, Elsevier Ltd., Amsterdam, (1991)

Katsuno, H., Sugimoto, M., *Symposium on Alkylation, Aromatization, Isomerization of Short Chain Hydrocarbons over Heterogeneous Catalysis, American Chemical Society*, New York, August 25-30, (1991), p.723

Kokes,R.J., Dent,A.L., *Advances in Catalysis*, **23**, p.1, (1972)

Lane, G.S., Modica, F.S., Miller, J.T., *J. Catal.*, **129**, p.145, (1991)

Le Van Mao,R., Levesque,P., Sjiariel,B., *Can. J. Chem. Eng.*, **64**, p.514, (1986)

Le Van Mao,R., Dufresne,L., *Appl. Catal.*, **52**, p.1, (1989)

Le Van Mao,R. and Yao,J., *Appl. Catal.*, **79**, p.77, (1991)

Lombardo,E.A., Hall,W.K., *J.Catal.*, **112**, p.565, (1988)

Lombardo,E.A., Pierantozzi,R., Hall,W.K., *J. Catal.*, **110**, p.171, (1988)

Magnoux,P., Machado,F., Guisnet,M., *New Frontiers in Catalysis, Proc. 10th Int. Conf. Catal.*, 19-24 July, (1992), Budapest, Hungary, p.435

Meisner,G.D., Iglesia,E., Baumgartner,J.E., Huang,E.S., *J. Catal.*, **140**, p.209, (1993)

Meriadeau,P., Naccache,C., *J. Mol. Catal.*, **50**, L7, (1989)

Meriaudeau,P., Sapaly,G., Naccache,C., *Studies in Surface Science and Catalysis*, **49B**, p.1423, Elsevier Ltd., Amsterdam, (1989)

Meriaudeau, P., Naccache, C., *Studies in Surface Science and Catalysis*, **68**, p.767, Elsevier Ltd., Amsterdam, (1991)

Meriaudeau, P., Naccache, C., *Studies in Surface Science and Catalysis*, **69**, p.405, Elsevier Ltd., Amsterdam, (1991)

Meriaudeau,P., Naccache,C., *Appl. Catal.*, **73**, L13, (1991)

Mole,T., Anderson,J.R., *Appl. Catal.*, **17**, p.141, (1985)

Norval, G.W., Phillips, M.J., Missen, R.W., *Appl. Catal.*, **54**, p.37, (1989)

Norval, G.W., Crimi, C., Phillips,M.J., *J. Catal.*, **113**, p.263, (1988)

Ono, Y., Kitagawa,H., Sendoda, Y., *J. Chem. Soc. Faraday Trans. 1*, **83**, p.2913, (1987)

Osaka,O., Nakashiro,K., Ono,Y., *Bull. Chem. Soc. Jpn.*, **66**, p.755, (1992)

Parera, J.M., Beltramini, J.N., Querini , C.A., Martinelli, E.E., Churin, E.J., Aloe, P.E., Figoli, N.S., *J. Catal.*, **99**, p.39, (1986)

Petit,L., Bournonville,J.P., Rattz,F., *Studies in Surface Science and Catalysis*, **49B**, p.1163, Elsevier Ltd., Amsterdam, (1989)

Planelles,J., Sanchez Marin,J., Tomas,F., Corma,A., *J. Mol. Catal.*, **32**, p.365, (1985)

Price,G.L., Kanazirev,K., *J. Mol. Catal.*, **66**, p.115, (1991)

Price,G.L., Kanazirev,V., *J. Catal.*, **126**, p.267, (1990)

Roessner,F., Hagen,A., Mroczek,U., Karge,H.G., Steinberg,K-H., *New Frontiers in Catalysis, Proc. 10th Int. Conf. Catal.*, 19-24 July, (1992), Budapest, Hungary, p.1707

Romero,T., Arenas,B., Perozo,E., Bolivar,C., Browo,G., Marcano,P., Scott.,C, Perez Zurita,M.J., Goldwasser,J., *J. Catal.*, **124**, p.281, (1990) Sapre, A.V., Krambeck,F.J., "Chemical Reactions in Complex Mixtures", The Mobil Workshop, Van Nostrand Reinhold, NewYork, p.143, (1991)

Sapre, A.V., Krambeck,F.J., "Chemical Reactions in Complex Mixtures", The Mobil Workshop, Van Nostrand Reinhold, NewYork, p.91, (1991)

Scire,S., Maggiore,R., Galvagno,S., Crisafulli,C., Solarino,L., *React. Kinet., Catal. Lett.*, **40**, p.349, (1989)

Scurrell, M.S., *Appl. Catal.*, **32**, p.1, (1987)

Seally,S., private communication, (1993)

Shigeshi,R., Garforth,A., Harris,I., Dwyer,J., *J. Catal.*, **130**, p.423, (1991)

Sneddon, D., *Catal. Today*, **6(3)**, p.351, (1990)

Spinicci,R., Tofanari,A., *Appl. Catal.*, **1**, p.387, (1981)

Spinicci,R., Tofanari,A., *Appl. Catal.*, **44**, p.197, (1988)

Stull,D.R., Westrum, E.F., Sinke,G.C., The Chemical Thermodynamics of Organic Compounds, Wiley and Son Ltd., New York, (1969)

Tauser, S.J., Steger, J.J., *J. Catal.*, **125**, p.387, (1990)

van Koningsveld, H., van Bekkum, H., Jansen, J.C., *Acta. Cryst.*, **B34**, p.127, (1987)